Reducible M-curves for Le-networks in the totally-nonnegative Grassmannian and KP-II multiline solitons

REDUCIBLE M-CURVES FOR LE-NETWORKS IN THE TOTALLY-NONNEGATIVE GRASSMANNIAN AND KP–II MULTILINE SOLITONS

SIMONETTA ABENDA AND PETR G. GRINEVICH

Abstract. We associate real and regular algebraic–geometric data to each multi–line soliton solution of Kadomtsev-Petviashvili II (KP) equation. These solutions are known to be parametrized by points of the totally non–negative part of real Grassmannians $Gr^{\mathrm{TNN}}(k,n)$. In [3] we were able to construct real algebraic-geometric data for soliton data in the main cell $Gr^{\mathrm{TP}}(k,n)$ only. Here we do not just extend that construction to all points in $Gr^{\mathrm{TNN}}(k,n)$, but we also considerably simplify it, since both the reducible rational M–curve Γ and the real regular KP divisor on Γ are directly related to the parametrization of positroid cells in $Gr^{\mathrm{TNN}}(k,n)$ via the Le–networks introduced in [62]. In particular, the direct relation of our construction to the Le–networks guarantees that the genus of the underlying smooth M–curve is minimal and it coincides with the dimension of the positroid cell in $Gr^{\mathrm{TNN}}(k,n)$ to which the soliton data belong to. Finally, we apply our construction to soliton data in $Gr^{\mathrm{TP}}(2,4)$ and we compare it with that in [3].

2010 MSC. 37K40; 37K20; 14H50; 14H70.

Keywords. Total positivity, totally non-negative Grassmannians, KP hierarchy, real solitons, M-curves, Le–diagrams, planar bipartite networks in the disk, Baker–Akhiezer function.

Contents

This research has been partially supported by GNFM-INDAM and RFO University of Bologna, by the Russian Foundation for Basic Research, grant 17-01-00366, by the program "Fundamental problems of nonlinear dynamics", Presidium of RAS. Partially this research was fulfilled during the visit of the second author (P.G.) to IHES, Universit Paris-Saclay, France in November 2017.

1. Introduction

The deep relation between the asymptotic behavior of real bounded multi–line KP* soliton solutions, asymptotic web networks and total positivity has been unveiled in a series of papers (see [11, 12, 17, 18, 20, 44, 45, 46, 47, 72] and references therein). On the other side, real regular KP finite-gap solutions are associated to M–curves [25], and soliton solutions can be obtained as degenerations of complex finite-gap ones, when some cycles on the spectral curves shrink to double points. As pointed out by S.P. Novikov, it is natural to check whether **real regular** degenerate solutions may be obtained by degenerating **real regular** finite-gap solutions. In particular, in the case of real bounded multi-line KP solitons, this means to investigate whether they can be obtained by degenerating smooth M–curves to rational (reducible) ones. Therefore we have

*Throughout the paper, we always use the notation KP for KP II, with the heat conductivity operator in the Lax pair.

started to search for new relations between total positivity in Grassmannians [52, 53, 62, 63, 64] and M–curves [38, 37, 59, 70], by connecting two relevant approaches used in KP theory to classify solutions, the Sato Grassmannian [65] and KP finite–gap theory [48, 49, 25], and in [3] we have succeeded in establishing a new connection between classical total positivity [42, 61] and rational degenerations of M–curves when the KP soliton data belonging to the main cells, $Gr^{\rm TP}(k,n) \subset Gr^{\rm TNN}(k,n)$.

Here we construct an analogous connection between all positroid cells in $Gr^{\rm TNN}(k,n)$ and M–curves. More precisely, we provide a new interpretation of minimal parametrizations of g–dimensional positroid cells $\mathcal{S}_{\mathcal{M}}^{\rm TNN} \subset Gr^{\rm TNN}(k,n)$ via degree g real and regular KP divisors on reducible M–curves which are rational degenerations of genus g M–curves, using the Le–networks introduced in [62]. To the Le–graph representing $\mathcal{S}_{\mathcal{M}}^{\rm TNN}$ [62], we canonically associate an universal reducible curve $\Gamma = \Gamma(\mathcal{S}_{\mathcal{M}}^{\rm TNN})$ with $g+1$ ovals which is a rational degeneration of a genus g smooth M–curve. Then we establish a canonical relation between points in $\mathcal{S}_{\mathcal{M}}^{\rm TNN}$ parametrized by Le–networks and degree g divisors on Γ. Since such networks provide a minimal parametrization of positroid cells [62] and the degree of the KP divisor coincides with the dimension of $\mathcal{S}_{\mathcal{M}}^{\rm TNN}$, our parametrization is optimal for generic soliton data.

The starting point is the fact that regular multi–line KP solitons are obtained in well–defined finite–dimensional reductions of the Sato Grassmannian [65]. More precisely, each family of KP real regular multiline soliton solutions corresponds to soliton data in a uniquely identified d–dimensional irreducible positroid cell $\mathcal{S}_{\mathcal{M}}^{\rm TNN}$ in a totally non–negative Grassmannian $Gr^{\rm TNN}(k,n)$[†] (see [18, 46, 47] and references therein). In this setting, the soliton data are a set of ordered phases $\mathcal{K} = \{\kappa_1 < \cdots < \kappa_n\}$ and a point $[A] \in \mathcal{S}_{\mathcal{M}}^{\rm TNN}$. Then the corresponding KP multiline soliton solution is real regular for real times and the direct spectral approach provides a k point divisor on a rational curve Γ_0 with n marked points corresponding to the phases $\mathcal{K}$ and a marked point corresponding to the essential singularity of the normalized KP wave function [54]. However, these spectral data are, in general, insufficient to reconstruct soliton data varying in $\mathcal{S}_{\mathcal{M}}^{\rm TNN}$ since $\max\{k, n-k\} \leq d \leq k(n-k)$.

On the other side, in principle, soliton solutions can be obtained by degenerating finite-gap solutions on smooth curves in the limit when some gaps degenerate to double points, as it was

[†]Each family of soliton solutions is also realized in an infinite number of d–dimensional reducible positroid cells in $Gr^{\rm TNN}(k',n')$ with $k' \geq k$ and $n' > n$.

first observed in [60] for the case of the Korteweg–de Vries equation.[‡] In particular, finite-gap KP solutions were constructed in [48, 49]: they are parametrized by degree g non-special divisors on genus g Riemann surfaces with a marked point. Real regular finite-gap KP solutions correspond to algebraic data on genus g M-curves satisfying natural constraints [25]: by definition, the curve has $g+1$ real ovals, and one of them contains the marked point, while each other oval contains exactly one divisor point.

Therefore, in order to obtain a one–to–one correspondence between soliton data varying in a given positroid cell and KP divisors, it is natural to impose that Γ_0 is an irreducible component of a reducible spectral curve. This approach is fully justified analytically by the extension of finite–gap theory to degenerate solutions, like solitons, on reducible curves in [50]. However, as remarked in [50], the finite–gap approach on reducible curves is ill–defined, in the sense that, due to degeneracy, there is not a unique way to extend the Baker–Akhiezer function. It is then relevant to search for canonical constructions compatible with the degeneration from regular finite–gap solutions. Since real regular quasi–periodic KP solutions are parametrized by real and regular divisors on smooth M–curves [25], we construct reducible curves Γ, which are rational degenerations of smooth M–curves, and KP divisors satisfying reality and regularity conditions compatible with those settled in [25]. The relevance of the construction proposed in this paper relies on the fact that, on one side, it perfectly matches the reality problem for KP finite–gap theory and, on the other side, provides a canonical parametrization of positroid cells. More precisely, in this paper:

(1) We associate a canonical reducible M–curve Γ to the Le–graph $\mathcal{G}$ describing the corresponding cell and we prove that it is a rational degeneration of a smooth M–curve of genus equal to the dimension g of the positroid cell. This curve Γ contains the rational curve Γ_0 coming from the direct spectral analysis as one of its irreducible components;
(2) We then provide a parametrization of each g–dimensional positroid cell by real regular degree g non–special divisors $\mathcal{D}_{\mathrm{KP},\Gamma}$. The Sato divisor coincides with $\mathcal{D}_{\mathrm{KP},\Gamma} \cap \Gamma_0$.

We have decided to treat the Le–network case separately both because the reducible curve for the Le–network is the rational degeneration of a smooth M–curve of **minimal genus** equal to the dimension of the positroid cell $\mathcal{S}_{\mathcal{M}}^{\mathrm{TNN}}$ and because we get a parametrization of $\mathcal{S}_{\mathcal{M}}^{\mathrm{TNN}}$ via degree g

[‡] Using other degenerations analogous to those in [23], one can construct other interesting classes of KP solutions, including the rational ones. For additional information about singular spectral curves in soliton theory see [67].

non–special KP divisors. Moreover, the explicit use of Le–networks is directly connected to the construction proposed in [3] for the case $\mathcal{S}_{\mathcal{M}}^{\mathrm{TNN}} = Gr^{\mathrm{TP}}(k,n)$ and it also considerably simplifies it. Finally, throughout this paper, we carry out explicitly the construction for the usual acyclic orientation of the Le–network and we postpone to [4] the proof of the invariance of the KP divisor with respect to changes of orientation of the network and the generalization of this construction to all Postnikov networks.

Before outlining our construction, we would like to point out that there are other well-known relations of different nature between networks, algebraic curves and integrable systems in literature. In dimer models with periodic boundary conditions (models on tori) the Riemann surfaces arise as the spectral curves for operators on networks on tori [43], and such spectral curves, which are generically regular, may be associated to classical or quantum integrable systems [35]. Another big area of activity is currently associated with the use of planar networks in the disk for the computation of scattering amplitudes in $N = 4$ super Yang-Mills on-shell diagrams, see [7, 8, 9] and references therein. We have noticed an analogy between the momentum–helicity conservation relations in the trivalent planar networks in the approach of [7, 8] and the relations satisfied by the vacuum and dressed edge wave functions in our approach. Consequently, a relevant open problem is whether our approach for KP may be interpreted as a scalar analog of a field theoretic model. Finally another relevant open problem is the connection of our construction to that in [47] where the asymptotic behavior of the multiline KP soliton solutions in the (x,y)-plane for large time t are shown to give rise to soliton webs interpreted in terms of real tropical geometry [40] and cluster algebras [28]. In our approach the KP solution plays the role of a potential in the spectral problem and its asymptotic behavior should be put in relation to that of KP zero divisors on Γ.

Total positivity itself, since its appearance in [66], naturally arises in many applications in connection with some reality properties of the system. In particular, important connections between positivity and oscillatory properties of mechanical systems were found in [30, 31]. The extension of the positivity property to integral kernels was investigated in [42]. Extension of total positivity to split reductive connected algebraic groups and flag manifolds was developped in [52, 53]. Total positivity in classical and generalized sense is also one of the basic concepts in the theory of cluster manifolds and cluster algebras [27, 28], see also the book [32]. Applications of the theory of total positivity in Lie groups to the study of homomorphisms of the fundamental group of a closed surface into a Lie group is considered in [26]. Non-negativity of systems of

modified Bessel functions of the first kind arising in the solutions to a model of overdamped Josephson junction was studied in [13, 14]. Of course, this list of literature is far from being complete.

Finally the positroid stratification of $Gr^{\mathrm{TNN}}(k,n)$ [62] is naturally related to the Gelfand-Serganova stratification of the complex Grassmannian $Gr(k,n)$ [33, 34]. As observed in [62], the real positivity condition essentially simplifies the problem, whereas the geometrical structure of the strata for complex Grassmannians can be as complicated as essentially any algebraic variety [55]. Let us point out that full Gelfand-Serganova stratification corresponds to the action of all complex KP flows on the Grassmannians. In particular, the factor-space of the Grassmannians by the action of compact tori corresponding to pure imaginary times has interesting topology studied in [15, 16].

Outline of the main construction. In this paper, to any given ordered n-set of real phases $\mathcal{K}$ and g-dimensional positroid cell in $\mathcal{S}^{\mathrm{TNN}}_{\mathcal{M}} \subset Gr^{\mathrm{TNN}}(k,n)$, we associate a canonical curve Γ which is a rational degeneration of a smooth M-curve of minimal genus g, and we parametrize these cells via real regular KP divisors on these curves. For any soliton data $(\mathcal{K},[A])$, $[A] \in \mathcal{S}^{\mathrm{TNN}}_{\mathcal{M}}$, the divisor can be made non-special by a proper choice of the normalization time $\vec{t}_0$. In our construction an essential tool is the parametrization of all positroid cells in $Gr^{\mathrm{TNN}}(k,n)$ by the Le–networks introduced in [62], which, in particular, guarantees both the non-specialty of the divisor and the minimality of the genus.

Indeed, given $\mathcal{K}$ and the planar trivalent bipartite Le–graph $\mathcal{G}$ in the disk representing $\mathcal{S}^{\mathrm{TNN}}_{\mathcal{M}}$, to such data we associate a unique reducible rational curve $\Gamma = \Gamma(\mathcal{G},\mathcal{K})$ using the following natural correspondence:

(1) The boundary of the disk corresponds to the rational component Γ_0 containing the essential singularity of the KP wave function and the Sato divisor, while the n boundary vertices correspond to the n marked phases κ_j on Γ_0;
(2) Each bivalent or trivalent internal vertex corresponds to a rational component of Γ. The black and white colors are related to the different analytic properties of the KP wave function on the corresponding rational components. The divisor points are associated to white trivalent vertices through linear relations;
(3) Each edge corresponds to a double point of Γ where different components are glued. Thanks to the trivalency assumption, each $\mathbb{CP}^1$ component carries three marked points

and we avoid the introduction of parameters marking double points, and the curve Γ is the same for all points in $\mathcal{S}_{\mathcal{M}}^{\mathrm{TNN}}$;

(4) Faces of the graph correspond to ovals of Γ;

(5) The canonical acyclic orientation of the Le–graph in [62] is associated to a well-defined choice of coordinates on the rational components of Γ.

We remark that the above correspondence is a minor modification of a special case in the representation of reducible curves by dual graphs (see, for example, [6], Section X). Non rational components are allowed in degenerate finite–gap theory on reducible curves as well; however, the rational ansatz for $\Gamma\backslash\Gamma_0$ considerably simplifies the overall construction.

By our construction, Γ is a real curve with $g+1$ ovals and is the rational degeneration of an M–curve of genus g. If the soliton data belong to the top cell $Gr^{\mathrm{TP}}(k,n)$, then $g=k(n-k)$ and the curve $\Gamma(\xi)$ constructed in [3] corresponds to a particular desingularization of $\Gamma(\mathcal{G})$ which reduces the number of rational components to $k+1$. We thouroughly discuss such desingularization in the simplest non–trivial case of soliton data in $Gr^{\mathrm{TP}}(2,4)$.

Then, we fix a point $[A]\in\mathcal{S}_{\mathcal{M}}^{\mathrm{TNN}}$ and extend its KP wave function from Γ_0 to Γ. We must control that at each pair of double points the values of the normalized KP wave function coincide for all times. In particular, this requirement has to be satisfied at the double points connecting components to Γ_0. Moreover, if we have linear relations between the values of the normalized KP wave function at the marked points of any given component, then its meromorphic extension to the whole curve is canonical. To define the wave function at all double points, we use the canonically oriented Le–network $\mathcal{N}$ representing $[A]$.

On $\mathcal{N}$ we first construct a system of **edge** vectors satisfying linear relations at the vertices. Each component of a given edge vector coincides, up to a sign, with the sum of the weights of all paths starting at the given edge and ending at the same boundary sink vertex. We remark that, for soliton data in $Gr^{\mathrm{TP}}(k,n)$, the recursive construction of such system of vectors generalizes the algebraic construction in [3].

We then use this system of vectors to construct both a vacuum edge wave function $\Phi(\vec{t})$ and its dressing $\Psi(\vec{t})$ on the Le–network. At this step, we modify the original network adding an univalent internal vertex next to each boundary source vertex using Postnikov move (M2) in order that the vacuum edge wave function satisfies Sato boundary conditions on Γ_0 and an edge vector corresponds to each Darboux point in Γ. Then, using the linear relations satisfied by the vacuum edge wave function at the vertices, we associate a canonical real number, which we

call vacuum network divisor number, to each trivalent white vertex of the modified network $\mathcal{N}'$. Similarly, using the same linear relations for the dressed edge wave function, we also associate another canonical real number, which we call dressed network divisor number, to any trivalent white vertex of $\mathcal{N}'$ not containing a Darboux edge.

Moreover, thanks to these linear relations, the normalized dressed wave function admits degree one meromorphic extension on each component corresponding to a trivalent white vertex of $\mathcal{N}$, and admits constant in the spectral parameter extension on each other component. The dressed network divisor numbers become the coordinates of the divisor points on the corresponding components. The full KP divisor is the sum of these points on $\Gamma\backslash\Gamma_0$ and the Sato divisor on Γ_0, it is effective, non-special and has degree g. Finally, we check that each finite oval of Γ contains exactly one divisor point.

We would like to remark that the divisors on networks introduced in our text are different from the commonly used divisors on graphs, see for example, [10]. To each trivalent white vertex we associate not only the multiplicity of divisor (it is always 1 in our setting), but also its position on the real part of the corresponding rational component, which is a real number.

Plan of the paper: We did our best to make the paper self–contained. In Section 2 and in Appendix A, we briefly present a review of the necessary results respectively for KP soliton theory and totally non–negative Grassmannians. In Section 3 we outline the main construction and state the principal theorems. In Section 4, we link the main algebraic construction in [3] to the Le–networks and extend it to any positroid cell. The construction of the system of edge vectors on the Le–networkn and the proof of the main Theorem on the characterization of the vacuum divisor is carried out in Section 5. In section 6 we apply our construction to soliton data in $Gr^{\mathrm{TP}}(2,4)$ and compare it with [3].

Notations: We use the following notations throughout the paper:

(1) k and n are positive integers such that $k < n$;
(2) for $s \in \mathbb{N}$ let $[s] = \{1, 2, \dots, s\}$; if $s, j \in \mathbb{N}$, $s < j$, then $[s, j] = \{s, s+1, s+2, \dots, j-1, j\}$;
(3) $\vec{t} = (t_1, t_2, t_3, \dots)$, where $t_1 = x$, $t_2 = y$, $t_3 = t$. Throughout the paper we assume that $\vec{t}$ always has only a finite number of non-zero components, but this number can be arbitrarily large;
(4) $\theta(\zeta, \vec{t}) = \sum_{s=1}^{\infty} \zeta^s t_s$,
(5) we denote the real phases $\kappa_1 < \kappa_2 < \dots < \kappa_n$ and $\theta_j \equiv \theta(\kappa_j, \vec{t})$.

2. KP–II multi-line solitons

In this section, we review the characterization of real bounded regular multiline KP soliton solutions via Darboux transformations, Sato's dressing transformations and finite gap–theory. The KP-II equation [41]

$$(-4u_t + 6uu_x + u_{xxx})_x + 3u_{yy} = 0, \tag{2.1}$$

is the first non–trivial flow of an integrable hierarchy [19, 24, 39, 58, 65]. In the following we denote $\vec{t} = (t_1 = x, t_2 = y, t_3 = t, t_4, \dots)$. The family of solutions we consider belong to the class of real regular exact KP solutions used, in particular, to model the shallow water waves in the approximation where the surface tension is negligible.

2.1. **The heat hierarchy and the dressing transformation.** Multiline KP solitons may be realized starting from the soliton data $(\mathcal{K}, [A])$, where $\mathcal{K}$ is a set of real ordered phases $\kappa_1 < \cdots < \kappa_n$, $A = (A^i_j)$ is a $k \times n$ real matrix of rank k and $[A]$ denotes the point in the finite dimensional real Grassmannian $Gr(k, n)$ corresponding to A. Following [57], see also [29], multiline KP soliton solutions to the KP equation are defined as

$$u(\vec{t}) = 2\partial_x^2 \log(\tau(\vec{t})), \tag{2.2}$$

where

(2.3)

$$\tau(\vec{t}) = Wr(f^{(1)}, \dots, f^{(k)}) \equiv \det \begin{vmatrix} f^{(1)} & \dots & f^{(k)} \\ \partial_x f^{(1)} & \dots & \partial_x f^{(k)} \\ \vdots & \ddots & \vdots \\ \partial_x^{n-1} f^{(1)} & \dots & \partial_x^{n-1} f^{(k)} \end{vmatrix} = \sum_I \Delta_I(A) \prod_{\substack{i_1 < i_2 \\ i_1, i_2 \in I}} (\kappa_{i_2} - \kappa_{i_1}) e^{\sum_{i \in I} \theta_i}$$

is the Wronskian of k linear independent solutions to the heat hierarchy $\partial_{t_l} f = \partial_x^l f$, $l = 2, 3, \dots$, of the form $f^{(i)}(\vec{t}) = \sum_{j=1}^n A^i_j e^{\theta_j}$, $i \in [k]$. In (2.3), the sum is over all k–element ordered subsets I in $[n]$, *i.e.* $I = \{1 \le i_1 < i_2 < \cdots < i_k \le n\}$ and $\Delta_I(A)$ are the maximal minors of the matrix A. Since we obtain the same KP solution by linearly recombining the heat hierarchy solutions, $u(\vec{t})$ is associated to the equivalence class $[A]$ of A, which is a point in the Grassmannian $Gr(k, n)$.

$u(x, y, t, \vec{0})$ is regular and bounded for all real x, y, t if and only if $\Delta_I(A) \ge 0$, for all I [47]. In such case, let $Mat^{\mathrm{TNN}}_{k,n}$ and GL^+_k, respectively denote the set of real $k \times n$ matrices of maximal rank k with non–negative maximal minors $\Delta_I(A)$, and the group of $k \times k$ matrices with positive determinants. Since left multiplication by elements in GL^+_k preserves $u(\vec{t})$ in (2.2),

we conclude that the soliton data $[A]$ is a point in the totally non–negative Grassmannian [62] $Gr^{\mathrm{TNN}}(k,n) = GL_k^+ \backslash Mat_{k,n}^{\mathrm{TNN}}$.

Any given soliton solution is associated to an infinite set of soliton data $(\mathcal{K}, [A])$, but there exists a unique minimal pair (k,n), such that the soliton solution can be realized with n phases $\kappa_1 < \cdots < \kappa_n$ and $[A] \in Gr^{\mathrm{TNN}}(k,n)$, but not with $n-1$ phases and $[A'] \in Gr^{\mathrm{TNN}}(k',n')$, where (k',n') is either $(k,n-1)$ or $(k-1,n-1)$.

Definition 2.1. Regular and irreducible soliton data [17]. *We call $(\mathcal{K}, [A])$ regular soliton data if $\mathcal{K} = \{\kappa_1 < \cdots < \kappa_n\}$ and $[A] \in Gr^{TNN}(k,n)$. We call the regular soliton data $(\mathcal{K}, [A])$ irreducible if $[A]$ is a point in the irreducible part of the real Grassmannian, i.e. if the reduced row echelon matrix A has the following properties:*

(1) Each column of A contains at least a non–zero element;

(2) Each row of A contains at least one nonzero element in addition to the pivot.

If either (1) or (2) doesn't occur, we call the soliton data $(\mathcal{K}, [A])$ reducible.

Remark 2.1. ***Reducible soliton data*** [17]. *If (1) in Definition 2.1 is violated for column l, then the phase κ_l does not appear in the solution (2.2). Then, one may remove such phase from $\mathcal{K}$, remove the zero column from A (see also Remark A.2) and realize the soliton in $Gr^{TNN}(k,n-1)$.*

If (2) in Definition 2.1 is violated for the row l corresponding to the pivot index i_l, then the heat hierarchy solution $f^{(l)}(\vec{t})$ contains only the phase κ_{i_l}, and such phase is missing in all other heat hierarchy solutions associated to RREF (reduced row echelon form) matrix. $f^{(l)}(\vec{t})$ is factored out in (2.3), and again, κ_{i_l} is missing in (2.2). So one may eliminate such phase from $\mathcal{K}$, remove the corresponding row and pivot column from A, change all signs in the new matrix to the right of the removed column and above the removed row and realize the soliton in $Gr^{TNN}(k-1,n-1)$ (see also Remark A.2).

For generic choices of the phases $\mathcal{K}$, the combinatorial classification of the irreducible part $Gr^{\mathrm{TNN}}(k,n)$ rules the classification of the asymptotic properties of multi–soliton solutions both in the (x,y) plane at fixed time t and in the tropical limit $(t \to \pm\infty)$ (see [11, 12, 17, 18, 20, 44, 45, 46, 47, 72] and references therein).

The following spectral data are associated to each soliton data $(\mathcal{K}, [A])$, $[A] \in Gr^{\mathrm{TNN}}(k,n)$: an irreducible rational curve, which we denote Γ_0, a marked point $P_0 \in \Gamma_0$, a degree k real divisor, which we call Sato divisor, and a KP wave function meromorphic on $\Gamma_0 \backslash \{P_0\}$, which we call the Sato KP wave function. The unnormalized Sato wave function can be obtained from

the dressing (inverse gauge) transformation [65] of the vacuum (zero–potential) eigenfunction $\phi^{(0)}(\zeta,\vec{t}) = \exp(\theta(\zeta,\vec{t}))$, which solves

$$\partial_x\phi^{(0)}(\zeta,\vec{t}) = \zeta\phi^{(0)}(\zeta,\vec{t}), \qquad \partial_{t_l}\phi^{(0)}(\zeta,\vec{t}) = \zeta^l\phi^{(0)}(\zeta,\vec{t}), \quad l \geq 2. \tag{2.4}$$

The operator $W = 1 - \mathfrak{w}_1(\vec{t})\partial_x^{-1} - \cdots - \mathfrak{w}_k(\vec{t})\partial_x^{-k}$, where $\mathfrak{w}_1(\vec{t}),\ldots,\mathfrak{w}_k(\vec{t})$ are the solutions to the following linear system of equations $\partial_x^k f^{(i)} = \mathfrak{w}_1\partial_x^{k-1}f^{(i)} + \cdots + \mathfrak{w}_k f^{(i)}$,$i \in [k]$, is the dressing (*i.e.* gauge) operator for the soliton data $(\mathcal{K},[A])$. Indeed W satisfies Sato equations $\partial_{t_l}W = B_lW - W\partial_x^l$, $l \geq 1$, with $B_l = (W\partial_x^l W^{-1})_+$ (the symbol $(H)_+$ denotes the differential part of the operator H). Therefore $L = W\partial_x W^{-1} = \partial_x + \frac{u(\vec{t})}{2}\partial_x^{-1} + \cdots$, $u(\vec{t}) = 2\partial_x\mathfrak{w}_1(\vec{t})$ and $\psi^{(0)}(\zeta;\vec{t}) = W\phi^{(0)}(\zeta;\vec{t})$ are, respectively, the KP-Lax operator, the KP–potential (KP solution) and the KP-eigenfunction, *i.e.* $L\psi^{(0)}(\zeta;\vec{t}) = \zeta\psi^{(0)}(\zeta;\vec{t})$, $\partial_{t_l}\psi^{(0)}(\zeta;\vec{t}) = B_l\psi^{(0)}(\zeta;\vec{t})$, forall $l \geq 2$.

The Darboux dressing operator $\mathfrak{D}$ is defined as

$$\mathfrak{D} \equiv W\partial_x^k = \partial_x^k - \mathfrak{w}_1(\vec{t})\partial_x^{k-1} - \cdots - \mathfrak{w}_k(\vec{t}) \tag{2.5}$$

and the KP-eigenfunction may be also represented by

$$\mathfrak{D}\phi^{(0)}(\zeta;\vec{t}) = W\partial_x^k\phi^{(0)}(\zeta;\vec{t}) = \left(\zeta^k - \mathfrak{w}_1(\vec{t})\zeta^{k-1} - \cdots - \mathfrak{w}_k(\vec{t})\right)\phi^{(0)}(\zeta;\vec{t}) = \zeta^k\psi^{(0)}(\zeta;\vec{t}). \tag{2.6}$$

Definition 2.2. Sato divisor *Let the regular soliton data be $(\mathcal{K},[A])$, $\mathcal{K} = \{\kappa_1 < \cdots < \kappa_n\}$, $[A] \in Gr^{TNN}(k,n)$. We call Sato divisor at time $\vec{t}_0$, $\mathcal{D}_{\mathrm{S},\Gamma_0}(\vec{t}_0)$, the set of the roots of the characteristic equation associated to the Dressing transformation*

$$\mathcal{D}_{\mathrm{S},\Gamma_0}(\vec{t}_0) = \{\gamma_j^{(\mathrm{S})}(\vec{t}_0),\ j \in [k] :\ (\gamma_j^{(\mathrm{S})}(\vec{t}_0))^k - \mathfrak{w}_1(\vec{t})(\gamma_j^{(\mathrm{S})}(\vec{t}_0))^{k-1} - \cdots - \mathfrak{w}_k(\vec{t}_0) = 0\,\}. \tag{2.7}$$

In [54] it is proven the following proposition

Proposition 2.1. ***The Sato divisor*** [54]. *Let the regular soliton data be $(\mathcal{K},[A])$, $\mathcal{K} = \{\kappa_1 < \cdots < \kappa_n\}$, $[A] \in Gr^{TNN}(k,n)$. Then for all real $\vec{t}_0$ the Sato divisor $\mathcal{D}_{\mathrm{S},\Gamma_0}(\vec{t}_0)$ is real and satisfies $\gamma_j^{(\mathrm{S})}(\vec{t}) \in [\kappa_1,\kappa_n]$, $j \in [k]$. Moreover for almost all $\vec{t}_0$ the Sato divisor points are distinct.*

Remark 2.2. Sato divisor for reducible regular soliton data *In the case of reducible regular soliton data $(\mathcal{K},[A])$, $\mathcal{K} = \{\kappa_1 < \cdots < \kappa_n\}$, $[A] \in Gr^{TNN}(k,n)$ (see Remark 2.1), we use the reduced Sato divisor $\mathcal{D}'_{\mathrm{S},\Gamma_0}(\vec{t}_0)$ of the corresponding maximally reduced positroid cell $Gr^{TNN}(k',n')$.*

More precisely, if the representative RREF matrix A in $Gr^{TNN}(k,n)$, contains a zero column in position l, then $k' = k$ and $\mathcal{D}_{\mathrm{S},\Gamma_0}(\vec{t}_0) = \mathcal{D}'_{\mathrm{S},\Gamma_0}(\vec{t}_0)$ for any $\vec{t}_0$, since the reducible and the reduced Darboux transformations coincide $\mathfrak{D}^{(k)} = \mathfrak{D}^{(k')}$.

Instead, if for some $r \in [k]$ and $i_r \in [r,n]$, the r–th row of the RREF matrix A contains only the pivot element: $A^r_j = \delta_{j,i_r}$, then, for all $\vec{t}_0$, $\kappa_{i_r} \in \mathcal{D}_{\mathrm{S},\Gamma_0}(\vec{t}_0)$, $k' = k-1$ and $\mathcal{D}'_{\mathrm{S},\Gamma_0}(\vec{t}_0) = \mathcal{D}_{\mathrm{S},\Gamma_0}(\vec{t}_0)\backslash\{\kappa_{i_r}\}$. Indeed, the characteristic polynomial associated to the Darboux differential operator $\mathfrak{D}$ satisfies $\zeta^k - \zeta^{k-1}\mathfrak{w}_1(\vec{t}) - \cdots - \mathfrak{w}_k(\vec{t}) = (\zeta - \kappa_{i_r})\left(\zeta^{k-1} - \mathfrak{w}'_1(\vec{t})\zeta^{k-2} - \cdots - \mathfrak{w}'_{k-1}(\vec{t})\right)$. Then $\mathfrak{D}' = W'\partial_x^{k-1} = \partial_x^{k-1} - \mathfrak{w}'_1(\vec{t})\partial_x^{k-2} - \cdots - \mathfrak{w}'_{k-1}(\vec{t})$ is the Darboux transformation associated to the reduced soliton data $(\mathcal{K}', [A'])$, with $\mathcal{K}' = \mathcal{K}\backslash\{\kappa_{i_r}\}$, $[A'] \in Gr^{TNN}(k-1, n-1)$ and A' related to A as in Remark 2.1.

Definition 2.3. ***Sato algebraic–geometric data*** *Let $(\mathcal{K}, [A])$ be given regular soliton data with $[A]$ belonging to a d dimensional positroid cell in $Gr^{TNN}(k,n)$. Let $\vec{t}_0$ such that the Sato divisor consists of k simple poles. Let Γ_0 be a copy of $\mathbb{CP}^1$ with marked points P_0, local coordinate ζ such that $\zeta^{-1}(P_0) = 0$ and $\zeta(\kappa_1) < \zeta(\kappa_2) < \cdots < \zeta(\kappa_n)$.*

Then to the data $(\mathcal{K}, [A], \Gamma_0\backslash\{P_0\}, \vec{t}_0)$ we associate the Sato divisor $\mathcal{D}_{\mathrm{S},\Gamma_0} = \mathcal{D}_{\mathrm{S},\Gamma_0}(\vec{t}_0)$ as in Definition (2.2) and the normalized Sato wave function

$$\hat{\psi}(P,\vec{t}) = \frac{\mathfrak{D}\phi^{(0)}(P;\vec{t})}{\mathfrak{D}\phi^{(0)}(P;\vec{t}_0)} = \frac{\psi^{(0)}(P;\vec{t})}{\psi^{(0)}(P;\vec{t}_0)}, \qquad \forall P \in \Gamma_0\backslash\{P_0\}, \tag{2.8}$$

with $\mathfrak{D}\phi^{(0)}(\zeta;\vec{t})$ as in (2.6).

By definition $(\hat{\psi}_0(P,\vec{t})) + \mathcal{D}_{\mathrm{S},\Gamma_0}(\vec{t}_0) \geq 0$, for all $\vec{t}$.

Remark 2.3. ***Incompleteness of Sato algebraic–geometric data*** *Let $1 \leq k < n$ and let $\vec{t}_0$ be fixed. Given the phases $\kappa_1 < \cdots < \kappa_n$ and the spectral data $(\Gamma_0\backslash\{P_0\}, \mathcal{D}_{\mathrm{S},\Gamma_0})$, where $\mathcal{D}_{\mathrm{S},\Gamma_0} = \mathcal{D}_{\mathrm{S},\Gamma_0}(\vec{t}_0)$ is a k point divisor satisfying Proposition 2.1, it is, in general, impossible to identify uniquely the point $[A] \in Gr^{TNN}(k,n)$ corresponding to such spectral data. Indeed, if we assume that the soliton data belong to an irreducible positroid cell of dimension d, then $\max\{k, n-k\} \leq d \leq k(n-k)$. Otherwise, an analogous inequality holds for the reduced Sato divisor.*

2.2. **Finite-gap KP solutions and their multi-line soliton limits.** Soliton KP solutions can be obtained from the finite-gap ones by proper degenerations of the spectral curve [49, 24].

The spectral data for periodic and quasiperiodic solutions of the KP equation (2.1) in the finite-gap approach [48, 49] are: a finite genus g compact Riemann surface Γ with a marked point P_0, a local parameter $1/\zeta$ near P_0 and a non-special divisor $\mathcal{D} = \gamma_1 + \ldots + \gamma_g$ of degree g in Γ. The Baker-Akhiezer function $\hat{\psi}(P,\vec{t})$, $P \in \Gamma$, is defined by the following analytic properties:

(1) For any fixed $\vec{t}$ the function $\hat{\psi}(P,\vec{t})$ is meromorphic in P on $\Gamma\backslash P_0$.

(2) On $\Gamma\backslash P_0$ the function $\hat{\psi}(P,\vec{t})$ is regular outside the divisor points γ_j and has at most first order poles at the divisor points. Equivalently, if we consider the line bundle $\mathcal{L}(\mathcal{D})$ associated to $\mathcal{D}$, then for each fixed $\vec{t}$ the function $\hat{\psi}(P,\vec{t})$ is a holomorphic section of $\mathcal{L}(\mathcal{D})$ outside P_0.

(3) $\hat{\psi}(P,\vec{t})$ has an essential singularity at the point P_0 with the following asymptotic:

$$\hat{\psi}(\zeta,\vec{t}) = e^{\zeta x+\zeta^2 y+\zeta^3 t+\cdots}\left(1-\chi_1(\vec{t})\zeta^{-1}-\cdots-\chi_k(\vec{t})\zeta^{-k}-\cdots\right).$$

For generic data these properties define an unique function, which is a common eigenfunction to all KP hierarchy auxiliary linear operators $-\partial_{t_j}+B_j$, where $B_j=(L^j)_+$, and the Lax operator is $L=\partial_x+\frac{u(\vec{t})}{2}\partial_x^{-1}+u_2(\vec{t})\partial_x^{-2}+\ldots$. All these operators commute and the potential $u(\vec{t})$ satisfies the KP hierarchy. In particular, the KP equation arises in the Dryuma-Zakharov-Shabat commutation representation [21], [71] as the compatibility for the second and the third operator: $[-\partial_y+B_2,-\partial_t+B_3]=0$, with $B_2\equiv(L^2)_+=\partial_x^2+u$, $B_3=(L^3)_+=\partial_x^3+\frac{3}{4}(u\partial_x+\partial_x u)+\tilde{u}$ and $\partial_x\tilde{u}=\frac{3}{4}\partial_y u$.

The Its-Matveev formula represents the KP hierarchy solution $u(\vec{t})$ in terms of the Riemann theta-functions associated with Γ (see, for example, [22]). After fixing a canonical basis of cycles $a_1,\ldots,a_g,b_1,\ldots,b_g$ and a basis of normalized holomorphic differentials $\omega_1,\ldots,\omega_g$ on Γ such that $\oint_{a_j}\omega_l=2\pi i\delta_{jl}$, $\oint_{b_j}\omega_l=B_{lj}$, $j,l\in[g]$, the KP solution takes the form $u(\vec{t})=2\partial_x^2\log\theta(\sum_j t_jU^{(j)}+z_0)+c_1$, where θ is the Riemann theta function and $U^{(j)}$ are the vectors of the b–periods of the following normalized meromorphic differentials, holomorphic on $\Gamma\backslash\{P_0\}$ and with principal parts $\hat{\omega}^{(j)}=d(\zeta^j)+O(1)$, at P_0 (see [48, 25]).

The real regular solutions are the most relevant in physical applications. In [25] the necessary and sufficient conditions on spectral data to generate real regular KP hierarchy solutions for all real $\vec{t}$ were established, under the assumption that Γ is smooth and has genus g:

(1) Γ possesses an antiholomorphic involution $\sigma:\Gamma\to\Gamma$, $\sigma^2=\mathrm{id}$, which has the maximal possible number of fixed components (real ovals). This number is equal to $g+1$, therefore (Γ,σ) is an M-curve.

(2) P_0 lies in one of the ovals, and each other oval contains exactly one divisor points. The oval containing P_0 is called "infinite" and all other ovals are called "finite".

The set of real ovals divides Γ into two connected components. Each of these components is homeomorphic to a sphere with $g+1$ holes. In Figure 1(left) we show an example for $g=2$.

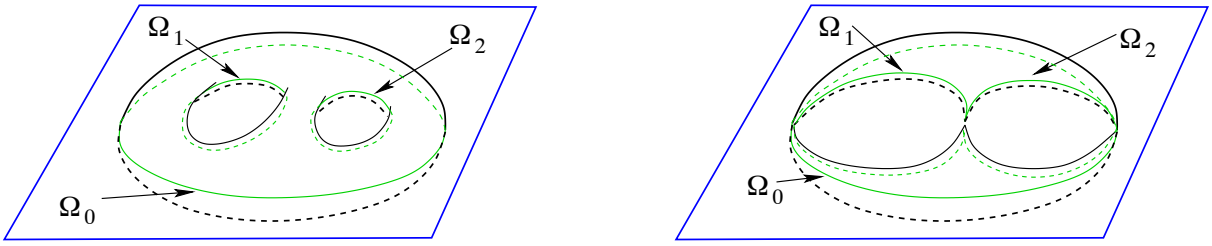

FIGURE 1. *Left: a genus 2 regular* M*-curve with 3 real ovals invariant w.r.t. the involution σ (orthogonal reflection with respect to the horizontal plane). Right: its degeneration is a reducible* M*-curve still possessing 3 real ovals.*

The sufficient condition of the Theorem in [25] still holds true if the spectral curve Γ degenerates in such a way that the divisor remains in the finite ovals at a finite distance from the essential singularity [25]. Of course, this condition is not necessary for degenerate curves, but the properties of the Sato divisor established in [54] are compatible with such an ansatz. Moreover, in [50], it has been proven that the algebraic–geometric approach goes through also for degenerate finite–gap solutions on **reducible** curves. Such inverse spectral problem is ill–posed, since there is not a unique reducible curve associated to the given soliton data. Finally there is also no a priori reason why, given one such reducible curve, the divisor on it should satisfy any reality condition.

In [3], we have proven that the multiline soliton solutions corresponding to points in $Gr^{\mathrm{TP}}(k,n)$ may indeed be obtained as limits of real regular finite-gap solutions on smooth M–curves: to any soliton datum in $Gr^{\mathrm{TP}}(k,n)$ and any $\xi \gg 1$, we have associated a curve Γ_ξ, which is the rational degeneration of a smooth M–curve of minimal genus $k(n-k)$ and a degree $k(n-k)$ divisor satisfying the reality conditions of Dubrovin and Natanzon's theorem. In Figure 1(right) we show the rational degeneration of the genus $g=2$ curve associated to soliton data in $Gr^{\mathrm{TP}}(1,3)$ and $Gr^{\mathrm{TP}}(2,3)$ in [1, 3].

The main objective of this paper is therefore twofold: **provide a canonical construction of a reducible rational M–curve of minimal genus $g=d$ for any fixed positroid cell in $Gr^{\mathbf{TNN}}(k,n)$ and show that real and regular divisors on such curve provide a parametrization of the cell**. We therefore give the following definition:

Definition 2.4. ***Real regular algebraic-geometrical data associated with a given soliton solution.*** *Assume that we have fixed soliton data $(\mathcal{K},[A])$, where $\mathcal{K}$ is a collection of real phases*

$\kappa_1 < \kappa_2 < \ldots < \kappa_n$, $[A] \in Gr^{TNN}(k,n)$. Let d be the dimension of the positroid cell to which $[A]$ belongs.

Assume that we have a reducible connected curve Γ with a marked point P_0, a local parameter $1/\zeta$ near P_0. In addition, assume that the curve Γ may be obtained from a rational degeneration of a smooth M*-curve of genus g, with $g \geq d$, and that the antiholomorphic involution preserves the maximum number of the ovals in the limit, so that Γ possesses $g+1$ real ovals.*

Assume that $\mathcal{D}$ is a degree g non-special divisor on $\Gamma \backslash P_0$, and that $\hat{\psi}$ is the normalized Baker-Ahkiezer function associated to such data, i.e. for any $\vec{t}$ its pole divisor is contained in $\mathcal{D}$: $(\hat{\psi}(P,\vec{t})) + \mathcal{D} \geq 0$ on $\Gamma \backslash P_0$, where (f) denotes the divisor of f.

We say that ***the algebraic-geometrical data Γ, $\mathcal{D}$ are associated to the soliton data*** *$(\mathcal{K}, [A])$,* ***if*** *the irreducible component Γ_0 of Γ containing P_0 is $\mathbb{CP}^1$, and the restriction of $\hat{\psi}$ to Γ_0 coincides with Sato normalized dressed wave function for the soliton data $(\mathcal{K}, [A])$. In particular, for such data the restriction of $\mathcal{D}$ to Γ_0 coincides with the Sato divisor.*

We say that the ***divisor $\mathcal{D}$ satisfies the reality and regularity conditions*** *if P_0 belongs to one of the fixed ovals and the boundary of each other finite oval contains exactly one divisor point.*

We remark that the simplicity and reality of the Sato divisor points proven in [54] is compatible with the reality and regularity of the algebraic-geometrical data associated with a given soliton solution in the Definition above, provided that the reducible curve Γ possesses k distinct ovals containing the Sato divisor points.

3. Algebraic-geometric approach for KP soliton data in $Gr^{\mathrm{TNN}}(k,n)$: the main construction

Since $Gr^{\mathrm{TNN}}(k,n)$ is topologically the closure of $Gr^{\mathrm{TP}}(k,n)$, one can try to extend **indirectly** the construction of [3] to soliton data in $Gr^{\mathrm{TNN}}(k,n)$ considering the latter as the limit of a sequence of soliton data in $Gr^{\mathrm{TP}}(k,n)$. But this limiting procedure is very non-trivial, and it provides only an upper bound for the genus: $g \leq k(n-k)$.

In the following we present a **direct** construction of algebraic geometric data associated to points in $Gr^{\mathrm{TNN}}(k,n)$ which is naturally related to the characterization of positroid cells in [62] and provides optimal genus spectral curves. Moreover, the present construction unveils the relation of the algebraic construction in [3] with Le-networks in $Gr^{\mathrm{TP}}(k,n)$. The starting point are the algebraic geometric data associated to $(\mathcal{K}, [A])$ via Sato dressing (see Definition 2.3):

(1) A rational curve Γ_0 equipped with a finite number of marked points: the ordered real phases $\kappa_1 < \cdots < \kappa_n$, and the essential singularity P_0 of the wave function;
(2) The Sato divisor $\mathcal{D}_{\mathrm{S},\Gamma_0}(\vec{t}_0)$ for the soliton data defined in Definition 2.2;
(3) The normalized wave function $\hat{\psi}(P,\vec{t})$ on $\Gamma_0\backslash\{P_0\}$ defined in (2.8).

As pointed out in Section 2.1, in general, the Sato divisor does not parametrize the whole positroid cell to which $[A]$ belongs to. Therefore, in general, we cannot reconstruct the soliton data $[A]$ just from the Sato divisor at $\vec{t}_0$.

Below, to any regular soliton data $(\mathcal{K},[A])$, we associate a well–defined curve Γ containing Γ_0 as a connected component, and a unique KP divisor on it using the Le–network $\mathcal{N}$ representing $[A]$. In particular, we show that Γ is reducible and a rational degeneration of a M-curve having the minimal possible genus, $g = d = \dim \mathcal{S}^{\mathrm{TNN}}_{\mathcal{M}}$, under genericity assumption on the soliton data. Finally, the set of poles of $\hat{\psi}$ exactly coincides with $\mathcal{D}_{\mathrm{KP},\Gamma}$ for generic $\vec{t}$.

Main construction *Assume we are given a real regular bounded multiline KP soliton solution generated by the following soliton data:*

(1) A set of n real ordered phases $\mathcal{K} = \{\kappa_1 < \kappa_2 < \cdots < \kappa_n\}$;
(2) A point $[A] \in \mathcal{S}^{TNN}_{\mathcal{M}} \subset Gr^{TNN}(k,n)$, where $\mathcal{S}^{TNN}_{\mathcal{M}}$ is a positroid stratum of dimension d.

We represent $[A]$ with its canonically oriented bipartite trivalent Le–network $\mathcal{N}$. We recall that $\mathcal{N}$ provides a representation of the points of the cell depending exactly by d parameters. Let us also denote $\mathcal{G}$ the Le–graph representing $\mathcal{S}^{TNN}_{\mathcal{M}}$. Then, we associate the following algebraic-geometric objects to the soliton data $(\mathcal{K},[A])$:

(1) A reducible M–curve $\Gamma = \Gamma(\mathcal{G})$ with $g+1$ ovals which is the rational degeneration of a smooth M–curve of genus $g = d$. In our approach, Γ_0 is one of the irreducible components of Γ. The marked point P_0 belongs to the intersection of Γ_0 with an oval (infinite oval);
(2) An unique real and regular degree g non–special KP divisor $\mathcal{D}_{\mathrm{KP},\Gamma} = \mathcal{D}_{\mathrm{KP},\Gamma}(\mathcal{K},[A]) \subset \Gamma\backslash\{P_0\}$ such that any finite oval contains exactly one divisor point and $\mathcal{D}_{\mathrm{KP},\Gamma} \cap \Gamma_0$ coincides with Sato divisor $\mathcal{D}_{\mathrm{S},\Gamma_0}(\vec{t}_0)$ for some initial time $\vec{t}_0$;
(3) An unique KP wave–function $\hat{\psi}(P,\vec{t})$ on $\Gamma\backslash\{P_0\}$ as in Definition 2.4 such that
  (a) Its restriction to $\Gamma_0\backslash\{P_0\}$ coincides with the normalized Sato wave function (2.6);
  (b) Its pole divisor has degree $\mathfrak{d} \leq g$ and is contained in $\mathcal{D}_{\mathrm{KP},\Gamma}$.

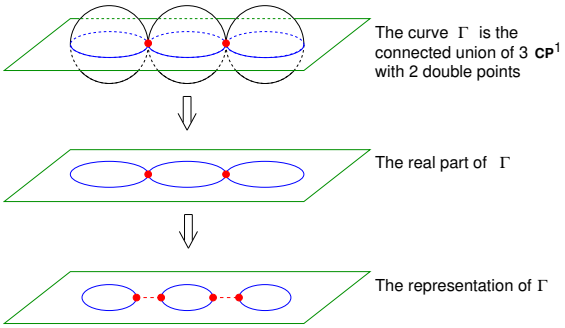

FIGURE 2. *The model of a reducible rational curve* Γ *with three components and one oval.*

Remark 3.1. *Here and in the following, when we refer to the Sato divisor for reducible real and regular soliton data, we mean the reduced Sato divisor defined in Remark 2.2. In particular, the KP divisor* $\mathcal{D}_{\mathrm{KP},\Gamma}$ *restricted to* Γ_0 *is the reduced Sato divisor.*

Remark 3.2. *In* [4] *we extend the main construction using any oriented bipartite trivalent network in the disk representing* $[A]$ *in Postnikov equivalence class* [62].

3.1. **The reducible rational curve** Γ**.** Given the oriented graph $\mathcal{G}$ representing a given positroid cell $\mathcal{S}_{\mathcal{M}}^{\mathrm{TNN}} \subset Gr^{\mathrm{TNN}}(k,n)$, the curve $\Gamma = \Gamma(\mathcal{G})$ is obtained gluing a finite number of copies of $\mathbb{CP}^1$, corresponding to the internal vertices in $\mathcal{G}$, and one copy of $\mathbb{CP}^1 = \Gamma_0$, corresponding to the boundary of the disk. We glue these components at pairs of points corresponding to its edges. We also fix a local affine coordinate ζ on each component (see Definition 3.1), therefore we have complex conjugation $\zeta \to \bar{\zeta}$ at each component. The points with real ζ form the real part of the given component. By construction (see Definition 3.1), the coordinates at each pair of glued points P, Q, are real. We then topologically represent the real part of Γ as a union of circles (ovals), where the latter correspond to the faces of $\mathcal{G}$.

We use the same representation for real rational curves as in [3] (see Fig. 2). We draw only the real part of each component and we represent it with a circle. Then we schematically represent the real part of Γ by drawing these circles separately and connecting the glued points by dashed lines. The planarity of the Le–graph implies that Γ is a reducible rational M–curve.

Construction 3.1. ***The curve*** $\Gamma = \Gamma(\mathcal{G})$**.** *Let* $\mathcal{K} = \{\kappa_1 < \cdots < \kappa_n\}$ *and let* $\mathcal{S}_{\mathcal{M}}^{TNN} \subset Gr^{TNN}(k,n)$ *be the positroid cell corresponding to the realizable matroid* $\mathcal{M}$*. Let* $\mathcal{G}$ *be the planar connected acyclically oriented trivalent bipartite Le–graph in the disk of Definition A.4 representing* $\mathcal{S}_{\mathcal{M}}^{TNN}$*. Let* $I = \{1 \le i_1 < \cdots < i_k \le n\}$ *be the set of the pivot indexes (i.e the lexicographically*

minimal base of $\mathcal{M}$) and, for any $r \in [k]$, let N_r be the number of filled boxes in the r-th row of the corresponding Le–diagram (see (A.3) in Appendix A). Finally, let $1 \leq j_1 < j_2 < \cdots < j_{N_r} \leq n$ be the non–pivot indexes of the boxes B_{i_r,j_s} in the Le–diagram with index $\chi^{i_r}_{j_s} = 1$, $s \in [N_r]$, where notations are consistent with (A.3) and (A.4) in Appendix A.

TABLE 1. The correspondence between the Le–graph $\mathcal{G}$ and the reducible rational curve Γ

$\mathcal{G}$	Γ
Boundary of disk	*Copy of* $\mathbb{CP}^1$ *denoted* Γ_0
Boundary vertex b_l	*Marked point* κ_l *on* Γ_0
Internal black vertex V'_{ij}	*Copy of* $\mathbb{CP}^1$ *denoted* Σ_{ij}
Internal white vertex V_{ij}	*Copy of* $\mathbb{CP}^1$ *denoted* Γ_{ij}
Edge	*Double point*
Face	*Oval*

The curve $\Gamma = \Gamma(\mathcal{G})$ is associated to $\mathcal{G}$ according to Table 1, after reflecting the graph w.r.t. a line orthogonal to the one containing the boundary vertices (we reflect the graph to have the natural increasing order of the phases on $\Gamma_0 \subset \Gamma$). More precisely, Γ is the connected union of $2n + k + 1$ copies of $\mathbb{CP}^1$ denoted as Γ_0, $\Sigma_{i_r j_s}$, $\Gamma_{i_r j_s}$, Γ_{i_r}, for $r \in [k]$, $s \in [N_r]$

$$\Gamma = \Gamma_0 \bigsqcup_{r=1}^{k} \left(\Gamma_{i_r} \sqcup \left(\bigsqcup_{s=1}^{N_r} \Gamma_{i_r j_s} \sqcup \Sigma_{i_r j_s} \right) \right)$$

according to the following rules (see also Figures 3 and 4):

(1) Γ_0 is the copy of $\mathbb{CP}^1$ corresponding to the boundary of the disk. It has $n + 1$ marked points: P_0 such that $\zeta^{-1}(P_0) = 0$ and the points $\kappa_1 < \cdots < \kappa_n$ corresponding to the boundary vertices $b_1, \ldots, b_n$ on $\mathcal{G}$;

(2) A copy of $\mathbb{CP}^1$ corresponds to any internal vertex of $\mathcal{G}$. For any fixed $r \in [k]$ and $s \in [N_r]$ we denote $\Gamma_{i_r j_s}$ (resp. $\Sigma_{i_r j_s}$) the copy of $\mathbb{CP}^1$ corresponding to the white vertex $V_{i_r j_s}$ (resp. black vertex $V'_{i_r j_s}$);

(3) We denote Γ_{i_r} the copy of $\mathbb{CP}^1$ corresponding to the internal white vertex V_{i_r} joined by an edge to the source b_{i_r}, $r \in [k]$;

(4) On each copy of $\mathbb{CP}^1$ corresponding to an internal vertex V, we mark as many points as edges at V. We number the edges at V anticlockwise in increasing order, so that, on

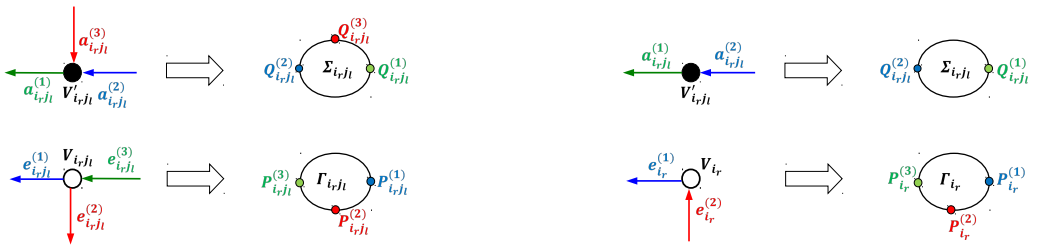

FIGURE 3. *The correspondence between marked points on copies $\Gamma_{i_r j_l}$ and $\Sigma_{i_r j_l}$ and edges of white and black vertices. The rule at the marked points corresponding to the edges of a bivalent white vertex at a boundary source b_{i_r} is justified by the necessity of adding a third marked point (Darboux point) on Γ_{i_r}.*

the corresponding copy of $\mathbb{CP}^1$, the marked points are numbered clockwise because of the mirror rule (see Figure 3). We use the following numbering rule:

- *(a) The unique horizontal edge pointing inward at the white vertex $V_{i_r i_s}$ is numbered 3, for any $r \in [k]$, $s \in [N_r]$. Therefore $\Gamma_{i_r j_s}$, $r \in [k]$, $s \in [N_r - 1]$, has 3 real ordered marked points which we denote $P^{(1)}_{i_r j_s}, P^{(2)}_{i_r j_s}, P^{(3)}_{i_r j_s}$ (see Figure 3[bottom, left]) and $\Gamma_{i_r j_{N_r}}$ has two marked points $P^{(2)}_{i_r j_s}, P^{(3)}_{i_r j_s}$;*
- *(b) At each white vertex V_{i_r} we have a horizontal edge marked $e^{(1)}_{i_r}$ and a vertical edge marked $e^{(2)}_{i_r}$ which correspond to the marked points $P^{(1)}_{i_r}, P^{(2)}_{i_r} \in \Gamma_{i_r}$. On each Γ_{i_r}, $r \in [k]$, we add an extra point, the Darboux point $P^{(3)}_{i_r}$, which we use to rule the position of the vacuum divisor;*
- *(c) The unique edge pointing outward at a black vertex $V'_{i_r j_s}$, $r \in [k]$, $s \in [N_r - 1]$, is always numbered 1. We denote $Q^{(m)}_{i_r j_s}$, $m \in [3]$ (resp. $m \in [2]$) the marked points on $\Sigma_{i r j_s}$ corresponding to the trivalent (resp. bivalent) black vertex $V'_{i_r j_s}$.*

(5) We glue copies of $\mathbb{CP}^1$ in pairs at the marked points corresponding to the end points of the corresponding edge on $\mathcal{G}$ (see Figure 4). More precisely:

(6) **Horizontal gluing rules for fixed** $r \in [k]$*:*

- *(a) If, for some $r \in [k]$, $N_r = 0$, then $P^{(1)}_{i_r} \in \Gamma_{i_r}$ is not glued to any other marked point;*
- *(b) If, for some $r \in [k]$, $N_r > 0$, then $P^{(1)}_{i_r} \in \Gamma_{i_r}$ is glued to $Q^{(2)}_{i_r j_1} \in \Sigma_{i_r j_1}$;*
- *(c) For any $s \in [N_r - 1]$, $P^{(1)}_{i_r j_s} \in \Gamma_{i_r j_s}$ is glued to $Q^{(2)}_{i_r j_{s+1}} \in \Sigma_{i_r j_{s+1}}$;*
- *(d) For any $s \in [N_r]$, $P^{(3)}_{i_r j_s} \in \Gamma_{i_r j_s}$ is glued to $Q^{(1)}_{i_r j_s} \in \Sigma_{i_r j_s}$;*
- *(e) $P^{(3)}_{i_r j} \in \Gamma_{i_r}$ is not glued to any other marked point.*

(7) **Vertical gluing rules***:*

- *(a) For any $r \in [k]$, $\kappa_{i_r} \in \Gamma_0$ is glued to $P^{(2)}_{i_r} \in \Gamma_{i_r}$;*

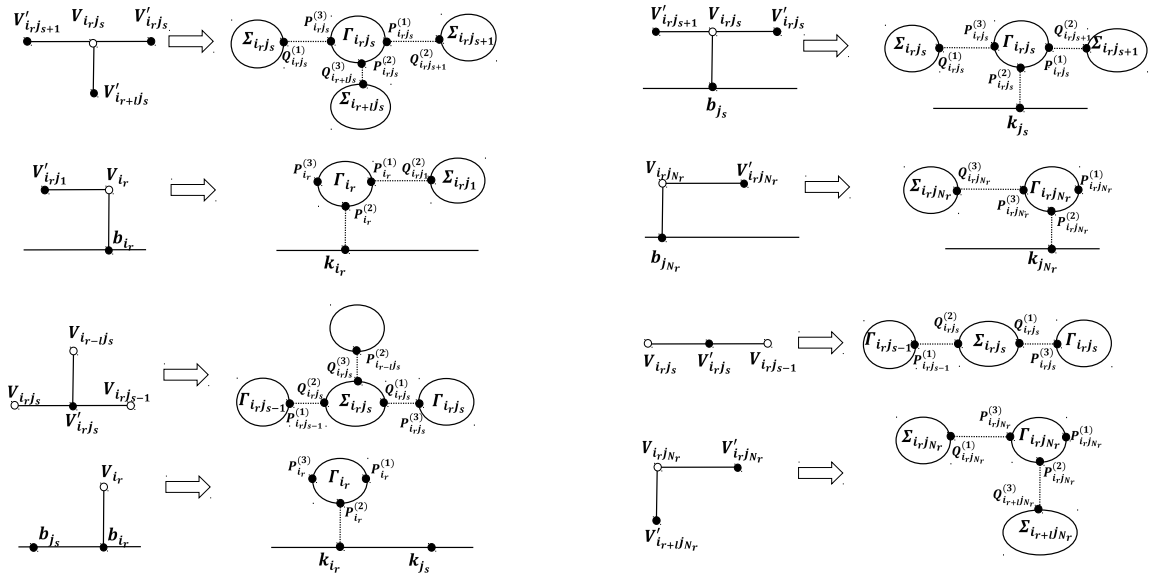

FIGURE 4. *The gluing rules on* Γ *are modeled on the bipartite Le–graph* $\mathcal{G}$ *reflected w.r.t. the vertical axis. The dotted lines mark the points where we glue different copies of* $\mathbb{CP}^1$.

(b) *For any* $j \in \bar{I}$ *such that* $\bar{r} = \max\{r \in [k] : \chi_j^{i_r} = 1\} > 0$, $\kappa_j \in \Gamma_0$ *is glued to* $P^{(2)}_{i_{\bar{r}}j} \in \Gamma_{i_{\bar{r}}j}$;

(c) *If, for some* $j \in \bar{I}$, $\chi_j^{i_r} = 0$ *for all* $r \in [k]$, *then* $\kappa_j \in \Gamma_0$ *is not glued to any other marked point;*

(d) *For any fixed* $r \in [2,k]$ *and any fixed* $s \in [N_r]$, *let* $\bar{r} = \max\{l \in [1, r-1] : \chi_{j_s}^{i_l} = 1\}$. *Then* $Q^{(3)}_{i_r j_s} \in \Sigma_{i_r j_3}$ *is glued to* $P^{(2)}_{i_{\bar{r}} j_s} \in \Gamma_{i_{\bar{r}} j_s}$.

(8) *The faces of* $\mathcal{G}$ *correspond to the ovals of* Γ. *We label the ovals* Ω_0, $\Omega_{i_r j_s}$, $s \in [N_r]$, $r \in [k]$, *as the corresponding faces of* $\mathcal{N}$.

Remark 3.3. ***Universality of the reducible rational curve*** Γ**.** *Let us point out that, for any fixed positroid cell* $\mathcal{S} = \mathcal{S}^{TNN}_{\mathcal{M}}$, *the construction of* Γ *does* ***not*** *require the introduction of any parameter. Therefore it provides an* ***universal*** *curve* Γ *for the whole positroid cell. In the next section we introduce the parametrization of* $\mathcal{S}^{TNN}_{\mathcal{M}}$ *via KP divisors on* Γ.

Remark 3.4. ***The role of bivalent vertices, the reduced graph*** $\mathcal{G}_{red}$ ***and the reduced*** M**−*curve*** $\Gamma(\mathcal{G}_{red})$ *The number of copies of* $\mathbb{CP}^1$ *used to construct* Γ *above is* ***excessive*** *in the sense that both the number of ovals and the* ***KP divisor*** *are invariant if we eliminate from* $\mathcal{G}$ *all copies of* $\mathbb{CP}^1$ *corresponding to bivalent vertices and change edge weights following* [62]. *In this procedure we maintain a bivalent vertex in* $\mathcal{G}_{red}$ *for each component which disconnects from the*

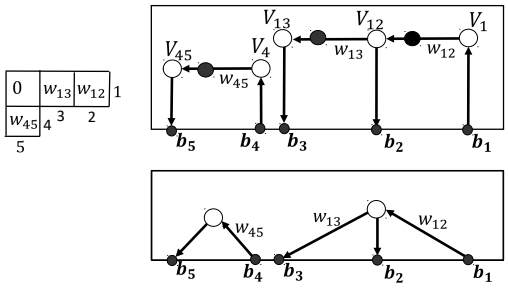

FIGURE 5. *The Le–networks corresponding to the Le–graph $\mathcal{G}$ [top] and its reduction $\mathcal{G}_{red}$ [bottom] for the same Le–tableau of a positroid cell of dimension $d = 3$ in $Gr^{TNN}(2,5)$ [left]. The weight is one for any edge not marked in the Figure.*

graph upon removing the boundary of the disk and consists of a single boundary source connected to a single boundary sink. We show a simple example in Figure 5. In the following, we denote $\mathcal{G}_{red}$ the reduced trivalent graph and $\Gamma(\mathcal{G}_{red})$ the reducible rational curve associated to it.

For the construction of the ***reducible rational*** `M`*-curve we can use both $\mathcal{G}$ and $\mathcal{G}_{red}$ graphs. In Sections 4 and 5 we use the Le–graph $\mathcal{G}$ to evidence the recursive construction in the proof. However, it is also possible to directly construct the KP wave function and its divisor on $\Gamma(\mathcal{G}_{red})$, since, by our construction, the KP wave function is constant with respect to the spectral parameter on each $\mathbb{CP}^1$ corresponding to a bivalent vertex.*

For constructing a regular perturbed `M`*-curve of genus equal to d it is convenient to start from $\Gamma(\mathcal{G}_{red})$ since it corresponds to a nodal plane curve of degree lesser than that for $\Gamma(\mathcal{G})$. In Section 6, we use $\Gamma(\mathcal{G}_{red})$ in the construction of the plane curve and of the KP divisor for soliton data in $Gr^{TP}(2,4)$.*

Remark 3.5. ***Comparison with the construction in*** [3]**.** *In* [3]*, to any given soliton data $(\mathcal{K}, [A])$, $[A] \in Gr^{TP}(k,n)$, we associate a curve obtained gluing $k+1$ copies of $\mathbb{CP}^1$ at double points whose position is ruled by a parameter $\xi \gg 1$. We then control the asymptotic leading behavior in ξ of the vacuum wave function via an algebraic construction using the positivity properties of a specific representative matrix of $[A]$. In this approach the number of $\mathbb{CP}^1$ components is much smaller, but we have to introduce extra parameters marking the positions of the glued points. In practice one can obtain such curve from the universal one by a proper desingularization of some double point (see also Section 6, where we desingularize explicitly $\Gamma(\mathcal{G}_{red})$ to $\Gamma(\xi)$ when $[A] \in Gr^{TP}(2,4)$).*

Proposition 3.1. ***The oval structure of*** Γ**.** *Let* $\mathcal{K} = \{\kappa_1 < \cdots < \kappa_n\}$ *and* $\mathcal{S}_{\mathcal{M}}^{TNN} \subset Gr^{TNN}(k,n)$ *be a positroid cell of dimension* d*. Let* Γ *be as in Construction 3.1. Then* Γ *possesses* $d+1$ *ovals which we label* Ω_0, $\Omega_{i_r j_s}$, $s \in [N_r]$, $r \in [k]$, $N_r \geq 1$*. Moreover the ovals are uniquely identified by the following properties:*

(1) Ω_0 *is the unique oval whose boundary contains both* κ_1 *and* κ_n*;*

(2) For any $r \in [k]$, $s \in [2, N_r]$, $\Omega_{i_r j_s}$ *is the unique oval whose boundary contains both* $P^{(2)}_{i_r j_s} \in \Gamma_{i_r j_s}$ *and* $P^{(2)}_{i_r j_{s-1}} \in \Gamma_{i_r j_{s-1}}$*;*

(3) For any $r \in [k]$, $\Omega_{i_r j_1}$ *is the unique oval whose boundary contains both* $P^{(2)}_{i_r j_1} \in \Gamma_{i_r j_1}$ *and* $P^{(2)}_{i_r} \in \Gamma_{i_r}$*.*

The proof is straightforward and we omit it. We remark that $\Gamma(\mathcal{G}_{\rm red})$ has the same number of ovals as $\Gamma(\mathcal{G})$.

Let d be the dimension of the **irreducible** positroid cell $\mathcal{S}_{\mathcal{M}}^{\rm TNN} \subset Gr^{\rm TNN}(k,n)$. Let $\mathcal{G}_{\rm red}$ be its reduced graph as in Remark 3.4 and suppose that it has n_b bivalent vertices after the reduction. Then $\Gamma(\mathcal{G}_{\rm red})$ is a partial normalization [6] of a connected reducible nodal plane curve with $d+1$ ovals obtained by gluing $2d-n+n_b+1$ copies of $\mathbb{CP}^1$. The curve $\Gamma(\mathcal{G}_{\rm red})$ is a rational degeneration of a genus d smooth M–curve. The total number of edges of $\mathcal{G}_{\rm red}$ is $3d-n+n_b$, and each of them corresponds to an handle of the desingularized M–curve. In the next Proposition we verify that the genus of the latter coincides with the dimension of $\mathcal{S}_{\mathcal{M}}^{\rm TNN}$.

Proposition 3.2. $\Gamma(\mathcal{G}_{red})$ ***is the rational degeneration of a smooth*** M***-curve of genus*** d**.** *Let* $\mathcal{K} = \{\kappa_1 < \cdots < \kappa_n\}$ *and* $\mathcal{S}_{\mathcal{M}}^{TNN} \subset Gr^{TNN}(k,n)$ *be an irreducible positroid cell of dimension* d*. Let* Γ *be as in Construction 3.1 and* $\Gamma(\mathcal{G}_{red})$ *be the its reduction obtained by eliminating the components corresponding to bivalent vertices eliminated in* $\mathcal{G}_{red}$*. Then* $\Gamma(\mathcal{G}_{red})$ *is a rational degeneration of a regular* M*–curve of genus* d *equal to the dimension of the positroid cell, possessing* $d+1$ *ovals.*

Proof. The only untrivial statement is the one concerning the genus of the perturbed curve. Let n_b be the number of bivalent vertices survived the reduction of the graph $\mathcal{G}$ according to Remark 3.4. By definition, $\Gamma(\mathcal{G}_{\rm red})$ is represented by $2d-n+n_b+1$ copies of $\mathbb{CP}^1$ connected at $3d-n+n_b$ pairs of double points. The regular curve is obtained opening a gap at each pair of these double points. We perform this desingularization respecting the real structure and keeping the number of real ovals fixed.

By construction, the desingularized curve has genus $g = \#\text{handles} - \#\mathbb{CP}^1 + 1 = 3d - n + n_b - (2d - n + n_b + 1) + 1 = d$, and it possesses $d + 1$ real ovals, therefore it is an M-curve. $\square$

3.2. **The planar representation of the desingularized curve.** Generic Riemann surfaces cannot be holomorphically mapped into $\mathbb{CP}^2$ without self-intersections [36], therefore partial normalization is necessary if the number of $\mathbb{CP}^1$ copies is sufficiently high. In our construction we have $2d - n + n_b + 1$ copies of $\mathbb{CP}^1$, which may be lines, quadrics or rational cubics in $\mathbb{CP}^2$. Denote the numbers of lines, quadrics and cubics by n_1, n_2, n_3 respectively. Clearly $n_1 + n_2 + n_3 = 2d - n + n_b + 1$, the total degree of the rational reducible curve $\Gamma(\mathcal{G}_{\text{red}})$ is $n_1 + 2n_2 + 3n_3$. The total number of singularities before normalization is

$$n_s = \frac{n_1(n_1-1)}{2} + 2n_1n_2 + 3n_1n_3 + 2n_2(n_2-1) + 6n_2n_3 + \frac{9n_3(n_3-1)}{2} + n_3$$

The last term in the above sum takes into account that all cubics are rational and each has one cusp. When we desingularize $\Gamma(\mathcal{G}_{\text{red}})$ to the genus d curve, $n_s - 3d + n - n_b$ intersections have to remain intersections for its plane curve model, and they are resolved after normalization.

Let us provide evidence that we have enough parameters. Let us assume that Γ_0 is defined by $\mu = 0$, and we have 3 systems of linear functions $l_j = a_j\lambda + b_j\mu$, $j \in [n_1]$, $l'_j = a'_j\lambda + b'_j\mu$, $j \in [n_2]$, $l''_j = a''_j\lambda + b''_j\mu$, $j \in [n_3]$ such that

(1) All slopes are pairwise distinct and all a_j, a'_j, a''_j are non-zero;
(2) The system of lines Γ_0, $\mathcal{L}_j : \{l_j - \alpha_j = 0\}$ intersect only in pairs.

The quadrics and cubics are represented by $\mathcal{Q}_j = 0$, $j \in [n_2]$ and $\mathcal{C}_i = 0$, $i \in [n_3]$ respectively, where $\mathcal{Q}_j = y - \alpha'_{j,2}(l'_j)^2 - \alpha'_{j,1}l'_j - \alpha'_{j,0}$ and $\mathcal{C}_i = y - \alpha''_{i,3}(l''_i)^3 - \alpha''_{i,2}(l''_i)^2 - \alpha''_{i,1}l''_i - \alpha''_{i,0}$.

The coefficients α, α', α'' have to be chosen so that all lines, quadrics and cubics intersect Γ_0 at proper points. We also assume that all $\alpha'_{j,2}$, $\alpha''_{i,3}$ are sufficiently large, so that all quadrics and cubics are small perturbations of pairs or triples of parallel lines respectively, and all intersections of components are real.

The unperturbed curve has then the following form

$$\Pi_0(\lambda,\mu) = 0, \quad \text{where } \Pi_0(\lambda,\mu) = \mu \prod_{i_1\in[n_1]} \mathcal{L}_{i_1} \prod_{i_2\in[n_2]} \mathcal{Q}_{i_2} \prod_{i_3\in[n_3]} \mathcal{C}_{i_3}.$$

We use the following collection of perturbative terms: $\{\Pi^{[0,1]}_{i_1}; \Pi^{[0,2],k}_{i_2}, k \in [2]; \Pi^{[0,3],k}_{i_3}, k \in [3]; \Pi^{[1,1]}_{i_1,j_1}; \Pi^{[1,2],k}_{i_1,i_2}, k \in [2]; \Pi^{[1,3],k}_{i_1,i_3}, k \in [3]; \Pi^{[2,2],k_1,k_2}_{i_2,j_2}, k_1,k_2 \in [2]; \Pi^{[2,3],k_1,k_2}_{i_2,i_3}, k_1 \in [2], k_2 \in [3]; \Pi^{[3,3],k_1,k_2}_{i_3,j_3}, k_1,k_2 \in [3]\}$,

where $i_l, j_l \in [n_l]$, $l \in [3]$, $i_1 < j_1$, $i_2 < j_2$, $i_3 < j_3$, and

$$\Pi_{i_1}^{[0,1]} = \frac{\Pi_0}{\mu \mathcal{L}_{i_1}}, \quad \Pi_{i_2}^{[0,2],k} = \frac{\Pi_0 (l'_{i_2})^{k-1}}{\mu \mathcal{Q}_{i_2}}, \quad \Pi_{i_3}^{[0,3],k} = \frac{\Pi_0 (l''_{i_3})^{k-1}}{\mu \mathcal{C}_{i_3}},$$

$$\Pi_{i_1,j_1}^{[1,1]} = \frac{\Pi_0}{\mathcal{L}_{i_1}\mathcal{L}_{j_1}}, \quad \Pi_{i_1,i_2}^{[1,2],k} = \frac{\Pi_0 (l'_{i_2})^{k-1}}{\mathcal{L}_{i_1}\mathcal{Q}_{i_2}}, \quad \Pi_{i_1,i_3}^{[1,3],k} = \frac{\Pi_0 (l''_{i_3})^{k-1}}{\mathcal{L}_{i_1}\mathcal{C}_{i_3}},$$

$$\Pi_{i_2,j_2}^{[2,2],k_1,k_2} = \frac{\Pi_0 (l'_{i_2})^{k_1-1}(l'_{j_2})^{k_2-1}}{\mathcal{Q}_{i_2}\mathcal{Q}_{j_2}}, \quad \Pi_{i_2,i_3}^{[2,3],k_1,k_2} = \frac{\Pi_0 (l'_{i_2})^{k_1-1}(l''_{i_3})^{k_2-1}}{\mathcal{Q}_{i_2}\mathcal{C}_{i_3}}, \quad \Pi_{i_3,j_3}^{[3,3],k_1,k_2} = \frac{\Pi_0 (l''_{i_3})^{k_1-1}(l''_{j_3})^{k_2-1}}{\mathcal{C}_{i_3}\mathcal{C}_{j_3}}.$$

We then consider the following perturbation of our rational curve $\Pi_0(\lambda, \mu) = 0$:

$$\Pi(\lambda, \mu) = 0, \quad \text{where} \quad \Pi(\lambda, \mu) = \Pi_0 + \sum \epsilon_s^r \Pi_s^r, \tag{3.1}$$

where the sum runs over all perturbation terms described above. The perturbed curve in $\mathbb{CP}^2$ has the same structure at the infinite line as the original rational curve. The number of perturbation parameters ϵ_s^r in (3.1) coincides with the number of intersections in $\Pi_0(\lambda, \mu) = 0$. For sufficiently small ϵ_s^r we have the following map

$$\{\epsilon_s^r\} \to \Pi(\mathcal{R}_s^r), \tag{3.2}$$

where $\mathcal{R}_s^r$ are the solutions of the system

$$\partial_\lambda \Pi(\lambda, \mu) = 0, \quad \partial_\mu \Pi(\lambda, \mu) = 0. \tag{3.3}$$

For the unperturbed curve, the set $\{\mathcal{R}_s^r\}$ coincides with the intersection points, therefore for small ϵ_s^r we have a natural enumeration. The map (3.2) is analytic for $|\epsilon_s^r| \ll 1$ and its Jacobian is non-zero, therefore it is locally invertible, and at each double point we can open a gap in the desired direction, or keep the point double.

Let us remark that these arguments are analogous to arguments used in [51].

3.3. **The KP divisor on Γ.** Throughout this section we fix a set of phases $\mathcal{K} = \{\kappa_1 < \cdots < \kappa_n\}$ and a positroid cell $\mathcal{S}_{\mathcal{M}}^{\mathrm{TNN}} \subset Gr^{\mathrm{TNN}}(k, n)$of dimension g. Γ is the curve of Construction 3.1 associated to such data with marked point $P_0 \in \Gamma_0$.

In this section we state the main results of our paper: for any soliton data $(\mathcal{K}, [A])$, $[A] \in \mathcal{S}_{\mathcal{M}}^{\mathbf{TNN}}$, we construct a unique real and regular degree g KP divisor $\mathcal{D}_{\mathbf{KP},\Gamma}$ on Γ as follows:

(1) We first construct a unique degree g effective real and regular **vacuum** divisor $\mathcal{D}_{\mathrm{vac},\Gamma}$ and a unique real and regular **vacuum** wave function $\hat{\phi}(P, \vec{t})$ on Γ satisfying appropriate boundary conditions (Theorem 3.1);

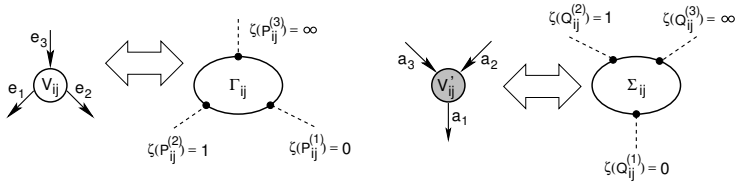

FIGURE 6. *Local coordinates on the components Γ_{ij} and Σ_{ij}: the marked point $P_{ij}^{(s)} \in \Gamma_{ij}$ corresponds to the edge e_s at the white vertex V_{ij} and the marked point $Q_s \in \Gamma_{ij}$ corresponds to the edge a_s at the black vertex V'_{ij}.*

(2) We then apply the Darboux dressing to such vacuum wave function and define the normalized **dressed divisor** $\mathcal{D}_{\mathrm{KP},\Gamma}$, which, by construction is effective and of degree g;

(3) $\mathcal{D}_{\mathrm{KP},\Gamma}$ has minimal degree g and is the **KP divisor** for the given soliton data on the spectral curve Γ, since its restriction to Γ_0 coincides with the Sato divisor defined in Section 2.1, and, by construction, it satisfies the reality and regularity conditions of Definition 2.4 (see Theorem 3.2).

Remark 3.6. ***Parametrization of positroid cells.*** *In our construction we associate a system of edge vectors to each Le–network in $\mathcal{S}_{\mathcal{M}}^{TNN}$. The properties of such edge vectors guarantee that the non–normalized KP wave function has untrivial dependence on $\vec{t}$ at all double points of Γ. Therefore, for any $[A_0] \in S$ it is possible to find an initial time $\vec{t}_0$ such that the degree g KP divisor $\mathcal{D}_{\mathrm{KP},\Gamma} = \mathcal{D}_{\mathrm{KP},\Gamma}(\vec{t}_0)$ is non–special for any point $[A] \in S$ sufficiently near to $[A_0]$ in the natural metric associated to the reduced row echelon matrix representation of such points. It is in this sense that we obtain a parametrization of $\mathcal{S}_{\mathcal{M}}^{TNN}$ via degree g non–special KP divisors.*

We start introducing local affine coordinates on each copy of $\mathbb{CP}^1$ and we use the same symbol ζ for any such affine coordinate to simplify notations (see also Figure 6).

Definition 3.1. Local affine coordinate on Γ *On each copy of $\mathbb{CP}^1$ the local coordinate ζ is uniquely identified by the following properties:*

(1) On Γ_0, $\zeta^{-1}(P_0) = 0$ and $\zeta(\kappa_1) < \cdots < \zeta(\kappa_n)$. To abridge notations, we identify the ζ–coordinate with the marked points $\kappa_j = \zeta(\kappa_j)$, $j \in [n]$;

(2) On the component Γ_{ij} corresponding to the internal white vertex V_{ij}:

$$\zeta(P_{ij}^{(1)}) = 0, \;\; \zeta(P_{ij}^{(2)}) = 1, \;\; \zeta(P_{ij}^{(3)}) = \infty,$$

while on the component Σ_{ij} corresponding to the internal black vertex V'_{ij}:

$$\zeta(Q_{ij}^{(1)}) = 0, \;\; \zeta(Q_{ij}^{(2)}) = 1, \;\; \zeta(Q_{ij}^{(3)}) = \infty.$$

In the following Definitions we state the desired properties for both the vacuum divisor and the vacuum wave function on Γ.

Definition 3.2. ***Real and regular vacuuum divisor compatible with $\mathcal{S}_{\mathcal{M}}^{TNN}$.*** *Let Ω_0 be the infinite oval containing the marked point $P_0 \in \Gamma_0$ and let Ω_j, $j \in [g]$ be the finite ovals of Γ. Let $P_3^{(i_r)}$, $r \in [k]$ be the Darboux points in Γ.*

We call a degree g divisor $\mathcal{D}_{\mathrm{vac},\Gamma} \in \Gamma \backslash \Gamma_0$ a real and regular vacuum divisor compatible with $\mathcal{S}_{\mathcal{M}}^{TNN}$ if:

1. *$\mathcal{D}_{\mathrm{vac},\Gamma}$ is contained in the union of all the ovals of Γ;*
2. *There is exactly one divisor point on each component of Γ corresponding to a trivalent white vertex or a bivalent white vertex containing a Darboux point;*
3. *In any Ω_j, $j \in [g]$, the total number of vacuum divisor poles plus the number of Darboux points is 1 mod 2;*
4. *In Ω_0, the total number of vacuum divisor poles plus the number of Darboux points plus k is 0 mod 2.*

Definition 3.3. A real and regular vacuum wave function on Γ corresponding to $\mathcal{D}_{\mathbf{vac},\Gamma}$: *Let $\mathcal{D}_{\mathrm{vac},\Gamma}$ be a degree g real regular divisor on Γ as in Definition 3.2. A function $\hat{\phi}(P, \vec{t})$, where $P \in \Gamma \backslash \{P_0\}$ and $\vec{t}$ are the KP times, is called a real and regular vacuum wave function on Γ corresponding to $\mathcal{D}_{\mathrm{vac},\Gamma}$ if:*

1. *There exists $\vec{t}_0$ such that $\hat{\phi}(P, \vec{t}_0) = 1$ at all points $P \in \Gamma \backslash \{P_0\}$;*
2. *The restriction of $\hat{\phi}$ to $\Gamma_0 \backslash \{P_0\}$ coincides with the following normalization of Sato's wave function, $\hat{\phi}(\zeta(P), \vec{t}) = e^{\theta(\zeta, \vec{t} - \vec{t}_0)}$, where $\theta(\zeta, \vec{t}) = \sum_{l \geq 1} t_l \zeta^l$;*
3. *For all $P \in \Gamma \backslash \Gamma_0$ the function $\hat{\phi}(P, \vec{t})$ satisfies all equations (2.4) of the vacuum hierarchy;*
4. *If both $\vec{t}$ and $\zeta(P)$ are real, then $\hat{\phi}(\zeta(P), \vec{t})$ is real. Here $\zeta(P)$ is the local affine coordinate on the corresponding component of Γ as in Definition 3.1;*
5. *$\hat{\phi}$ takes equal values at pairs of glued points $P, Q \in \Gamma$, for all $\vec{t}$: $\hat{\phi}(P, \vec{t}) = \hat{\phi}(Q, \vec{t})$;*
6. *For each fixed $\vec{t}$ the function $\hat{\phi}(P, \vec{t})$ is meromorphic of degree $\leq g$ in P on $\Gamma \backslash \{P_0\}$: for any fixed $\vec{t}$ we have $(\hat{\phi}(P, \vec{t})) + \mathcal{D}_{\mathrm{vac},\Gamma} \geq 0$ on $\Gamma \backslash P_0$, where (f) denotes the divisor of f. Equivalently, for any fixed $\vec{t}$ on $\Gamma \backslash \{P_0\}$ the function $\hat{\phi}(\zeta, \vec{t})$ is regular outside the points of $\mathcal{D}_{\mathrm{vac},\Gamma}$ and at each of these points either it has a first order pole or it is regular;*
7. *For each $P \in \Gamma \backslash \{P_0\}$ outside $\mathcal{D}_{\mathrm{vac},\Gamma}$ the function $\hat{\phi}(P, \vec{t})$ is regular in $\vec{t}$ for all times.*

Definition 3.4. A real and regular vacuum wave function on Γ for the soliton data $(\mathcal{K}, [A])$: *Let $\mathcal{K}$, Γ and $\hat{\phi}(P, \vec{t})$ be as in Construction 3.1 and in Definition 3.3. Let $[A] \in \mathcal{S}_{\mathcal{M}}^{TNN}$. The function $\hat{\phi}(P, \vec{t})$ is a real and regular vacuum wave function for the soliton data $(\mathcal{K}, [A])$ if, at each Darboux point $P_{i_r}^{(3)}$, $r \in [k]$ and for all $\vec{t}$,*

$$\hat{\phi}(P_{i_r}^{(3)}, \vec{t}) \equiv f^{(r)}(\vec{t}), \tag{3.4}$$

where $f^{(r)}(\vec{t})$, $r \in [k]$, generate the Darboux transformation for the soliton data.

Theorem 3.1. ***Existence and uniqueness of a real and regular divisor and vacuum wave function on Γ satisfying appropriate boundary conditions.*** *Let $(\mathcal{K}, [A])$ be given soliton data with $[A] \in \mathcal{S}_{\mathcal{M}}^{TNN}$ of dimension g, and let Γ be as in Construction 3.1 with Darboux points $\{P_{i_r}^{(3)}, r \in [k]\}$. Then, we can fix an initial time $\vec{t}_0$ such that to the following data $(\mathcal{K}, [A]; \Gamma, P_0, P_{i_1}^{(3)}, \dots, P_{i_k}^{(3)}; \vec{t}_0)$ we associate*

1. *A **unique** real and regular degree g vacuum divisor $\mathcal{D}_{\mathrm{vac},\Gamma}$ as in Definition 3.2,*
2. *A **unique** real and regular vacuum wave function $\hat{\phi}(P, \vec{t})$ corresponding to this divisor satisfying Definitions 3.3 and 3.4.*

Moreover, at the Darboux points, $\hat{\phi}(P, \vec{t})$ satisfies

$$\hat{\phi}(P_{i_r}^{(3)}, \vec{t}) \equiv \frac{\sum_{l=1}^{n} A_l^r \exp(\theta_l(\vec{t}))}{\sum_{l=1}^{n} A_l^r \exp(\theta_l(\vec{t}_0))}, \quad r \in [k], \qquad \forall \vec{t}, \tag{3.5}$$

where $f^{(r)}(\vec{t})$ are the generators of the Darboux transformation associated to the RRE representative matrix A.

We prove Theorem 3.1 in Section 5. More precisely, we construct a unique vacuum wave function on Γ using the algebraic recursion settled in Section 4.2. We first modify the LE-network moving the boundary sources to convenient inner vertices, added in correspondence of the Darboux points in Γ. Then we assign a vector constructed in Section 4.1 to each vertical edge of this modified network and use the linear relations at the inner vertices to extend this system of vectors to all its edges. We use this system of vectors to define a unique vacuum edge wave function (v.e.w.) satisfying the necessary boundary conditions. By construction, the linear relations at trivalent white vertices define a degree g divisor with the required reality and regularity conditions (see Lemma 5.4). Finally, we construct the degree g real and regular vacuum wave function on Γ imposing that it takes the value of the normalized v.e.w. at the marked points (double points and Darboux points) which correspond to the edges (see Theorem 5.1).

Definition 3.5. ***The dressing of the vacuum wave function on*** Γ**.** *Let* Γ *and* $\hat{\phi}$ *be as in Theorem 3.1 for given soliton data* $(\mathcal{K}, [A])$*. Then the corresponding* ***Darboux transformed wave function*** *is defined by:*

$$\psi(P, \vec{t}) = \mathfrak{D}\hat{\phi}(P, \vec{t}), \qquad P \in \Gamma \backslash \{P_0\}, \ \forall \vec{t}, \tag{3.6}$$

where $\mathfrak{D}$ *is the Darboux dressing differential operator for the soliton data* $(\mathcal{K}, [A])$ *defined in (2.5). Let the initial condition* $\vec{t}_0$ *be such that* $\mathfrak{D}\hat{\phi}(P, \vec{t}_0) \neq 0$ *at all double points* $P \in \Gamma$*. We define the* ***normalized dressed wave function*** $\hat{\psi}(P, \vec{t})$ *as*

$$\hat{\psi}(P, \vec{t}) = \frac{\psi(P, \vec{t})}{\psi(P, \vec{t}_0)}. \tag{3.7}$$

We define the ***normalized dressed divisor*** *as*

$$\mathcal{D}_{\mathrm{KP},\Gamma} = \mathcal{D}_{\mathrm{dr},\Gamma} + (\psi(P, \vec{t}_0)). \tag{3.8}$$

where the non-effective divisor $\mathcal{D}_{\mathrm{dr},\Gamma}$ *is defined by*

$$\mathcal{D}_{\mathrm{dr},\Gamma} = \mathcal{D}_{\mathrm{vac},\Gamma} + kP_0 - \sum_{r=1}^{k} P_{i_r}. \tag{3.9}$$

Remark 3.7. *For reducible soliton data* $[A]$ *in* $Gr^{TNN}(k, n)$ *with* s *isolated boundary sources we have two Darboux dressings: the reducible* k*-th order dressing operator and the reduced* $(k-s)$*-order dressing operator (see Remarks 2.1 and 2.2). The normalized dressed wave function is the same for both dressings, while the* $\mathcal{D}_{\mathrm{KP},\Gamma}$ *divisor associated to the reducible dressing operator contains* s *extra points in the intersection of the finite ovals with* Γ_0*, so that we have more than one divisor point in some of the finite ovals. Therefore, in such case, in the Definition above we use the* $(k-s)$*-th order reduced dressing operator. The extra* s *divisor points may be interpreted as being originated from real and regular divisor data on regular* M*–curves of genus* $g+s$ *under the assumption that* s *ovals degenerate to points in the solitonic limit.*

Lemma 3.1. *(1) For any* $\vec{t}$ *we have the following inequality on* $\Gamma \backslash P_0$*:*

$$(\psi(P, \vec{t})) + \mathcal{D}_{\mathrm{dr},\Gamma} \geq 0. \tag{3.10}$$

(2) The number of poles minus the number of zeroes for $\mathcal{D}_{\mathrm{dr},\Gamma}$ *(counted with multiplicities, if necessary) at each finite oval is odd and at the infinite oval it is even.*

The first property follows directly from the definition of $\psi(P,\vec{t})$. The second statement simply follows from properties of the vacuum wave function constructed in Theorem 3.1, namely equation (3.4) in Definition 3.4, properties (3)-(4) in Definition 3.2 and formula (3.9).

Lemma 3.2. *(1) For any $\vec{t}$ we have the following inequality on $\Gamma\backslash P_0$:*

$$(\hat{\psi}(P,\vec{t})) + \mathcal{D}_{\mathrm{KP},\Gamma} \geq 0. \tag{3.11}$$

(2) The divisor $\mathcal{D}_{\mathrm{KP},\Gamma}$ is effective and has degree g.

(3) All poles of $\mathcal{D}_{\mathrm{KP},\Gamma}$ lie at the finite ovals, and each finite oval contains exactly one pole of $\mathcal{D}_{\mathrm{KP},\Gamma}$.

The first statement follows immediately from the definition of $\hat{\psi}(P,\vec{t})$ and $\mathcal{D}_{\mathrm{KP},\Gamma}$. The second statement follows immediately from (3.8). The third statement follows from the fact that $\psi(P,\vec{t}_0)$ is real at all real ovals and from Lemma 3.1.

Theorem 3.2. ***The effective divisor on*** Γ. *Assume that $\hat{\phi}$ is the real and regular vacuum wave function on Γ of Theorem 3.1 for the given soliton data $(\mathcal{K},[A])$. Let $\hat{\psi}$ be the normalized dressed wave function from Definition 3.5.*

Then the divisor $\mathcal{D}_{\mathrm{KP},\Gamma}$ is the KP divisor on Γ for the soliton data $(\mathcal{K},[A])$, and it satisfies the reality and regularity conditions of Definition 2.4, whereas $\hat{\psi}$ is the KP wave function on Γ for the soliton data $(\mathcal{K},[A])$. Moreover, the degree of the effective pole divisor of $\hat{\psi}$ coincides with g, the dimension of the positroid cell of $[A]$.

The proof of the Theorem easily follows from Lemmas 3.1, 3.2 and Theorem 3.1. We remark that the Darboux transformation automatically creates the Sato divisor on Γ_0.

Remark 3.8. $\mathcal{D}_{\mathbf{KP},\Gamma}$ ***is the KP divisor on*** $\Gamma(\mathcal{G}_{\boldsymbol{red}})$. *In our construction each KP divisor point either belongs to Γ_0 or to a copy of $\mathbb{CP}^1$ represented by a trivalent white vertex. Below we prove that the value of the normalized KP wave function is constant with respect to the spectral parameter on each component corresponding to a bivalent vertex; therefore the elimination of bivalent vertices doesn't affect either the value of the normalized KP wave function on the $\mathbb{CP}^1$ components corresponding to trivalent white vertices or the position of the KP divisor points.*

Remark 3.9. ***Invariance of the KP divisor*** *In* [4] *we prove that $\hat{\psi}$ and $\mathcal{D}_{\mathrm{KP},\Gamma}$ do not depend neither on the orientation of the network nor on the choice of the position of the Darboux points.*

4. A system of vectors on the Le–network

In the previous Section we constructed the spectral curve Γ associated with the given positroid cell $\mathcal{S}_{\mathcal{M}}^{\mathrm{TNN}}$ and the ordered set $\mathcal{K}$. The final goal of the main construction is the computation of the divisor corresponding to a given point $[A] \in S$. At this aim, in this and in the next sections, we first introduce a system of edge vectors on the Le–network and we use it to compute the values of the vacuum and dressed wave functions at all marked points of the curve.

The construction of a system of vectors at the edges of the Le–network is based on an algebraic procedure analogous to the one introduced in [3] on the main cell. In [3], we related a specific representation of the rows of the banded matrix in $[A] \in Gr^{\mathrm{TP}}(k,n)$ to the leading order behavior in the parameter ξ of the vacuum wave function at double points and Darboux points. Here we use an excessive number of copies of $\mathbb{CP}^1$ to relate the system of edge vectors to the **exact behavior** of both the vacuum and the dressed wave functions at the marked points of Γ. Moreover, both the vectors and the wave functions satisfy linear relations at the vertices of the Le-network which are used to construct the vacuum and the dressed divisors.

In this section we first use the Le–network $\mathcal{N}$ to express each row of the RREF representative matrix as a linear combination with positive coefficients of a minimal number of some basic row vectors. This construction is a generalization of the Principal Algebraic Lemma in [3] and easily follows from [62]. Then, in Section 4.2 we present a recursive construction of these basic vectors, generalizing the corresponding theorem in [3]. In [4], we generalize the construction of edge vectors to any planar trivalent bipartite network $\mathcal{N}$ in the disk representing a given point of $Gr^{\mathrm{TNN}}(k,n)$.

4.1. Representation of the rows of the RREF matrix using the Le–tableau.

The notations used in this section are the same as in the Appendix. We fix the positroid cell $\mathcal{S}_{\mathcal{M}}^{\mathrm{TNN}} \subset Gr^{\mathrm{TNN}}(k,n)$ and the planar bipartite trivalent acyclically oriented Le–graph $\mathcal{G}$ representing it, whereas $\mathcal{N}$ is the Le–network on $\mathcal{G}$ representing $[A] \in \mathcal{S}_{\mathcal{M}}^{\mathrm{TNN}}$. In the following A is the representative matrix in RREF of $[A]$, I is the lexicographically minimal base in the matroid $\mathcal{M}$ and $\bar{I} = [n] \backslash I$. Each row r of A may be expressed as a linear combination with **positive coefficients** $c_{l_s}^r$ of $N_r + 1$ vectors $E^{(r)}[l_s]$, $s \in [0, N_r]$, computed using $\mathcal{N}$. Each coefficient $c_{l_s}^r$ is the weight of the directed path from the boundary source b_{i_r} to the internal white vertex $V_{i_r l_s}$. The absolute value of the j-th component of the vector $E^{(r)}[l_s]$ is the sum of the weights of all possible paths starting downwards at $V_{i_r l_s}$ and zig–zagging to the destination b_j, while its sign

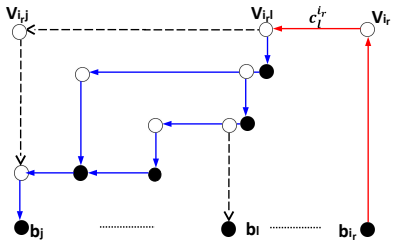

FIGURE 7. *The coefficient $c_l^{i_r}$ is the weight of the directed path from the source b_{i_r} to the white internal vertex $V_{i_r l}$, while $E_j^{(r)}[l]$, the j–th component of $E^{(r)}[l]$, has absolute value equal to the sum of the weights of all the directed paths which start downwards at the internal vertex $V_{i_r l}$ and zig–zag to the boundary sink b_j. The sign of $E_j^{(r)}[l]$ is equal to the number of boundary sources b_{i_s} with $i_s \in]i_r, j[$.*

depends on the number of boundary sources passed before reaching the destination (see Lemma 4.1).

Let us fix $r \in [k]$ and let $i_r \in I$ be the corresponding pivot index. Let $l \in \bar{I}$ such that the box $B_{i_r l}$ has index $\chi_l^{i_r} = 1$ and let $V_{i_r l}$ be the corresponding white vertex in $\mathcal{N}_t$. Let us consider all directed paths P starting at b_{i_r}, moving horizontally from V_{i_r} to $V_{i_r l}$, moving downwards at $V_{i_r l}$ and then zigzagging towards any possible destination $j \in \bar{I}$. Necessarily $j \geq l$; moreover, for $l = j$, there is exactly one such path from b_{i_r} to b_l. For $j \in \bar{I}$ and $j \geq l$, let us define

$$\begin{aligned} \mathcal{P}_{lj}^{(r)} &= \{\, P_{lj}^{(r)} : b_{i_r} \mapsto b_j \;:\; P_{lj}^{(r)} \text{ moves downwards at the white vertex } V_{i_r l} \,\}, \\ \bar{\mathcal{P}}_{lj}^{(r)} &= \{\, \bar{P}_{lj}^{(r)} : V_{i_r l} \mapsto b_j \;:\; \bar{P}_{lj}^{(r)} \text{ moves downwards at the white vertex } V_{i_r l} \,\}, \end{aligned} \tag{4.1}$$

and denote by $P_{i_r l}$ the path from the source b_{i_r} to the white vertex $V_{i_r l}$. Then for any $P_{lj}^{(r)} \in \mathcal{P}_{lj}^{(r)}$ there exists a unique path $\bar{P}_{lj}^{(r)} \in \bar{\mathcal{P}}_{lj}^{(r)}$ such that $P_{lj}^{(r)} = P_{i_r l} \sqcup \bar{P}_{lj}^{(r)}$. Define

$$c_l^i \equiv \prod_{e \in P_{i_r l}} w_e. \tag{4.2}$$

Then the weight of the path $P_{lj}^{(r)}$ is $w(P_{lj}^{(r)}) = \prod_{e \in P_{lj}^{(r)}} w_e = c_l^i \left(\prod_{e \in \bar{P}_{lj}^{(r)}} w_e \right) = c_l^i \, w(\bar{P}_{lj}^{(r)})$ and, for any $j \in \bar{I}$, $j > i_r$, the matrix entry in reduced row echelon form as in (A.2), may be re–expressed as

$$A_j^{r_i} = (-1)^{\sigma_{i_r j}} \sum_{s=1}^{N_r} c_{l_s}^i \sum_{\bar{P}_{l_s j}^{(r)} \in \bar{\mathcal{P}}_{l_s j}^{(r)}} w(\bar{P}_{l_s j}^{(r)}) = (-1)^{\sigma_{i_r j}} \sum_{l \leq j} c_l^i \sum_{\bar{P}_{lj}^{(r)} \in \bar{\mathcal{P}}_{lj}^{(r)}} w(\bar{P}_{lj}^{(r)}),$$

where $\sigma_{i_r j}$ is the number of boundary sources in $]i_r, j[$. In [62] the matrix elements $A_j^{r_i}$ are computed using columns instead of rows.

Finally, for any $r \in [k]$, $i_r \in I$, $l \in \bar{I}$, $l > i_r$, and such that $\chi_l^{i_r} = 1$, let us define the row vector $E^{(r)}[l] = (E_1^{(i)}[l], \dots, E_n^{(i)}[l])$, with

$$E_j^{(r)}[l] \;=\; \begin{cases} 0 & \text{if } j < l \text{ or } j \in I, \\ (-1)^{\sigma_{i_r j}} \sum\limits_{\bar{P}_{lj}^{(r)} \in \bar{\mathcal{P}}_{lj}^{(r)}} w(\bar{P}_{lj}^{(r)}) & \text{if } l, j \in \bar{I} \text{ and } j \geq l. \end{cases} \tag{4.3}$$

In the expression above the entry $E_j^{(r)}[l] = 0$ if there is no path moving downwards at the vertex $V_{i_r l}$ and reaching destination b_j. Finally we associate to the boundary source a vector

$$E^{(r)}[i_r] = (0, \dots, 0, 1, 0, \dots, 0), \tag{4.4}$$

with non zero entry in the i_r-th column. Then the following Lemma holds true.

Lemma 4.1. *Let A be the reduced row echelon form matrix representing a given point in the matroid stratum $\mathcal{S}_{\mathcal{M}}^{TNN} \subset Gr^{TNN}(k,n)$ and let D be the corresponding Le–diagram. Let $E^{(r)}[i]$, $E^{(r)}[l]$, c_l^i as in (4.2), (4.3) and (4.4), with $r \in [k]$, $i_r \in I$, $l \in \bar{I}$, such that the box $B_{i_r l}$ is filled by 1. Then, the r–th row of A is*

$$A[r] = E^{(r)}[i_r] + \sum_{s=1}^{N_r} c_{l_s}^r E^{(r)}[l_s], \tag{4.5}$$

where the sum runs over the indexes $l_s \in \bar{I}$ such that the index in (A.4) is $\chi_{l_s}^{i_r} = 1$.

The proof is trivial and is omitted. Let us remark that the vectors $E^{(r)}[i_r]$, $E^{(r)}[l_s]$, $s \in N_r$, form a minimal system of vectors to represent the r-th row of the reduced row echelon matrix.

4.2. **Recursive construction of the row vectors $E^{(r)}[l]$ using the Le–diagram.** In Theorem 4.1 we provide a recursive representation for the above system of vectors using the Le–tableau starting from the last row ($r = k$) and moving upwards till the first row ($r = 1$).

For any fixed $r \in [k]$, we first complete the system of vectors introduced in the previous section to a convenient basis in $\mathbb{R}^n$, given by the rows of $n \times n$ matrix $\hat{E}^{(r)}$. For $r = k$, we use the canonical basis in $\mathbb{R}^n$. We pass from the basis associated to the r-th row to the one associated to the $(r-1)$–th row applying a transition matrix $C^{[r-1,r]}$: $\hat{E}^{(r-1)} = C^{[r-1,r]} \hat{E}^{(r)}$. Each transition matrix $C^{[r-1,r]}$ keeps track of empty and non–empty boxes of the r–th row of the Le-tableau, and is upper triangular by definition. The choice of signs in $C^{[r-1,r]}$ in (4.6) keeps track of the sign changes when passing a pivot column. We also complete each set of coefficients c_l^r in (4.2) to a row vector $\hat{c}^{(r)}$, with l indexing the column position.

This construction is a corollary to the Lindström lemma in the case of acyclic graphs and, for points $[A] \in Gr^{\mathrm{TP}}(k,n)$, is also the combinatorial version of the recursive algebraic construction in [3] for a different choice of the basic vectors and therefore of the representative matrix A. In [4] we give general rules to construct well defined systems of vectors on any network and for any orientation.

Theorem 4.1 is used in section 5.1 to define a vacuum edge wave function and its dressing on $\mathcal{N}$. Such vacuum edge wave function (respectively its dressing)

(1) rules the behavior of the vacuum wave function (respectively the dressed wave function) on Γ at all marked points;
(2) satisfies linear relations at the inner vertices of $\mathcal{N}$ which are used to detect the position of the vacuum (resp. dressed) divisor points.

Theorem 4.1. (The recursive algebraic construction) *Let $[A] \in \mathcal{S}_{\mathcal{M}}^{TNN} \subset Gr^{TNN}(k,n)$ with pivot set $I = \{1 \le i_1 < i_2 < \cdots < i_k \le n\}$. Let T and $\mathcal{N}$ respectively be the Le–tableau and its acyclically oriented bipartite Le–network. For any $r \in [k]$, $j \in \bar{I}$, let the index $\chi_j^{i_r}$ be as in (A.4). Let us define the following collections of $n \times n$ invertible matrices $\hat{E}^{(r)}$, $n \times n$ transition matrices $C^{[r-1,r]}$ and row vectors $\hat{c}^{(r)}$, $r \in [k]$, associated to $\mathcal{N}$:*

(1) $\hat{E}^{(k)}$ is the $n \times n$ identity matrix and we denote its row vectors as $\hat{E}^{(k)}[l]$, $l \in [n]$;
(2) For $r \in [k]$, define the $n \times n$ transition matrix $C^{[r-1,r]}$ as follows:

$$C_j^{[r-1,r],l} = \begin{cases} \delta_j^l, & \text{if } l \in [1, i_r[, \quad j \in [n], \\ -1 & \text{if } l = j = i_r, \\ -\hat{w}_{i_r j}^{(r)}, & \text{if } l = i_r, \quad j \in]i_r, n] \text{ and } \quad \chi_j^{i_r} = 1, \\ -\hat{w}_{lj}^{(r)}, & \text{if } l, j \in \bar{I} \cap]i_r, n], \quad j \ge l, \quad \chi_j^{i_r}\chi_l^{i_r} = 1, \\ -\delta_j^l, & \text{if } l \in \bar{I} \cap]i_r, n], \quad \chi_l^{i_r} = 0, \quad j \in [n], \\ -\delta_j^l, & \text{if } l \in I \cap]i_r, n], \quad j \in [n], \\ 0 & \text{otherwise,} \end{cases} \tag{4.6}$$

where

(a) for $l, j \in \bar{I} \cap]i_r, n]$, $j \ge l$, $\hat{w}_{lj}^{(r)}$ is the weight of the directed horizontal path from the black vertex $V'_{i_r l}$ to the white vertex $V_{i_r j}$. In particular $\hat{w}_{ll}^{(r)} = 1$;
(b) for $l = i_r$ and $j \in \bar{I}$, $\hat{w}_{i_r j}^{(r)}$ is the weight of the directed horizontal path from the vertex V_{i_r} to the white vertex $V_{i_r j}$.

(3) The matrices $\hat{E}^{(r-1)}$ are recursively computed as r decreases from k to 2, by

$$\hat{E}^{(r-1)} = C^{[r-1,r]}\hat{E}^{(r)}. \tag{4.7}$$

(4) For any $r \in [k]$, the l–element of the row vector $\hat{c}^{(r)}$, $l \in [n]$, is

$$\hat{c}_l^{(r)} = \begin{cases} 1 & \text{if } l = i_r, \\ c_l^r & \text{if } \chi_l^{i_r} = 1, \\ 0 & \text{otherwise}, \end{cases} \tag{4.8}$$

with c_l^r as in (4.2).

Then

(1) For $r \in [k-1]$ $\hat{E}^{(r)}$ is the $n \times n$ matrix such that

$$\hat{E}^{(r)}[l] = \begin{cases} \hat{E}^{(k)}[l] & \text{if } l \le i_r, \\ (-1)^{\sigma_{sr}} A[s] & \text{if } l = i_s, \text{ and } s \in]r,k], \\ E^{(r)}[l] & \text{if } l \in \bar{I} \cap]i_r, n], \text{ and } \chi_l^r = 1, \end{cases} \tag{4.9}$$

with $E^{(r)}[l]$ as in (4.3) and $\sigma_{sr} = \#\{i_t \in I, r \le t < s\}$;

(2) For any $r \in [k]$,

$$A[r] = \sum_{l=1}^{n} \hat{c}_l^r \hat{E}^{(r)}[l] \equiv E^{(r)}[i_r] + \sum_{s=1}^{N_r} c_{l_s}^r E^{(r)}[l_s], \tag{4.10}$$

where the second sum is over the indexes such that $\chi_{l_s}^{i_r} = 1$.

Remark 4.1. Changing the orientation of the graph *Any change of orientation in $\mathcal{N}$ corresponds to the composition of elementary changes of orientation* [62]*, either corresponding to a change of the base in the matroid $\mathcal{M}$ of $[A]$ or to a change of orientation in a cycle of the graph. We postpone to* [4] *a thorough explanation of how the system of vectors on any given network representing $[A]$ is effected by such elementary changes and the proof that both the normalized dressed wave function and the effective KP divisor are not affected by them.*

Proof. (4.10) follows immediately from Lemma 4.1, (4.8) and (4.9).

The first statement in (4.9), $\hat{E}^{(r)}[l] = \hat{E}^{(k)}[l]$ for $l \le i_r$, $r \in [k]$ is trivial by definition of the transition matrix (4.6). The remaining statements in (4.9) follow by induction in the index r as it decreases from k to 1. Indeed, for $r = k$, the transition matrix $C^{[k-1,k]}$

(1) Leaves invariant all canonical basis vectors $\hat{E}^{(k)}[l]$ for all $l < i_k$;

(2) Transforms the canonical basis vector $\hat{E}^{(k)}[i_k]$ to $-A[k]$, if $l = i_k$;

(3) Changes the sign of the canonical basis vector, $\hat{E}^{(k-1)}[l] = -\hat{E}^{(k)}[l]$, if $l \in \bar{I} \cap]i_k, n]$ and $\chi_l^{i_k} = 0$;

(4) Acts untrivially only if $l \in \bar{I} \cap]i_k, n]$ and $\chi_l^{i_k} = 1$. In such case, the components of $\hat{E}^{(k-1)}[l]$ are transformed to

$$\hat{E}_j^{(k-1),l} = \begin{cases} 0 & \text{if } j < l, \\ -1 & \text{if } j = l, \\ 0 & \text{if } j > l \text{ and } \chi_j^{i_k} = 0, \\ -\hat{w}_{lj}^{(k)} & \text{if } j > l \text{ and } \chi_j^{i_k} = 1. \end{cases}$$

It is straightforward to verify that $\hat{E}^{(k-1)}[l] = E^{(k-1)}[l]$, if $l = i_{k-1}$ or $\chi_l^{i_{k-1}} = 1$, for $l \geq i_{k-1}$. Indeed if both $\chi_l^{i_{k-1}} = 1$ and $\chi_l^{i_k} = 1$, the white vertex $V_{i_{k-1}l}$ is joined to the black vertex $V'_{i_k l}$ by an edge of weight 1 so that by definition $\hat{E}^{(k-1)}[l] = E^{(k-1)}[l]$. If $\chi_l^{i_{k-1}} = 1$ and $\chi_l^{i_k} = 0$, the white vertex $V_{i_{k-1}l}$ is joined to the boundary vertex b_l by an edge of unit weight and $\hat{E}^{(k-1)}[l] = E^{(k-1)}[l]$.

Let us now suppose to have verified (4.9), for any $s \in [r, k]$ and let's verify it for $s = r - 1$. By definition

$$\hat{E}^{(r-1)} = C^{[r-1,r]}\hat{E}^{(r)} = C^{[r-1,r]}C^{[r,r+1]}\hat{E}^{(r+1)} = \cdots = \left(\prod_{s=r}^{k} C^{[s-1,s]}\right)\hat{E}^{(k)}. \tag{4.11}$$

Let $l \in \bar{I} \cap]i_{r-1}, n]$ be fixed. If $\chi_l^{i_{r-1}} = 0$, then there is no contribution to $A[r-1]$ from the vector $\hat{E}^{(r-1)}[l]$ since the coefficient $\hat{c}_l^{r-1} = 0$. Suppose now that $\chi_l^{i_{r-1}} = 1$ and consider the set $S = \{ s \in [r, k] \, : \, \chi_l^{i_s} = 1 \}$. If $S = \emptyset$, then the white vertex $V_{i_{r-1}l}$ is joined directly to the boundary sink b_l by an edge of unit weight and

$$\hat{E}^{(r-1)}[l] = (-1)^{k-r+1}\hat{E}^{(k)}[l] = (-1)^{k-r+1}E^{(k)}[l] = E^{(r-1)}[l].$$

Otherwise, let $\bar{s} = \min S$. In this case moving downwards from the white vertex $V_{i_{r-1}l}$ the first black vertex that we meet is $V'_{i_{\bar{s}}l}$ and such edge has unit weight. Then, using (4.11), we have

$$\hat{E}^{(r-1)}[l] = (-1)^{\bar{s}-r+1}\hat{E}^{(\bar{s})}[l] = (-1)^{\bar{s}-r+1}E^{(\bar{s})}[l] = E^{(r-1)}[l].$$

Finally let $l = i_r$. In such case

$$\hat{E}^{(r-1)}[i_r] = C^{[r-1,r]}[i_r]\hat{E}^{(r)} = -\sum_{j=1}^{n} \hat{c}_j^r \hat{E}^{(r)}[j] = -A[r].$$

since, by definition $C_j^{[r-1,r],i_r} = -\hat{c}_j^r$ and $\hat{c}_j^r$ is non zero if and only if $j = i_r$ or $j \in \bar{I} \cap]i_r, n]$ is such that $\chi_j^{i_r} = 1$. □

Remark 4.2. ***Comparison with the algebraic construction in*** [3] *Lemma 4.1 and Theorem 4.1 generalize the algebraic construction in* [3] *for points in* $Gr^{TP}(k,n)$ *to any point in* $Gr^{TNN}(k,n)$*. The main difference is in the choice of the representative matrix: here* A *is the RREF matrix while in* [3] *we use a matrix in banded form.*

Example 4.1. *Let us apply Theorem 4.1 to the Le–network in Figure 22 representing Example A.2.* $\hat{E}^{(4)} = Id_{9\times 9}$*, the only non–zero coefficients associated to the forth row of* A *are* $\hat{c}^4_7 = 1$*,* $\hat{c}^4_8 = w_{78}$ *and clearly* $A[4] = \hat{c}^4\hat{E}^{(4)}$*. Then*

$$\hat{E}^{(3)} \equiv C^{[3,4]} = \begin{pmatrix} I_{6\times 6} & & 0_{6\times 3} & \\ & -1 & -w_{78} & 0 \\ 0_{3\times 6} & 0 & -1 & 0 \\ & 0 & 0 & -1 \end{pmatrix},$$

where $0_{i\times j}$ *is the* $(i\times j)$ *null matrix, while* $I_{l\times l}$ *is the* $(l\times l)$ *identity matrix. The third row coefficient vector is* $\hat{c}^3 = (\,0\,,0\,,0\,,1\,,w_{45}\,,w_{45}w_{46}\,,0\,,w_{45}w_{46}w_{48}\,,w_{45}w_{46}w_{48}w_{49}\,)$*, and* $A[3] = \hat{c}^3\hat{E}^{(3)}$*. The transition matrix from the third to the second row* $C^{[2,3]}$*, the new basis vectors* $\hat{E}^{(2)}$ *and the coefficient vector* $\hat{c}^2$ *of the second row respectively are*

$$C^{[2,3]} = \begin{pmatrix} I_{3\times 3} & & & 0_{3\times 6} & & \\ & -1 & -w_{45} & -w_{45}w_{46} & 0 & -w_{45}w_{46}w_{48} & -w_{45}w_{46}w_{48}w_{49} \\ & 0 & -1 & -w_{46} & 0 & -w_{46}w_{48} & -w_{46}w_{48}w_{49} \\ & 0 & 0 & -1 & 0 & -w_{48} & -w_{48}w_{49} \\ 0_{6\times 3} & 0 & 0 & 0 & -1 & 0 & 0 \\ & 0 & 0 & 0 & 0 & -1 & -w_{49} \\ & 0 & 0 & 0 & 0 & 0 & -1 \end{pmatrix},$$

$$\hat{E}^{(2)} = C^{[2,3]}\hat{E}^{(3)} = \begin{pmatrix} Id_{3\times 3} & & & 0_{3\times 6} & & \\ & -1 & -w_{45} & -w_{45}w_{46} & 0 & w_{45}w_{46}w_{48} & w_{45}w_{46}w_{48}w_{49} \\ & 0 & -1 & -w_{46} & 0 & w_{46}w_{48} & w_{46}w_{48}w_{49} \\ & 0 & 0 & -1 & 0 & w_{48} & w_{48}w_{49} \\ 0_{6\times 3} & 0 & 0 & 0 & 1 & w_{78} & 0 \\ & 0 & 0 & 0 & 0 & 1 & w_{49} \\ & 0 & 0 & 0 & 0 & 0 & 1 \end{pmatrix},$$

$\hat{c}^2 = (\,0\,,1\,,w_{23}\,,0\,,w_{23}w_{25}\,,0\,,0\,,0\,,0\,)$*, and* $A[2] = \hat{c}^2\hat{E}^{(2)}$*. Finally, the transition matrix from the second to the first row* $C^{[1,2]}$*, the new basis vectors* $\hat{E}^{(1)}$ *and the coefficient vector* $\hat{c}^1$ *of the*

first row, respectively, are

$$C^{[1,2]} = \begin{pmatrix} 1 & 0 & 0 & 0 & 0 & \\ 0 & -1 & -w_{23} & 0 & -w_{23}w_{25} & \\ 0 & 0 & -1 & 0 & -w_{25} & 0_{5\times 4} \\ 0 & 0 & 0 & -1 & 0 & \\ 0 & 0 & 0 & 0 & -1 & \\ & & & 0_{5\times 1} & & -Id_{4\times 4} \end{pmatrix},$$

$$\hat{E}^{(1)} = C^{[1,2]}\hat{E}^{(2)} = \begin{pmatrix} 1 & 0 & 0 & 0 & 0 & 0 & 0 & 0 & 0 \\ 0 & -1 & -w_{23} & 0 & w_{23}w_{25} & w_{23}w_{25}w_{46} & 0 & -w_{23}w_{25}w_{46}w_{48} & -w_{23}w_{25}w_{46}w_{48}w_{49} \\ 0 & 0 & -1 & 0 & w_{25} & w_{25}w_{46} & 0 & -w_{25}w_{46}w_{48} & -w_{25}w_{46}w_{48}w_{49} \\ 0 & 0 & 0 & 1 & w_{45} & w_{45}w_{46} & 0 & -w_{45}w_{46}w_{48} & -w_{45}w_{46}w_{48}w_{49} \\ 0 & 0 & 0 & 0 & 1 & w_{46} & 0 & -w_{46}w_{48} & -w_{46}w_{48}w_{49} \\ 0 & 0 & 0 & 0 & 0 & 1 & 0 & -w_{48} & -w_{48}w_{49} \\ 0 & 0 & 0 & 0 & 0 & 0 & -1 & -w_{78} & 0 \\ 0 & 0 & 0 & 0 & 0 & 0 & 0 & -1 & -w_{49} \\ 0 & 0 & 0 & 0 & 0 & 0 & 0 & 0 & -1 \end{pmatrix},$$

$\hat{c}^1 = (\,1\,,0\,,0\,,0\,,w_{15}\,,w_{15}w_{16}\,,0\,,0\,,w_{15}w_{16}w_{19}\,)$, *and* $A[1] = \hat{c}^1\hat{E}^{(1)}$.

5. Proof of Theorem 3.1 on Γ

Throughout this Section we fix the KP regular soliton data, *i.e.* n ordered real phases $\mathcal{K} = \{\kappa_1 < \cdots < \kappa_n\}$ and a point $[A] \in \mathcal{S}^{\rm TNN}_{\mathcal{M}} \subset Gr^{\rm TNN}(k,n)$, $\dim \mathcal{S}^{\rm TNN}_{\mathcal{M}} = g$. $I = \{i_1, \dots, i_k\}$ is the lexicographically minimal base of $\mathcal{M}$ (the pivot set for any matrix A representing $[A]$); T and $\mathcal{N}$ are the Le–tableau and the acyclically oriented bipartite Le–network representing $[A]$, see [62] and, also, Appendix A. Finally, Γ is the curve associated to the Le–graph as in Construction 3.1.

The idea of the proof of Theorem 3.1 is to extend the vacuum wave function from Γ_0 to Γ using the network to define the values of the wave function at the double points and at the Darboux points so that it admits a good meromorphic extension, and the divisor has the desired properties. At this aim, we first modify the Le-network by adding an edge and an internal vertex in correspondence of each Darboux point in Γ, and transform the boundary sources into boundary sinks (see Figure 8). Then, in Section 5.1 we use the algebraic construction of the previous section to define a system of edge vectors and a vacuum and a dressed edge wave functions on the modified Le–network. In Section 5.2 we use the linear relations satisfied by the edge wave functions at the internal vertices to assign to each trivalent white vertex a pair of real numbers, which we call vacuum and dressed network divisor numbers respectively. Finally,

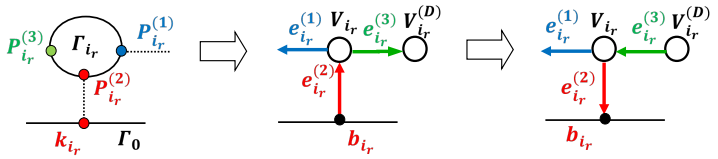

FIGURE 8. *The modified graph $\mathcal{N}'$ is obtained adding an edge $e_{i_r}^{(3)}$ at each pivot vertex V_{i_r} and a white vertex $V_{i_r}^{(D)}$. The orientation in $\mathcal{N}'$ is the same as in the initial network $\mathcal{N}$ except at the edge $e_{i_r}^{(2)}$.*

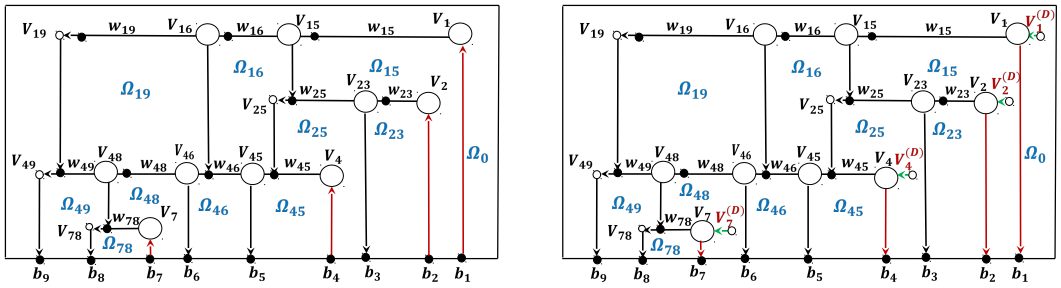

FIGURE 9. *The transformation from the Le-Network $\mathcal{N}$ (left) to the modified Le-network $\mathcal{N}'$ (right) for Example A.2 (see also Figure 19).*

in Section 5.3, we extend the normalized vacuum and dressed edge wave functions to Γ in such a way that the network divisor numbers become the local coordinates of the pole divisors of such wave functions, and we prove that the vacuum divisor satisfies the reality and regularity conditions of Theorem 3.1.

Definition 5.1. ***The planar oriented trivalent bipartite network $\mathcal{N}'$:*** *Denote $\mathcal{N}'$ the network obtained from $\mathcal{N}$ adding a unit edge $e_{i_r}^{(3)}$ at each pivot vertex V_{i_r} in the position corresponding to the Darboux point $P_{i_r}^{(3)} \in \Gamma_{i_r}$ and let $V_{i_r}^{(D)}$ be the white vertex at the other end of $e_{i_r}^{(3)}$. Such move corresponds to Move (M2) - unicolored edge contraction/uncontraction and still represents the same point in the Grassmannian* [62]. *Then orient all edges in $\mathcal{N}'$ as in $\mathcal{N}$ except the edges $e_{i_r}^{(2)}$, which point from V_{i_r} to b_{i_r}, and $e_{i_r}^{(3)}$, $r \in [k]$, which point from $V_{i_r}^{(D)}$ to V_{i_r}, for any $r \in [k]$ (see Figure 8).*

For an example of transformation from $\mathcal{N}$ to $\mathcal{N}'$ see Figure 9.

Remark 5.1. ***Data and notations.*** *From now on we use the modified network $\mathcal{N}'$ with the orientation as in Definition 5.1 and, in addition to the assumptions made in the beginning of this Section, we settle the following notations:*

(1) N_r, $r \in [k]$, is the number of filled boxes in the row r of the Le-tableaux of A, $\chi^i_j \in \{0,1\}$ is the index of the box $B_{i,j}$ (see (A.3) and (A.4));

(2) The pivot indexes are denoted $1 \le i_1 < \cdots < i_k \le n$ and, for any $r \in [k]$, $1 \le j_1 < j_2 < \cdots < j_{N_r} \le n$ are the non–pivot indexes of the boxes B_{i_r,j_s} of index $\chi^{i_r}_{j_s} = 1$, $s \in [N_r]$;

(3) The index $j_0 \equiv 0$ is associated to the vertices, $V_{i_r 0} \equiv V_{i_r}$, and to any quantity referring to them;

(4) The edges $e^{(m)}_{i_r j_l}$, $m \in [3]$, are enumerated with the indexes of its incident white vertex $V_{i_r j_l}$, $r \in [k]$ and $l \in [0, N_r]$ (see Figures 3 and 8). Finally, the vertices $V_{i_r j_{N_r}}$ have two edges which we label $e^{(2)}_{i_r j_l}$ and $e^{(3)}_{i_r j_l}$;

(5) The families of matrices $\hat{E}^{(r)}$ and vectors $\hat{c}^{(r)}$, $r \in [k]$, are as in Theorem 4.1;

(6) $\mathfrak{E}_\theta(\vec{t}) = (e^{\theta_1(\vec{t})}, \dots, e^{\theta_n(\vec{t})})$, where $\theta_j(\vec{t}) = \sum_{l \ge 1} \kappa^l_j t_l$ and $\vec{t} = (t_1 = x, t_2 = y, t_3 = t, t_4, \dots)$ are the KP times, and $\prec \cdot, \cdot \succ$ denotes the usual scalar product;

(7) On each component of Γ, ζ is the coordinate of Definition 3.1.

In the statements of the Theorems and in the Definitions below we shall not explicitly mention the above data.

5.1. **Vacuum and dressed edge wave functions on the modified Le–network.** We now define a system of vectors $\mathfrak{E}^{(m)}_{i_r j_l}$ on the edges of $\mathcal{N}'$ using the vectors introduced in Section 4. First of all, in $\mathcal{N}'$, for each fixed $r \in [k]$ and $l \in [0, N_r]$ we assign the row vector $E^{(r)}[j_l]$ to the vertical edge $e^{(2)}_{i_r j_l}$ at the white vertex $V_{i_r j_l} \in \mathcal{N}'$: $\mathfrak{E}^{(2)}_{i_r j_l} \equiv E^{(r)}[j_l]$. We then assign a vector also at each horizontal edge using linear relations at inner black and white vertices (see Definition 5.2). The vacuum edge wave function $\Phi^{(m)}_{ij}(\vec{t})$ at the edge $e^{(m)}_{ij} \in \mathcal{N}'$ is just the product of the edge vector $\mathfrak{E}^{(m)}_{ij}$ with the vector $\mathfrak{E}_\theta(\vec{t})$: $\Phi^{(m)}_{ij}(\vec{t}) = \prec \mathfrak{E}^{(m)}_{ij}, \mathfrak{E}_\theta(\vec{t}) \succ$.

Finally, by construction, the edge vector assigned to $e^{(3)}_{i_r}$ is the r-th row of the RREF matrix, for any $r \in [k]$, and, therefore, the vacuum edge wave function at $e^{(3)}_{i_r}$ coincides with one of the heat hierarchy solutions generating the Darboux transformation (see Lemma 5.2).

Definition 5.2. Edge vectors (e.v.) and vacuum edge wave function (v.e.w.) on $\mathcal{N}'$. *Let the soliton data and the notations be fixed as in Remark 5.1. To each edge of $\mathcal{N}'$, we associate an edge vector (e.v.) and a vacuum edge wave function (v.e.w.) depending on $\vec{t}$ as follows:*

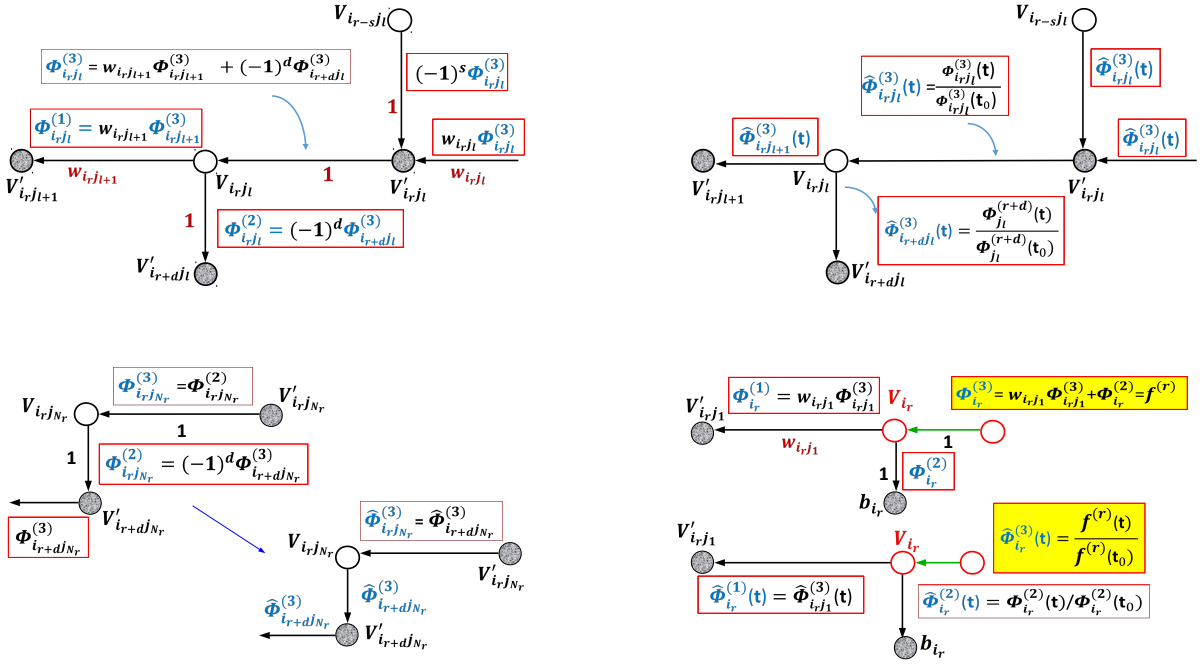

FIGURE 10. *The linear relations for the vacuum edge wave function* $\Phi^{(m)}_{i_rj_l}(\vec{t})$ *at white and black vertices [top,left]. The normalized v.e.w.* $\hat{\Phi}^{(m)}_{i_rj_l}(\vec{t})$ *takes the same value at all the edges at a given black vertex* $V'_{i_rj_l}$ *and different values at the edges at a given trivalent white vertex* $V_{i_rj_l}$ *[top right]. The same at the bivalent white vertex* $V_{i_rj_{N_r}}$ *[bottom,left] and at the vertex* V_{i_r}, $i_r \in I$ *[bottom, right]. Also the dressed edge wave function satisfies the same linear relations.*

(1) For any $r \in [k]$, *to the vertical edge* $e^{(2)}_{i_r}$ *joining the white vertex* V_{i_r} *to the boundary vertex* b_{i_r}, *we assign e.v. and v.e.w.*

$$\mathfrak{E}^{(2)}_{i_r} = \hat{E}^{(k)}[i_r], \qquad \Phi^{(2)}_{i_r}(\vec{t}) \equiv\prec \hat{E}^{(k)}[i_r], \mathfrak{E}_\theta(\vec{t}) \succ= e^{\theta_{ir}(\vec{t})}; \tag{5.1}$$

(2) For any fixed $r \in [k]$ *and* $l \in [N_r]$, *to the vertical edge* $e^{(2)}_{i_rj_l}$ *at the white vertex* $V_{i_rj_l}$ *we assign*

$$\mathfrak{E}^{(2)}_{i_rj_l} = \hat{E}^{(r)}[j_l], \qquad \Phi^{(2)}_{i_rj_l}(\vec{t}) \equiv\prec \mathfrak{E}^{(2)}_{i_rj_l}, \mathfrak{E}_\theta(\vec{t}) \succ; \tag{5.2}$$

(3) For any $r \in [k]$, *to the horizontal edge* $e^{(3)}_{i_rj_{N_r}}$ *joining the black vertex* $V'_{i_rj_{N_r}}$ *to the white vertex* $V_{i_rj_{N_r}}$ *of the r-th row we assign:*

$$\mathfrak{E}^{(3)}_{i_rj_{N_r}} = \mathfrak{E}^{(2)}_{i_rj_{N_r}}, \qquad \Phi^{(3)}_{i_rj_{N_r}}(\vec{t}) \equiv\prec \mathfrak{E}^{(3)}_{i_rj_{N_r}}, \mathfrak{E}_\theta(\vec{t}) \succ= \Phi^{(2)}_{i_rj_{N_r}}(\vec{t}) \tag{5.3}$$

(4) For any $r \in [k]$, $l \in [0, N_r - 1]$, *to the horizontal edge* $e^{(1)}_{i_rj_l}$ *joining the white vertex* $V_{i_rj_l}$ *to the black vertex* $V'_{i_rj_{l+1}}$ *we assign*

$$\mathfrak{E}^{(1)}_{i_rj_l} = w_{i_rj_{l+1}}\mathfrak{E}^{(3)}_{i_rj_{l+1}}, \qquad \Phi^{(1)}_{i_rj_l}(\vec{t}) \equiv\prec \mathfrak{E}^{(1)}_{i_rj_l}, \mathfrak{E}_\theta(\vec{t}) \succ= w_{i_rj_{l+1}}\Phi^{(3)}_{i_rj_{l+1}}(\vec{t}), \tag{5.4}$$

where $w_{i_r j_1}$ is the weight of $e^{(1)}_{i_r j_l}$. Here $j_0 = 0$;

(5) For any $r \in [k]$, $l \in [0, N_r - 1]$, to the edge $e^{(3)}_{i_r j_l}$ joining the black vertex $V'_{i_r j_l}$ to the white vertex $V_{i_r j_l}$ we assign

$$\mathfrak{E}^{(3)}_{i_r j_l} = \mathfrak{E}^{(1)}_{i_r j_l} + \mathfrak{E}^{(2)}_{i_r j_l}, \qquad \Phi^{(3)}_{i_r j_l}(\vec{t}) \equiv\prec \mathfrak{E}^{(3)}_{i_r j_l}, \mathfrak{E}_\theta(\vec{t}) \succ= \Phi^{(1)}_{i_r j_l}(\vec{t}) + \Phi^{(2)}_{i_r j_l}(\vec{t}), \tag{5.5}$$

i.e. the sum of the contributions from the edges to the left and below $V_{i_r j_l}$.

We illustrate Definition 5.2 in Figure 10.

Remark 5.2. ***Edge vectors and oriented paths in $\mathcal{N}'$.*** *It is easy to check that, for any given edge e, the absolute value of the j–th component of the vector at e is simply the sum of the weights of all the paths starting at e and having destination b_j and the sign of such component depends only on the number of boundary sources in $]i_r, j[$, where $r \in [k]$ is the biggest index such that there exists a walk from the Darboux source vertex $V^{(D)}_{i_r}$ to e. Recall that the acyclic orientation of $\mathcal{N}'$ is associated to the lexicographically minimal base I; therefore there is a canonical way to count the number of Darboux sources for any path from an internal edge e to a destination b_j, and it is also straightforward to check that all paths from e to b_j are assigned the same sign.*

Definition 5.3. The dressed edge wave function (d.e.w.) on $\mathcal{N}'$. *In the setting of Definition 5.2, for any fixed $r \in [k]$ and $l \in [0, N_r]$, we define the dressed edge wave function $\Psi^{(m)}_{i_r j_l}(\vec{t})$ on the edge $e^{(m)}_{i_r j_l} \in \mathcal{N}'$ as the dressing of the v.e.w. $\Phi^{(m)}_{i_r j_l}(\vec{t})$*

$$\Psi^{(m)}_{i_r j_l}(\vec{t}) = \mathfrak{D}\Phi^{(m)}_{i_r j_l}(\vec{t}), \tag{5.6}$$

where $\mathfrak{D}$ is the Darboux transformation associated to the given soliton data $(\mathcal{K}, [A])$.

Remark 5.3. *In* [4]*, we generalize the construction of edge vectors (and edge wave functions) to any network representing $[A]$ in Postnikov class and adapt the construction in* [62, 68] *to express the components of the edge vectors in case of non acyclic orientations. In the latter case one has to deal with sums over infinite number if paths.*

By construction, the system of edge vectors $\mathfrak{E}^{(m)}_{i_r, j_l}$, the v.e.w. $\Phi^{(m)}_{i_r j_l}(\vec{t})$ and the d.e.w. $\Psi^{(m)}_{i_r j_l}(\vec{t})$ on $\mathcal{N}'$ solve the following linear system at the inner vertices of $\mathcal{N}'$ under suitable boundary conditions.

Lemma 5.1. ***The linear system in $\mathcal{N}'$*** *Let $G_j(\vec{t})$, $j \in [n]$, be smooth functions in $\vec{t}$. Then there exists a unique function $G_e(\vec{t})$ defined on the edges e of $\mathcal{N}'$ satisfying for all $\vec{t}$:*

(1) *For any* $r \in [k]$ *and* $l \in [0, N_r]$, *on the unit edge* $e^{(3)}_{i_r j_l}$ *pointing in at the white vertex* $V_{i_r j_l}$, *define* $G_{e^{(3)}_{i_r,j_l}}$ *as the sum of the values of* G_e *on the edges* $e = e^{(1)}_{i_r j_l}, e^{(2)}_{i_r j_l}$ *pointing out at* $V_{i_r j_l}$*:*

$$G_{e^{(3)}_{i_r,j_l}}(\vec{t}) = G_{e^{(1)}_{i_r j_l}}(\vec{t}) + G_{e^{(2)}_{i_r j_l}}(\vec{t});$$

(2) *For any* $r \in [k]$ *and* $l \in [0, N_r - 1]$, *on the horizontal edge* $e^{(1)}_{i_r j_l}$ *of weight* $w_{i_r j_l}$ *pointing in at the black vertex* $V'_{i_r j_{l+1}}$, *define* $G_{e^{(1)}_{i_r,j_l}}$ *as*

$$G_{e^{(1)}_{i_r,j_l}}(\vec{t}) = w_{i_r j_{l+1}} G_{e^{(3)}_{i_r,j_{l+1}}}(\vec{t}),$$

where $e^{(3)}_{i_r,j_{l+1}}$ *is the unique edge pointing out at* $V'_{i_r j_{l+1}}$*;*

(3) *For any* $r \in [k]$, *the unit vertical edge* $e^{(2)}_{i_r}$ *joins the white vertex* V_{i_r} *to the boundary vertex* b_{i_r}. *Define*

$$G_{e^{(2)}_{i_r j_l}}(\vec{t}) = G_{i_r}(\vec{t});$$

(4) *For any* $r \in [N_r]$, *if the unit vertical edge* $e^{(2)}_{i_r,j_l}$ *joins the white vertex* V_{i_r,j_l} *to the boundary vertex* b_{j_l}, *define*

$$G_{e^{(2)}_{i_r j_l}}(\vec{t}) = G_{j_l}(\vec{t}).$$

Otherwise, the black vertex $V'_{i_{\bar{s}} j_l}$, *with* $\bar{s} = \min S$, *with* $S = \{ s \in [r+1, k] : \chi^{i_s}_{j_l} = 1 \} \neq \emptyset$ *as in the proof of Theorem 4.1, is the ending vertex of* $e^{(2)}_{i_r j_l}$, $d = d(i_r j_l) = \bar{s} - r$ *is the number of pivot indexes in the interval* $]i_r, j_l[$ *and define*

$$G_{e^{(2)}_{i_r j_l}}(\vec{t}) = (-1)^d G_{e^{(3)}_{i_{r+d} j_l}}(\vec{t}).$$

In particular, if we assign the boundary conditions $G_j(\vec{t}) \equiv \Phi^{(2)}_j(\vec{t})$, *(respectively* $G_j(\vec{t}) \equiv \Psi^{(2)}_j(\vec{t})$*), for all* $j \in [n]$, *then the edge function coincides with the v.e.w. of Definition 5.2 (respectively with the d.e.w. of Definition 5.3).*

Proof. First let $\mathcal{N}'$ correspond to an irreducible positroid cell $\mathcal{S}^{\mathrm{TNN}}_{\mathcal{M}} \subset Gr^{\mathrm{TNN}}(k, n)$ of dimension g. Then, the number of variables in the linear system defined in the above Lemma is equal to the number of edges, $3g + 2k$ ($g + k$ vertical edges and $2g + k$ horizontal edges). Any trivalent black vertex carries two equations, while each bivalent black vertex carries one condition. There are g internal black vertices, and $g - n + k$ of them are trivalent. Therefore the total number of equations at black vertices is $2g - n + k$. The total number of equations at white vertices is $g + k$, since the total number of internal white vertices is $g + 2k$, but the univalent Darboux vertices on $\mathcal{N}'$ do not carry any extra condition. So, we may freely impose a value to n variables (edges).

The presence of an isolated boundary sink b_j implies the addition of an internal univalent vertex joined to b_j: we have a new variable (the univalent edge) and no extra condition. The presence of an isolated boundary source b_i implies the addition of a bivalent vertex V_i and of an univalent Darboux vertex $V_i^{(D)}$: we have two variables and one equation.

The system is well-defined and the solution is unique because the network is acyclic. Finally the system can be solved recurrently. □

Remark 5.4. *We remark that the linear relations satisfied by the edge vectors, the vacuum edge wave function and its dressing at the black and white vertices (see Definition 5.2 and Figure 10) are of the same type as those imposed by momentum conservation at trivalent vertices of on–shell diagrams in* [7, 8] *(formulas (4.54) and (4.55) in* [7]*).*

Comparing Theorem 4.1 and Definition 5.2, it is not difficult to prove that the e.v. at the Darboux edge $e_{i_r}^{(3)}$ coincides with the r–th row of the RREF matrix A (see equation 5.8 below); therefore the v.e.w. at the same edge is $f^{(r)}(\vec{t})$ as required in Theorem 3.1.

Lemma 5.2. *Let the soliton data and the notations be fixed as in Remark 5.1. Let the e.v. and v.e.w. be as in Definition 5.2. Then,*

(1) for any $r \in [k]$ and $l \in [N_r]$, the edge vector at the edge joining $V_{i_r j_l}$, $V'_{i_r j_l}$ is

$$\mathfrak{E}^{(3)}_{i_r j_l} = \sum_{s=l}^{N_r} \hat{c}^r_{j_s} \hat{E}^{(r)}[j_s]; \tag{5.7}$$

(2) for any $r \in [k]$ the edge vector at the edge $e_{i_r}^{(3)}$ is the r–th row of the RREF matrix representing $[A] \in Gr^{TNN}(k,n)$ and the v.e.w. is the r–th generator of the dressing transformation associated to the soliton data $(\mathcal{K}, [A])$

$$\mathfrak{E}^{(3)}_{i_r} = A[r], \qquad \Phi^{(3)}_{i_r}(\vec{t}) = f^{(r)}(\vec{t}). \tag{5.8}$$

Therefore the d.e.w. satisfies $\Psi^{(3)}_{i_r}(\vec{t}) \equiv 0$, for all $r \in [k]$ and for all $\vec{t}$.

The proof of the Lemma easily follows comparing (5.7) and (5.8) with (4.2), (4.7), (4.8) and (4.10) in Theorem 4.1 and with (5.1)–(5.5) in Definition 5.2.

As remarked in the proof of Lemma 5.1, the edge vectors and vacuum and dressed edge wave functions on $\mathcal{N}'$ may be recursively computed using Theorem 4.1 starting from the last row of the corresponding Le–diagram ($r = k$) and moving up decreasing the index r till $r = 1$. For

simplicity, we illustrate the algorithm for the edge vectors only (see also Figure 10 for the edge wave functions).

Algorithm for the edge vectors: For any $r \in [k]$:

(1) If $N_r = 0$, *i.e.* all the boxes of the r–th row of the Le–diagram contain zeros, assign to the white vertex V_r the vector $\hat{E}^{(r)}[i_r] \equiv \hat{E}^{(k+1)}[i_r]$ and proceed to (3);

(2) Otherwise:

(a) Start from the leftmost white vertex of the line, $V_{i_r j_{N_r}}$ and assign to the edge joining $V_{i_r j_{N_r}}$ and $V'_{i_r j_{N_r}}$ the edge vector

$$\mathfrak{E}^{(3)}_{i_r j_{N_r}} = \hat{E}^{(r)}[j_{N_r}]$$

(b) For any l from $N_r - 1$ to 1, assign to the edge joining $V'_{i_r j_l}$ and $V_{i_r j_l}$, the vector

$$\mathfrak{E}^{(3)}_{i_r j_l} = w_{i_r j_{l+1}} \mathfrak{E}^{(3)}_{i_r j_{l+1}} + \hat{E}^{(r)}[j_l].$$

(c) At the white vertex V_r assign the vector

$$\mathfrak{E}^{(3)}_{i_r 0} = w_{i_r j_1} \mathfrak{E}^{(3)}_{i_r j_1} + \hat{E}^{(r)}[i_r] = A[r],$$

and go to (3).

(3) If $r = 1$, just end. Otherwise set the counter to $r - 1$ and repeat the whole procedure.

Example 5.1. *We illustrate such procedure for Example A.2 (see Figure 9[right]). At the horizontal edge joining V_{45} and V'_{45} we assign the edge vector*

$$\mathfrak{E}^{(3)}_{45} = E^{(3)}[5] + w_{46}\mathfrak{E}^{(3)}_{46} = (0, 0, 0, 0, 1, w_{46}, 0, -w_{46}w_{48}, -w_{46}w_{48}w_{49}),$$

since $\mathfrak{E}^{(3)}_{46} = E^{(3)}[6] + w_{48}\mathfrak{E}^{(3)}_{48} = E^{(3)}[6] + w_{48}(\hat{E}^{(3)}[8] + w_{49}\hat{E}^{(3)}[9])$, and the edge wave function

$$\Phi^{(3)}_{45}(\vec{t}) = e^{\theta_5(\vec{t})} + w_{46}e^{\theta_6(\vec{t})} - w_{46}w_{48}e^{\theta_8(\vec{t})} - w_{46}w_{48}w_{49}e^{\theta_9(\vec{t})}.$$

At the horizontal edge joining V_{25} and V'_{25} we associate the edge vector $\mathfrak{E}^{(3)}_{25} = E^{(2)}[5] = -\mathfrak{E}^{(3)}_{45}$ (compare with Example 4.1) and the edge wave function $\Phi^{(3)}_{25}(\vec{t}) = -\Phi^{(3)}_{45}(\vec{t})$ for all times $\vec{t}$.

5.2. **The vacuum and dressed network divisors.** We now assign two real numbers, a vacuum network divisor number $\gamma^{(\mathrm{vac})}_{ij}$ and a dressed network divisor number $\gamma^{(\mathrm{dr})}_{ij}$, to each trivalent white vertex of $\mathcal{N}'$ using the linear system considered in the previous section, after choosing a convenient initial time $\vec{t}_0$ with respect to which we normalize the wave functions. The fact that, for any soliton data $(\mathcal{K}, [A])$, there exists a proper choice of time $\vec{t}_0$ such that both the vacuum and the dressed wavefunctions are non zero at all double points using a is an essential condition to

construct non–special (vacuum and dressed) divisors on Γ. In particular, we use the fact that the all horizontal edge vectors on the r-th row have the highest non-zero component in position j_{N_r}, and these components share the same sign.

Lemma 5.3. ***Choice of the initial time.*** *Let the Le–network $\mathcal{N}'$, the v.e.w. $\Phi_{ij}^{(m)}(\vec{t})$ and the d.e.w. $\Psi_{ij}^{(m)}(\vec{t})$ be as in the previous section for the soliton data $(\mathcal{K}, [A])$. Then there exists x_0 such that for all real $x > x_0$:*

(1) The signs of $\Phi_{i_rj_l}^{(1)}(x, 0, 0, \ldots)$ and $\Phi_{i_rj_l}^{(3)}(x, 0, 0, \ldots)$, for any given $l \in [0, N_r]$, $r \in [k]$, are equal to the sign of their highest non zero coefficient;

(2) The d.e.w. $\Psi_{i_rj_l}^{(m)}(x, 0, 0, \ldots) \neq 0$ on any edge $e_{i_rj_l}^{(m)}$ distinct from the Darboux edges, $e_{i_rj_l}^{(m)} \notin \{e_{i_r}^{(3)} : r \in [k]\}$.

Proof. The first statement easily follows from the definition of the vacuum wave function, since no edge vector is null. For the second statement we recall that we use the reduced Darboux transformation if the soliton data belongs to a reducible cell. Therefore, we assume without loss of generality that $[A]$ belongs to an irreducible cell. The Darboux operator $\mathfrak{D}$ is a regular k-th order ordinary linear differential operator, and the d.e.w. is identically zero by definition at the Darboux edges $e_{i_r}^{(3)}$, $r \in [k]$ and nowhere else. At all other edges the d.e.w. is a linear combination of real exponentials divided by the τ-function. For this reason, the d.e.w. has only finite number of real zeroes, and, if x_0 is sufficiently big, $\Psi_{i_rj_l}^{(m)}(x, 0, 0, \ldots) \neq 0$. □

Definition 5.4. ***The vacuum network divisor $\mathcal{D}_{\mathbf{vac},\mathcal{N}'}$ and the dressed network divisor $\mathcal{D}_{\mathbf{dr},\mathcal{N}'}$.*** *Let $\Phi_{i_rj_l}^{(m)}(\vec{t})$, $\Psi_{i_rj_l}^{(m)}(\vec{t})$ be the vacuum and the dressed edge wave functions on the edges $e_{i_rj_l}^{(m)}$, $m \in [3]$, at $V_{i_rj_l}$ of the network $\mathcal{N}'$. Let $\vec{t}_0 = (x_0, 0, 0, \ldots)$ be fixed as in Lemma 5.3.*

We assign a vacuum network divisor number $\gamma_{i_rj_l}^{(\mathrm{vac})}$ to ***each*** *trivalent white vertex $V_{i_rj_l}$ ($r \in [k]$, $l \in [0, N_r - 1]$) :*

$$\gamma_{i_rj_l}^{(\mathrm{vac})} = \frac{\Phi_{i_rj_l}^{(1)}(\vec{t}_0)}{\Phi_{i_rj_l}^{(1)}(\vec{t}_0) + \Phi_{i_rj_l}^{(2)}(\vec{t}_0)} = \frac{\Phi_{i_rj_l}^{(1)}(\vec{t}_0)}{\Phi_{i_rj_l}^{(3)}(\vec{t}_0)}. \tag{5.9}$$

We call the collection of the g pairs: $\mathcal{D}_{\mathrm{vac},\mathcal{N}'} = \{(\gamma_{i_rj_l}^{(\mathrm{vac})}, V_{i_rj_l}),\ l \in [0, N_r - 1], r \in [k]\}$ the vacuum network divisor on $\mathcal{N}'$.

Analogously, we assign a dressed network divisor number $\gamma^{(\mathrm{dr})}_{i_r j_l}$ *to each trivalent white vertex* $V_{i_r j_l}$ ***not containing a Darboux edge*** *(*$r \in [k]$, $l \in [N_r - 1]$*):*

$$\gamma^{(\mathrm{dr})}_{i_r j_l} = \frac{\Psi^{(1)}_{i_r j_l}(\vec{t}_0)}{\Psi^{(1)}_{i_r j_l}(\vec{t}_0) + \Psi^{(2)}_{i_r j_l}(\vec{t}_0)} = \frac{\Psi^{(1)}_{i_r j_l}(\vec{t}_0)}{\Psi^{(3)}_{i_r j_l}(\vec{t}_0)}. \tag{5.10}$$

We call the collection of the pairs $\mathcal{D}_{\mathrm{dr},\mathcal{N}'} = \{(\gamma^{(\mathrm{dr})}_{i_r j_l}, V_{i_r j_l}),\ l \in [N_r - 1], r \in [k]\}$ *the dressed network divisor on* $\mathcal{N}'$*.*

Remark 5.5. *We do not assign neither vacuum nor dressed network divisor numbers to vertices connected with isolated boundary vertices, since these vertices are not trivalent in our construction.*

Remark 5.6. *If the Le-network corresponds to a point in an irreducible positroid cell in* $Gr^{TNN}(k, n)$*, then* $\mathcal{D}_{\mathrm{dr},\mathcal{N}'}$ *is a collection of* $g - k$ *pairs. If the Le-network corresponds to a point in a reducible positroid cell in* $Gr^{TNN}(k, n)$*, and the reduced cell belongs to* $Gr^{TNN}(k', n')$*, then* $\mathcal{D}_{\mathrm{dr},\mathcal{N}'}$ *is a collection of* $g - k'$ *pairs.*

Remark 5.7. *The vacuum and the dressed network divisors in Definition 5.4 are constructed using a certain orientation of the Le-network, but they behave differently with respect to changes of orientation and of the Darboux points positions* [4]*. Indeed, any such change induces an untrivial transformation of the vacuum network divisor numbers. On the contrary, in case of changes of orientation, the dressed divisor numbers transform in agreement with the change of coordinates induced on the components of* Γ*. Moreover, the dressed divisor numbers are invariant under changes of Darboux points positions. Therefore the position of the KP divisor in the ovals is independent on both the orientation of the network and the position chosen for the Darboux source points.*

In the next Lemma, we normalize the v.e.w. previously defined and characterize the vacuum network divisor.

Definition 5.5. ***The normalized vacuum edge wavefunction*** $\hat{\Phi}$***, and the KP edge wave function*** $\hat{\Psi}$***.*** *Let* $\Phi^{(m)}_{i_r j_l}(\vec{t})$ *and* $\Psi^{(m)}_{i_r j_l}(\vec{t})$ *be the vacuum and the dressed edge wave functions on* $\mathcal{N}'$ *with* $\vec{t}_0$ *as above.*

Then the normalized vacuum edge wave function on $\mathcal{N}'$ *is*

$$\hat{\Phi}^{(m)}_{i_r j_l}(\vec{t}) = \frac{\Phi^{(m)}_{i_r j_l}(\vec{t})}{\Phi^{(m)}_{i_r j_l}(\vec{t}_0)}, \qquad l \in [0, N_r],\ r \in [k],\ m \in [3], \tag{5.11}$$

and the KP edge wave function on $\mathcal{N}'$ is

$$\hat{\Psi}^{(m)}_{i_r j_l}(\vec{t}) = \begin{cases} \dfrac{\Psi^{(m)}_{i_r j_l}(\vec{t})}{\Psi^{(m)}_{i_r j_l}(\vec{t}_0)}, & \text{for all } m \in [3],\ l \in [N_r],\ r \in [k], \\ \dfrac{\mathfrak{D} e^{i\theta_{i_r}(\vec{t})}}{\mathfrak{D} e^{i\theta_{i_r}(\vec{t}_0)}}, & \text{if } m = 3, l = 0 \text{ i.e. on the Darboux edge } e^{(3)}_{i_r},\ r \in [k]. \end{cases} \tag{5.12}$$

Lemma 5.4. *Let $(\mathcal{K}, [A])$ and $\hat{\Phi}$, $\hat{\Psi}$ be as in the Definition 5.5 with $\vec{t}_0 = (x_0, 0 \dots)$ as in Lemma 5.3. Then they have the following properties:*

(1) $\hat{\Phi}^{(m)}_{i_r j_l}(\vec{t})$ and $\hat{\Psi}^{(m)}_{i_r j_l}(\vec{t})$ are regular functions of $\vec{t}$ for any $r \in [k]$, $l \in [0, N_r]$, $m \in [3]$;

(2) $\hat{\Phi}(\vec{t})$ ($\hat{\Psi}(\vec{t})$ respectively) takes the same value on all edges at any given black vertex and any given bivalent white vertex;

(3) For any fixed $r \in [k]$, $j \in [N_r - 1]$, $\hat{\Phi}(\vec{t})$ ($\hat{\Psi}(\vec{t})$ respectively) takes different values on the edges at the white trivalent vertex $V_{i_r j_l}$ for almost all $\vec{t}$, and the vacuum and dressed network divisor numbers $\gamma^{(\mathrm{vac})}_{i_r j_l}$, $\gamma^{(\mathrm{dr})}_{i_r j_l}$, defined in (5.9) are the unique numbers such that

$$\hat{\Phi}^{(3)}_{i_r j_l}(\vec{t}) \equiv \gamma^{(\mathrm{vac})}_{i_r j_l} \hat{\Phi}^{(1)}_{i_r j_l}(\vec{t}) + (1 - \gamma^{(\mathrm{vac})}_{i_r j_l}) \hat{\Phi}^{(2)}_{i_r j_l}(\vec{t}), \qquad \forall \vec{t};$$

$$\hat{\Psi}^{(3)}_{i_r j_l}(\vec{t}) \equiv \gamma^{(\mathrm{dr})}_{i_r j_l} \hat{\Psi}^{(1)}_{i_r j_l}(\vec{t}) + (1 - \gamma^{(\mathrm{dr})}_{i_r j_l}) \hat{\Psi}^{(2)}_{i_r j_l}(\vec{t}), \qquad \forall \vec{t}.$$

*Moreover, all $\gamma^{(\mathrm{vac})}_{i_r j_l}$ are **positive**;*

*(4) For any $r \in [k]$, such that b_{i_r} is not an isolated boundary vertex, the normalized v.e.w. takes different values on the edges at the white trivalent vertex V_{i_r} for almost all $\vec{t}$, and $\gamma^{(\mathrm{vac})}_{i_r}$ defined in (5.9) is the unique **positive** number such that*

$$\hat{\Phi}^{(3)}_{i_r}(\vec{t}) \equiv \gamma^{(\mathrm{vac})}_{i_r} \hat{\Phi}^{(1)}_{i_r}(\vec{t}) + (1 - \gamma^{(\mathrm{vac})}_{i_r}) \hat{\Phi}^{(2)}_{i_r}(\vec{t}), \qquad \forall \vec{t}.$$

If, for some $r \in [k]$, b_{i_r} is an isolated boundary vertex, the white vertex V_{i_r} is bivalent and $\hat{\Phi}^{(3)}_{i_r}(\vec{t}) \equiv \hat{\Phi}^{(2)}_{i_r}(\vec{t}) = \exp(\theta_{i_r}(\vec{t} - \vec{t}_0))$, $\forall \vec{t}$;

(5) For any $r \in [k]$, the normalized KP edge wave function takes the same value on the edges at the white trivalent vertex V_{i_r} for all $\vec{t}$,

$$\hat{\Psi}^{(1)}_{i_r}(\vec{t}) = \hat{\Psi}^{(2)}_{i_r}(\vec{t}) = \hat{\Psi}^{(3)}_{i_r}(\vec{t});$$

(6) The set of normalized v.e.w. $\hat{\Phi}^{(3)}_{i_r}(\vec{t})$ defined at the vertices V_{i_r}, $r \in [k]$,

(a) Form a basis of heat hierarchy solutions which satisfy $\mathfrak{D}\Phi^{(3)}_{i_r}(\vec{t}) \equiv 0$, for all $r \in [k]$, $\vec{t}$, with $\mathfrak{D} = W\partial_x^k \equiv \partial_x^k - \mathfrak{w}_1(\vec{t})\partial_x^{k-1} - \mathfrak{w}_2(\vec{t})\partial_x^{k-2} - \cdots - \mathfrak{w}_k(\vec{t})$, the Darboux transformation and W the Sato dressing operator for $(\mathcal{K}, [A])$;

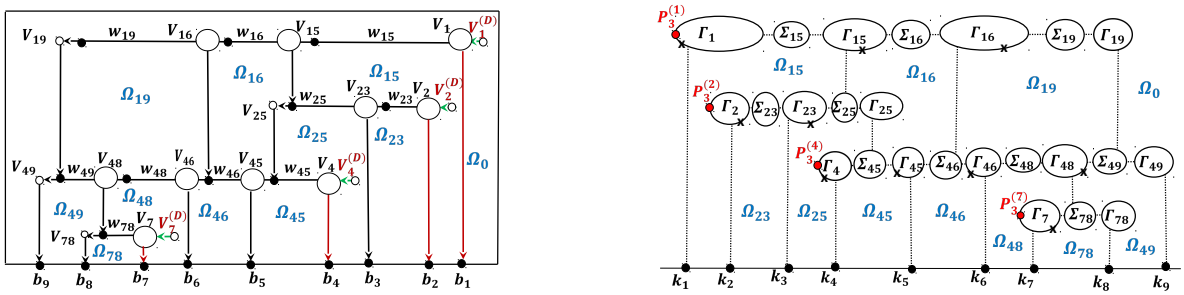

FIGURE 11. *The vacuum divisor (crosses) on the* M*–curve* Γ *[right] for Example A.2: the local coordinate of the vacuum divisor point on the component* $\Gamma_{ij} \subset \Gamma$ *[right] is the divisor number of the vertex* V_{ij} *on* $\mathcal{N}'$ *[left].*

(b) Generate the KP soliton solution $u(\vec{t})$ *associated to* $(\mathcal{K}, [A])$

$$u(\vec{t}) = 2\partial_{xx} \log(\tau(\vec{t})), \qquad \tau(\vec{t}) = \ Wr_x(\hat{\Phi}^{(3)}_{i_1}(\vec{t}), \dots, \hat{\Phi}^{(3)}_{i_k}(\vec{t}))$$

where Wr_x *denotes the Wronskian of* $\hat{\Phi}^{(3)}_{i_r}(\vec{t})$, $r \in [k]$, *with respect to* $x = t_1$.

The proof is trivial and is omitted. We illustrate the above statement in Figure 10.

Example 5.2. *Let's compute the normalized vacuum edge wave function for Example 5.1. At the vertex* V_{45} *the normalized vacuum edge wave function is*

$$\hat{\Phi}^{(3)}_{45}(\vec{t}) = \frac{e^{\theta_5(\vec{t})} + w_{46}e^{\theta_6(\vec{t})} - w_{46}w_{48}e^{\theta_8(\vec{t})} - w_{46}w_{48}w_{49}e^{\theta_9(\vec{t})}}{e^{\theta_5(\vec{t}_0)} + w_{46}e^{\theta_6(\vec{t}_0)} - w_{46}w_{48}e^{\theta_8(\vec{t}_0)} - w_{46}w_{48}w_{49}e^{\theta_9(\vec{t}_0)}}.$$

At the vertex V_{25} *we associate the* **opposite** *edge wave function* $\Phi^{(3)}_{25}(\vec{t}) = -\Phi^{(3)}_{45}(\vec{t})$ *and the* **same normalized** *edge wave function* $\hat{\Phi}^{(3)}_{25}(\vec{t}) = \hat{\Phi}^{(3)}_{45}(\vec{t})$ *for all times* $\vec{t}$. *We leave as an exercise to the reader the computation of the vacuum divisor numbers for this example (see also Figure 11).*

5.3. **From the edge wave functions on the network to the wave functions on the curve** Γ**.** In this section we define the normalized vacuum wave function $\hat{\phi}(P, \vec{t})$ and the normalized KP wave function $\hat{\psi}(P, \vec{t})$ on the curve Γ using the following construction:

Construction 5.1. ***The normalized vacuum and KP wave functions on*** Γ**.**

(1) On each component $\Gamma_{i_r j_s}$ *of* Γ *corresponding to a white vertex* $V_{i_r j_s}$ *carrying a vacuum (dressed) divisor number we assign a vacuum (dressed) divisor point* $P^{(\mathrm{vac})}_{i_r j_l}$ $(P^{(\mathrm{dr})}_{i_r j_l})$ *with coordinate equal to this number;*

(2) On Γ_0 *the normalized vacuum (dressed) wave functions coincide with the normalized vacuum (dressed Sato) wave functions respectively;*

(3) *On each marked point of* Γ *the value of the normalized vacuum (dressed) wave function is assigned equal to the value of the vacuum (dressed) edge wave function on the corresponding edge of* $\mathcal{N}'$*;*

(4) *On each component of* $\Gamma\backslash\Gamma_0$ *carrying no divisor points the corresponding function is extended as constant function in the spectral parameter. We use here that on each such component the values of the normalized (vacuum or KP) wave function are the same at all marked points;*

(5) *On each component of* $\Gamma\backslash\Gamma_0$ *carrying a divisor point the corresponding function is extended to an order 1 meromorphic function in the spectral parameter with a simple pole at the divisor point. More precisely, for* $r \in [k]$ *such that* $N_r > 0$, $\gamma^{(\mathrm{vac})}_{i_r j_s} = \frac{\Phi^{(1)}_{i_r j_s}(\vec{t}_0)}{\Phi^{(3)}_{i_r j_s}(\vec{t}_0)}$, $s \in [0, N_r - 1]$, *and*

$$\hat{\phi}_{i_r j_s}(\zeta, \vec{t}) = \frac{\Phi^{(1)}_{i_r j_s}(\vec{t})(\zeta - 1) + \Phi^{(2)}_{i_r j_s}(\vec{t})\zeta}{\Phi^{(3)}_{i_r j_s}(\vec{t}_0)\left(\zeta - \gamma^{(\mathrm{vac})}_{i_r j_s}\right)},$$

where $\hat{\phi}_{i_r j_s}(\zeta, \vec{t})$ *denotes the restriction of the normalized vacuum wave function to the component* Γ_{i_r, j_s}*. Similarly, for* $r \in [k]$ *such that* $N_r > 0$, $\gamma^{(\mathrm{dr})}_{i_r j_s} = \frac{\Psi^{(1)}_{i_r j_s}(\vec{t}_0)}{\Psi^{(3)}_{i_r j_s}(\vec{t}_0)}$, $s \in [N_r - 1]$, *and*

$$\hat{\psi}_{i_r j_s}(\zeta, \vec{t}) = \frac{\Psi^{(1)}_{i_r j_s}(\vec{t})(\zeta - 1) + \Psi^{(2)}_{i_r j_s}(\vec{t})\zeta}{\Psi^{(3)}_{i_r j_s}(\vec{t}_0)\left(\zeta - \gamma^{(\mathrm{dr})}_{i_r j_s}\right)},$$

where $\hat{\psi}_{i_r j_s}(\zeta, \vec{t})$ *denotes the restriction of the normalized KP wave function to the component* Γ_{i_r, j_s}*,* ζ *is the local coordinate on this component.*

The vacuum divisor $\mathcal{D}_{\mathrm{vac},\Gamma}$ is the sum of all points $P^{(\mathrm{vac})}_{i_r j_l}$, $r \in [k]$, $j \in [0, N_r - 1]$, assigned at $\Gamma\backslash\Gamma_0$, and it contains no points at Γ_0. The KP divisor $\mathcal{D}_{\mathrm{KP},\Gamma}$ on Γ is the sum of all points $P^{(\mathrm{dr})}_{i_r j_l}$, $r \in [k]$, $j \in [N_r - 1]$, assigned at $\Gamma\backslash\Gamma_0$ and of the Sato divisor $\mathcal{D}_{\mathrm{S},\Gamma_0}(\vec{t}_0)$ on Γ_0.

Finally, we check that we have the correct number of divisor points at each oval.

Theorem 5.1. The vacuum divisor (Theorem 3.1). *$\hat{\phi}$ as in Construction 5.1 is the real and regular vacuum wave function on Γ for the soliton data $(\mathcal{K}, [A])$, that is it satisfies all the properties of Definitions 3.3 and 3.4 on $\Gamma\backslash\{P_0\}$. In particular, it satisfies (3.5), that is*

$$\hat{\phi}(P^{(3)}_{i_r}, \vec{t}) = \frac{\sum_{l=1}^n A_l^r \exp(\theta_l(\vec{t}))}{\sum_{l=1}^n A_l^r \exp(\theta_l(\vec{t}_0))}, \qquad \text{for } r \in [k], \ \ \forall \vec{t},$$

where A is the RREF representative matrix in $[A]$. Finally the vacuum divisor $\mathcal{D}_{\mathrm{vac},\Gamma} = \{P^{(\mathrm{vac})}_{i_r j_l}\}$ of $\hat{\phi}$ satisfies:

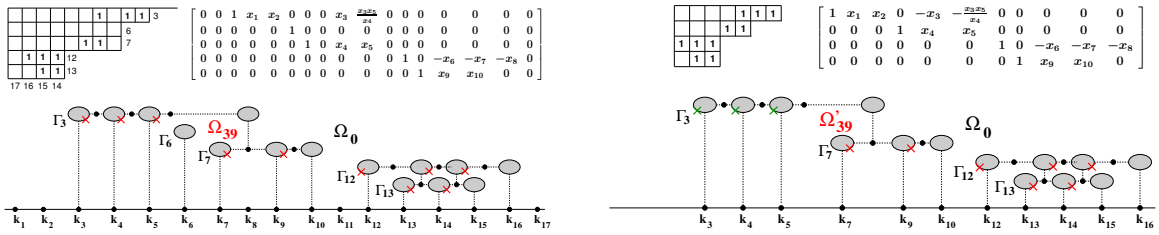

FIGURE 12. *We illustrate Case b) in the proof of Theorem 5.1 for the example discussed in Remark 5.9.*

(1) *It consists of g simple poles and no pole belongs to Γ_0;*

(2) *There is exactly one pole on each component $\Gamma_{i_r j_l}$ corresponding to a trivalent white vertex in $\mathcal{N}'$;*

(3) *For any finite oval Ω_s, $s \in [g]$, let $\nu_s = \#\{\mathcal{D}_{\mathrm{vac},\Gamma} \cap \Omega_s\}$ and $\mu_s = \#\{P_{i_r}^{(3)} \in \Omega_s,\ r \in [k]\}$ respectively be the number of poles and the number of Darboux points in Ω_s. Then*

$$\nu_s + \mu_s = \text{ odd number}, \qquad \text{for any } s \in [g]; \tag{5.13}$$

(4) *Let $\nu_0 = \#\{\mathcal{D}_{\mathrm{vac},\Gamma} \cap \Omega_0\}$ and $\mu_0 = \#\{P_{i_r}^{(3)} \in \Omega_0,\ r \in [k]\}$, respectively be the number of poles and the number of Darboux points in the infinite oval Ω_0. Then*

$$\nu_0 + \mu_0 - k = \text{ even number}. \tag{5.14}$$

Let us remark that $k - \mu_0$ is the number of Darboux source points not belonging to the infinite oval Ω_0, therefore, equivalently,

$$\nu_0 = \#\text{Darboux points not belongig to } \Omega_0 \mod 2. \tag{5.15}$$

Proof. The only untrivial statements are properties (3) and (4). Copies of $\mathbb{CP}^1$ corresponding to isolated boundary sources contribute to the counting only with a Darboux point, while those corresponding to not isolated boundary sources contribute with a pole and a Darboux point. Moreover, by definition, all poles have positive ζ–coordinate so that:

(1) for any fixed $r \in [k]$ and $l \in [N_r]$, the finite oval $\Omega_{i_r j_l}$ may contain only poles belonging either to $\Gamma_{i_r j_l}$ or to $\Gamma_{i_r j_{l-1}}$ or to $\Gamma_{i_{r+d}}$, with $d \in [k-r]$;

(2) Ω_0 may contain only poles belonging to Γ_{i_r}, with $r \in [k]$.

Let's prove (5.14) first.

Case a) First of all, consider the simplest situation in which the only Darboux point belonging to Ω_0 is $P_{i_1}^{(D)}$. In this case, $\mu_0 = 1$ in $\mathcal{N}'$, since $\Gamma_{i_s} \cap \Omega_0 \neq \emptyset$ if and only if $s = 1$. The pole on Γ_{i_1}

has ζ–coordinate

$$\gamma_{i_1}^{(\mathrm{vac})} = \frac{\Phi_{i_1}^{(1)}(\vec{t}_0)}{\Phi_{i_1}^{(1)}(\vec{t}_0) + e^{\theta_{i_1}(t_0)}} > 0$$

and $\mathrm{sign}(\Phi_{i_1}^{(1)}(\vec{t}_0)) = (-1)^{k-1}$ by construction (compare Lemma 5.4 with Theorem 4.1). Then, if k is even, $\gamma_{i_1}^{(\mathrm{vac})} > 1$, the vacuum divisor point $P_{i_1}^{(\mathrm{vac})} \in \Omega_0$, $\nu_0 = 1$ and (5.14) holds. If k is odd, $0 < \gamma_{i_1}^{(\mathrm{vac})} < 1$, $P_{i_1}^{(\mathrm{vac})} \notin \Omega_0$, $\nu_0 = 0$ and (5.14) again holds true.

Case b) Otherwise, the oval Ω_0 contains $d > 1$ Darboux points $P_{i_{s_1}}^{(D)}, \dots, P_{i_{s_d}}^{(D)}$, $1 \le s_1 < \cdots < s_d \le k$. Then, for any $l \in [d]$, there exists an index $\bar{\jmath}_l$ satisfying $1 \le i_{s_1} \le \bar{\jmath}_1 < i_{s_2} \le \bar{\jmath}_2 < \cdots < i_{s_d} \le \bar{\jmath}_d \le n$ such that, for any fixed $l \in [d]$, if $i_{s_l} = \bar{\jmath}_l$ then $b_{i_{s_l}}$ is an isolated boundary source in $\mathcal{N}$(an isolated boundary sink in $\mathcal{N}'$); otherwise $\bar{\jmath}_l$ is the maximum non pivot index such that there exists a path from the boundary source $b_{i_{s_l}}$ to the boundary sink $b_{\bar{\jmath}_l}$.

In this case, in $\mathcal{N}'$, $\Omega_0 \cap \Gamma_{i_r} \neq \emptyset$ if and only if $r \in \{s_1, \dots, s_d\}$. For any fixed $l \in [d]$, we apply the argument of Case a) to the subgraph of $\mathcal{N}'$ containing only boundary vertices between $b_{i_{s_l}}$ and $b_{\bar{\jmath}_l}$, and again (5.14) holds true. We refer to Figure 12 for an illustrating example.

To prove (5.13), we treat separately the cases:

(1) The finite oval Ω_{i_r,j_l} does not intersect Γ_0;

(2) The finite oval Ω_{i_r,j_l} intersects Γ_0;

In the first case there are no Darboux points belonging to Ω_{i_r,j_l}, whereas the only poles which may belong to Ω_{i_r,j_l} are those belonging to the upper components Γ_{i_r,j_l} and $\Gamma_{i_r,j_{l-1}}$. Let i_s be the biggest pivot index such that there exists a component with the first index i_s intersecting Ω_{i_r,j_l}. By construction, the vacuum wave function has the same sign at all horizontal edges with the same first index at time $\vec{t}_0$, and $\mathrm{sign}\,\Phi_{i_r j_l}^{(2)}(\vec{t}_0) = (-1)^{s-r}\mathrm{sign}\,\Phi_{i_s j_{N_s}}^{(3)}(\vec{t}_0)$, $\mathrm{sign}\,\Phi_{i_r j_{l-1}}^{(2)}(\vec{t}_0) = (-1)^{s-r}\mathrm{sign}\,\Phi_{i_s j_{N_s}}^{(3)}(\vec{t}_0)$. Therefore, only one pole belongs to Ω_{i_r,j_l} since $\Phi_{i_r j_l}^{(2)}(\vec{t}_0)\,\Phi_{i_r j_{l-1}}^{(2)}(\vec{t}_0) > 0$.

In the second case let us denote s_L and s_R respectively:

$$s_L = \min\{s \in [n], \kappa_s \in \Omega_{i_r,j_l}\}, \quad s_R = \max\{s \in [n], \kappa_s \in \Omega_{i_r,j_l}\}.$$

Let us remark that s_L and s_R may be both pivot or non-pivot indexes. Let us also introduce an index ν_{s_R} which tells whether the divisor point $\gamma_{s_R}^{(\mathrm{vac})}$ belong to Ω_{i_r,j_l} if $s_R \in I$.

$$\nu_{s_R} = \begin{cases} 0 & \text{if } s_R \notin I \\ 0 & \text{if } s_R \in I \text{ and } \gamma_{s_R}^{(\mathrm{vac})} \notin \Omega_{i_r,j_l} \\ 1 & \text{if } s_R \in I \text{ and } \gamma_{s_R}^{(\mathrm{vac})} \in \Omega_{i_r,j_l}. \end{cases}$$

Then

$$\operatorname{sign}\Phi^{(2)}_{i_r j_{l-1}}(\vec{t}_0) = (-1)^{\#(]i_r,s_L]\cap I)}, \quad \operatorname{sign}\Phi^{(2)}_{i_r j_l}(\vec{t}_0) = (-1)^{\#(]i_r,s_R]\cap I)+\nu_{s_R}}.$$

Therefore

$$\operatorname{sign}\left(\Phi^{(2)}_{i_r j_{l-1}}(\vec{t}_0)\,\Phi^{(2)}_{i_r j_l}(\vec{t}_0)\right) = (-1)^{\#(]s_L,s_R]\cap I)+\nu_{s_R}}. \tag{5.16}$$

If $s_R - s_L > 1$, then the boundary of Ω_{i_r,j_l} includes components associated to the boundary sources in $]s_L, s_R[$, behaving like components of the infinite oval in the intersection with Ω_{i_r,j_l}. Using (5.15) we immediately conclude that $\tilde{\nu}_0(i_r, j_l)$, the number of divisor points on the intersection of Ω_{i_r,j_l} with such components, is equal to the number of Darboux points in $]s_L, s_R[$ not belonging to $\Omega_{i_r,j_l} \mod 2$.

Therefore, substituting $\tilde{\nu}_0(i_r, j_l)$ into (5.16) we get

$$\operatorname{sign}\left(\Phi^{(2)}_{i_r j_{l-1}}(\vec{t}_0)\,\Phi^{(2)}_{i_r j_l}(\vec{t}_0)\right) = (-1)^{\tilde{\nu}_0(i_r,j_l)+\mu_{i_r,j_l}+\nu_{s_R}}, \tag{5.17}$$

where μ_{i_r,j_l} is the number of Darboux points in Ω_{i_r,j_l}.

If $\tilde{\nu}_0(i_r, j_l)+\mu_{i_r,j_l}+\nu_{s_R} = 0 \mod 2$, then $\#\big(\{\gamma^{(\mathrm{vac})}_{i_r,j_{l-1}}, \gamma^{(\mathrm{vac})}_{i_r,j_l}\}\cap\Omega_{i_r,j_l}\big) = 1$, otherwise $\#\big(\{\gamma^{(\mathrm{vac})}_{i_r,j_{l-1}}, \gamma^{(\mathrm{vac})}_{i_r,j_l}\}\cap \Omega_{i_r,j_l}\big) = 0 \mod 2$, and the proof of (5.13) is complete. □

Remark 5.8. *One may adapt this proof to check directly that the KP divisor has exactly one divisor point at each finite oval and no divisor points at the infinite oval, see* [5].

Remark 5.9. The effect of the isolated boundary vertices on the effective vacuum divisor. *Any KP soliton solution is associated to an unique irreducible cell in $Gr^{TNN}(k', n')$ which is obtained eliminating all isolated boundary vertices from the Le–diagram. Let I be the pivot set. The elimination of an isolated boundary vertex b_j, $j \in \bar{I}$, does not affect the vacuum divisor. The elimination of an isolated boundary vertex b_{i_s}, $i_s \in I$, produces a change of sign in the matrix elements in all the rows $r \in [1, s-1]$ which lie to the right of the i_s–th column. This change of sign is automatically encoded in the basis of vectors by the recursion associated to the reduced matrix, and effects both the sign of the vacuum edge wave function and the position of the vacuum divisor not just in the oval where we remove Γ_{i_s}, but also in all the ovals to the left and above it. We show an example in Figure 12 of both the reducible and reduced vacuum divisors. The original Le–diagram in Fig.12[above left] has RREF matrix A depending on 10 positive parameters x_l, $l \in [10]$ and the corresponding reducible rational* M*–curve is shown in Fig.12[bottom left]. The crosses are the divisor points of the KP vacuum wave function: here $k = 5$, $d = 2$, $s_1 = 1$, $s_2 = 4$, $i_1 = 3$, $i_4 = 12$, $j_1 = 10$ and $j_2 = 16$. The infinite oval*

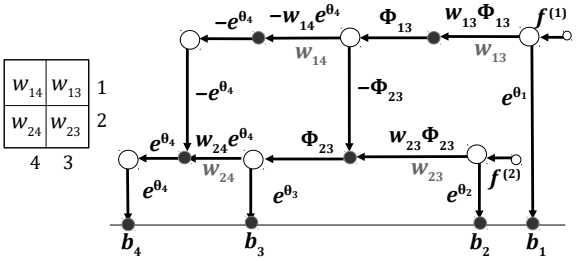

FIGURE 13. *The Le-tableau and vacuum edge wave function on the modified Le–network for soliton data in* $Gr^{TP}(2,4)$. $\Phi_{13}(\vec{t}) = -e^{\theta_3(\vec{t})} - (w_{14}+w_{24})e^{\theta_4(\vec{t})}$, *while* $\Phi_{23}(\vec{t}) = e^{\theta_3(\vec{t})} + w_{24}e^{\theta_4(\vec{t})}$.

Ω_0 *intersects* Γ_3 *and* Γ_{12} *and* $\mu_0 = 2$. $\Phi_{12}^{(1)}(\vec{t}_0)$ *has the sign of the entry* $A_{12}^4 = -x_8 < 0$, $\Phi^{(2)}(\vec{t}_0)) = \exp(\theta_{12}(\vec{t}_0)) > 0$ *so that* $\gamma_{12}^{(\mathrm{vac})} > 1$ *and* $P_{12}^{(\mathrm{vac})} \in \Omega_0$. $\Phi_3^{(1)}(\vec{t}_0)$ *has the sign of the entry* $A_{10}^1 = (x_3x_5)/x_4 > 0$, $\Phi^{(2)}(\vec{t}_0)) = \exp(\theta_3(\vec{t}_0)) > 0$ *so that* $\gamma_3^{(\mathrm{vac})} < 1$ *and* $P_3^{(\mathrm{vac})} \notin \Omega_0$. *In conclusion* $\nu_0 = 1$ *and* $k + \mu_0 + \nu_0 = 8$ *is even.*

The reduced Le–diagram and the reduced matrix (see Fig.12[top, right]) are obtained eliminating, respectively, all isolated boundary vertices. This transformation corresponds to the elimination of the component Γ_6 *in the reducible rational curve (Fig.12[bottom right]) and to the change of the vacuum pole divisor points (crosses) in the oval* Ω'_{39} *which corresponds to* Ω_{39} *and in all the ovals to the left and above such oval. All other vacuum divisor points (crosses) in the ovals to the right and below respectively of* Ω_{39} *and of* Ω'_{39} *are the same in Figure 12 [bottom, left] and 12[bottom, right].*

6. Construction of the plane curve and the divisor to soliton data in $Gr^{\mathrm{TP}}(2,4)$ and comparison with the construction in [3]

$Gr^{\mathrm{TP}}(2,4)$ is the main cell in $Gr^{\mathrm{TNN}}(2,4)$ and its elements $[A]$ are equivalence classes of real 2×4 matrices A with all maximal minors positive. Such matrices are parametrized by the four weights of the Le-tableau (see Figure 13), w_{ij}, $i = 1,2$, $j = 3,4$, and may be represented in the reduced row echelon form (RREF),

$$A = \begin{pmatrix} 1 & 0 & -w_{13} & -w_{13}(w_{14}+w_{24}) \\ 0 & 1 & w_{23} & w_{23}w_{24} \end{pmatrix}. \tag{6.1}$$

The generators of the Darboux transformation $\mathfrak{D} = \partial_x^2 - \mathfrak{w}_1(\vec{t})\partial_x - \mathfrak{w}_2(\vec{t})$ are

(6.2)

$$f^{(1)}(\vec{t}) = e^{\theta_1(\vec{t})} - w_{13}e^{\theta_3(\vec{t})} - w_{13}(w_{14}+w_{24})e^{\theta_4(\vec{t})}, \qquad f^{(2)}(\vec{t}) = e^{\theta_2(\vec{t})} + w_{23}e^{\theta_3(\vec{t})} + w_{23}w_{24}e^{\theta_4(\vec{t})}.$$

In [3] we have proposed a plane curve representation of $\Gamma(\xi)$ for soliton data in $Gr^{\mathrm{TP}}(2,4)$ as the product of a line, a quadric and a cubic and we have desingularized $\Gamma(\xi)$ to a genus 4 M–curve. In [2] and [5], we use the reduced Le–network $\mathcal{G}_{\mathrm{red}}$ to implement the construction of the present paper, and represent $\Gamma(\mathcal{G}_{\mathrm{red}})$ by five lines. We recall that the elimination of $\mathbb{CP}^1$ copies associated to bivalent vertices is fully justified since it does not effect neither the properties of the desigularized curve (see Section 3.1) nor the divisor (see Remark 3.8).

In [5] we also desingularize $\Gamma(\mathcal{G}_{\mathrm{red}})$ to a smooth genus 4 M–curve on which we numerically construct real–regular KP–II finite gap solutions, while in [2] evidence is provided that the asymptotic behavior of the KP soliton zero divisor in $\|(x,y)\| \gg 1$ for fixed time t is consistent with the characterization in [17].

In this section, we discuss the same example with a different spirit from our previous publications: we represent

$$\Gamma(\mathcal{G}_{\mathrm{red}}) = \Gamma_0 \sqcup \Gamma'_{13} \sqcup \Gamma_{23} \sqcup \Sigma'_{23} \sqcup \Sigma'_{24},$$

as five lines which are the limit of two lines and a cubic representing

$$\Gamma(\xi) = \Gamma_0 \sqcup \Gamma_1(\xi) \sqcup \Gamma_2(\xi), \quad \xi \gg 1,$$

so that $\Gamma(\mathcal{G}_{\mathrm{red}}) = \Gamma(\infty)$. We present the topological model of both $\Gamma(\mathcal{G}_{\mathrm{red}})$ and $\Gamma(\xi)$ when $\xi \gg 1$ in Figure 16[top].

$\Gamma(\xi)$ in Section 6.2 is the reducible curve obtained by the intersection of two lines representing Γ_0 and $\Gamma_2(\xi)$ and a cubic representing $\Gamma_1(\xi)$, such that

$$\Gamma_1(\infty) = \Gamma_{23} \sqcup \Sigma'_{23} \sqcup \Sigma'_{24}, \qquad \Gamma_2(\infty) = \Gamma'_{13}.$$

We remark that the above representation of $\Gamma(\xi)$ is different from that proposed in [3]. We also compute the KP divisors both on $\Gamma(\mathcal{G}_{\mathrm{red}})$ and $\Gamma(\xi)$. For $\xi \gg 1$, the KP divisor on $\Gamma(\xi)$ coincides at leading order with that of $\Gamma(\mathcal{G}_{\mathrm{red}})$ in appropriate coordinates. We remark that the KP divisor is independent on the plane curve representation. Finally, we desingularize both $\Gamma(\mathcal{G}_{\mathrm{red}})$ and $\Gamma(\xi)$ to genus 4 M–curves.

6.1. **A spectral curve for the reduced Le–network for soliton data in $Gr^{\mathrm{TP}}(2,4)$ and its desingularization.** We briefly illustrate the construction of the rational spectral curve $\Gamma(\mathcal{G}_{\mathrm{red}})$ for soliton data in $Gr^{\mathrm{TP}}(2,4)$. We reduce the degree of the curve from 11 to 5 by eliminating the $\mathbb{CP}^1$ components corresponding to bivalent vertices in $\mathcal{G}$. We represent the topological model of

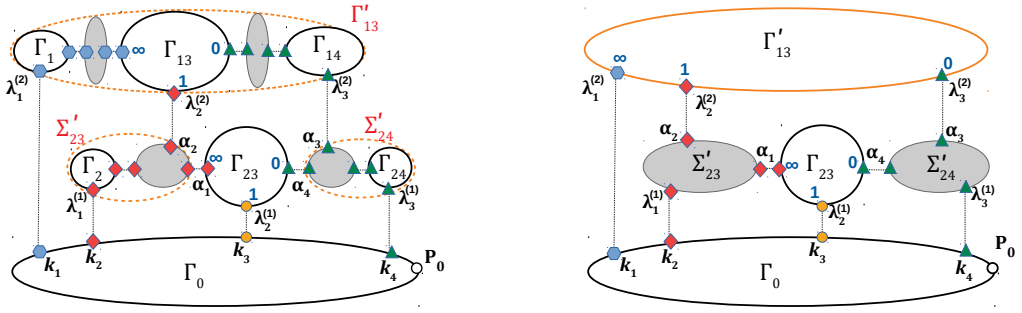

FIGURE 14. *The topological model of the spectral curves $\Gamma(\mathcal{G})$ [left] and $\Gamma(\mathcal{G}_{\rm red})$ [right] for soliton data $Gr^{TP}(2,4)$. In both figures, the value of the KP edge wave function is the same at all points marked with the same symbol.*

$\Gamma(\mathcal{G})$ and of $\Gamma(\mathcal{G}_{\rm red})$ in Figure 14: at all double points marked with the same symbol the value of the normalized dressed wave function is the same for all times.

The curve $\Gamma(\mathcal{G}_{\rm red})$ is the partial normalization of the nodal plane curve $\Pi_0(\lambda,\mu)=0$, with Π_0 as in (6.6), and it is the rational degeneration of the genus 4 M–curve Γ_ε in (6.7) for $\varepsilon\to 0$. Here we modify the plane curve representation in [5] so that the plane curve representing $\Gamma(\xi)$ is a rational deformation of $\Pi_0(\lambda,\mu)=0$ for $\xi\gg 1$. We plot both the topological model and the plane curve for this example in Figure 15.

The reducible rational curve $\Gamma(\mathcal{G}_{\rm red})$ is obtained gluing five copies of $\mathbb{CP}^1$: Γ_0, Γ'_{13}, Γ_{23}, Σ'_{23} and Σ'_{24} and it may be represented as a plane curve given by the intersection of five lines. To simplify its representation, we impose that Γ_0 is one of the coordinate axis in the (λ,μ)–plane, say $\mu=0$, that $P_0\in\Gamma_0$ is the infinite point, that the lines Σ'_{23}, Σ'_{24} are orthogonal to Γ_0, that Γ_{23} is parallel to the first bisector and that Γ'_{13} and Γ_{23} intersect at a finite point α_5:

(6.3)

$$\Gamma_0:\mu=0,\quad \Gamma'_{13}:\mu-c_{13}(\lambda-\kappa_1)=0,\quad \Gamma_{23}:\mu-\lambda+\kappa_3=0,\quad \Sigma'_{23}:\lambda-\kappa_2=0,\quad \Sigma'_{24}:\lambda-\kappa_4=0.$$

Notice that here we do not follow the generic construction of Section 3.2 and use parallel lines.

We choose

$$c_{13}=\frac{(\kappa_2+\kappa_4-2\kappa_3)(\kappa_4-\kappa_3)(\kappa_2-\kappa_1)+(\kappa_3-\kappa_1)(\kappa_3-\kappa_2)^2}{(\kappa_4-\kappa_1)(\kappa_2-\kappa_1)(\kappa_2+\kappa_4-2\kappa_3)},\tag{6.4}$$

so that it coincides at leading order in ξ with the coefficient of the line $\Gamma_2(\xi)$ in (6.8). Our representation fits generic values of κ_j. The figures in this and the following sections all refer to the case $\kappa_2+\kappa_4-2\kappa_3<0$.

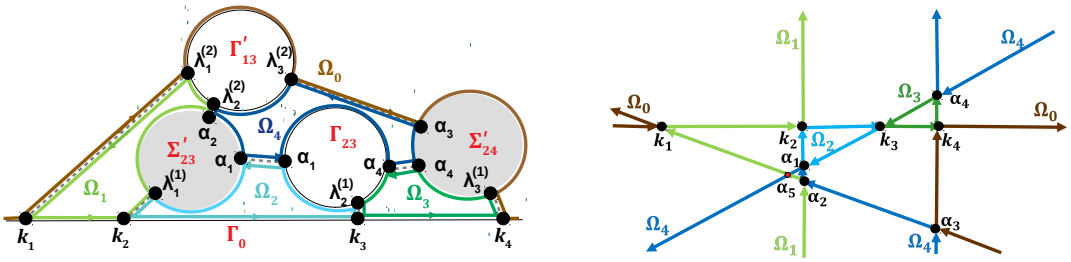

FIGURE 15. *The topological model of spectral curve for soliton data $Gr^{TP}(2,4)$, $\Gamma(\mathcal{G}_{\rm red})$ [left] is the partial normalization of the plane algebraic curve [right]. The ovals in the nodal plane curve are labeled as in the real part of its partial normalization.*

As usual we denote Ω_0 the infinite oval, that is $P_0 \in \Omega_0$, and Ω_j, $j \in [4]$, the finite ovals (see Figure 15). Since the singularity at infinity is completely resolved, the lines Σ'_{23} and Σ'_{24} do not intersect at infinity. Finally the ovals Ω_1 and Ω_4 are both finite since neither of them passes through P_0.

The relation between the coordinate λ in the plane curve representation and the coordinate ζ introduced in Definition 3.1 may be easily worked out at each component of $\Gamma(\mathcal{G}_{\rm red})$. On Γ'_{13}, we have 3 real ordered marked points, with ζ–coordinates: $\zeta(\lambda_3^{(2)}) = 0 < \zeta(\lambda_2^{(2)}) = 1 < \zeta(\lambda_1^{(2)}) = \infty$. Comparing with (6.3) we then easily conclude that

$$\lambda = \frac{\kappa_1(\kappa_4-\kappa_2)\zeta + (\kappa_2-\kappa_1)\kappa_4}{(\kappa_4-\kappa_2)\zeta + (\kappa_2-\kappa_1)}.$$

On Σ'_{23}, we have 3 real ordered marked points, and the following constraints: $\mu(\lambda_1^{(1)}) = \mu(\kappa_2) = 0$, $\mu(\alpha_1) = \kappa_2 - \kappa_3$, $\mu(\alpha_2) = \mu(\lambda_2^{(2)}) = c_{13}(\kappa_2 - \kappa_1)$. Similarly on Σ'_{24}, we have 3 real ordered marked points, and the following constraints: $\mu(\lambda_3^{(1)}) = \mu(\kappa_4) = 0$, $\mu(\alpha_4) = \kappa_4 - \kappa_3$, $\mu(\alpha_3) = \mu(\lambda_1^{(2)}) = c_{13}(\kappa_4 - \kappa_1)$. Analogously, on Γ_{23} in the initial ζ coordinates we have 3 real ordered marked points and $\zeta(\alpha_4) = 0 < \zeta(\lambda_2^{(1)}) = 1 < \zeta(\alpha_1) = \infty$, therefore the fractional linear transformation to the λ is:

$$\lambda = \frac{\kappa_2(\kappa_4-\kappa_3)\zeta + (\kappa_3-\kappa_2)\kappa_4}{(\kappa_4-\kappa_3)\zeta + (\kappa_3-\kappa_2)}.$$

We remark that Γ'_{13} and Γ_{23} intersect at

$$\alpha_5 = (\lambda_5, \mu_5) = \left(-\frac{\kappa_3 - c_{13}\kappa_1}{c_{13}-1}, -\frac{c_{13}(\kappa_3-\kappa_1)}{c_{13}-1} \right), \tag{6.5}$$

which does not correspond to any of the marked points of the topological model of Γ (see Figure 15). Such singularity is resolved in the partial normalization and therefore there are no extra

conditions to be satisfied by the vacuum and the dressed wave functions at α_5. Finally $\Gamma(\mathcal{G}_{\rm red})$ is represented by the reducible plane curve $\Pi_0(\lambda,\mu)=0$, with

$$\Pi_0(\lambda,\mu)=\mu\cdot\big(\mu-c_{13}(\lambda-\kappa_1)\big)\cdot\big(\lambda-\kappa_2\big)\cdot\big(\mu-\lambda+\kappa_3\big)\cdot\big(\lambda-\kappa_4\big). \tag{6.6}$$

The desingularization of $\Gamma(\mathcal{G}_{\rm red})$ gives a genus 4 M–curve Γ_ε for the following choice ($0<\varepsilon\ll 1$):

$$\Gamma_\varepsilon\ :\qquad \Pi(\lambda,\mu;\varepsilon)=\begin{cases}\Pi_0(\lambda,\mu)+\varepsilon^2\,(\lambda-\lambda_5)^2\,C_0(\lambda,\mu)=0, & \text{if } c_{13}\neq 1,\\ \Pi_0(\lambda,\mu)+\varepsilon^2 C_0(\lambda,\mu)=0, & \text{if } c_{13}=1,\end{cases} \tag{6.7}$$

where λ_5 is as in (6.5) and C_0 is a cubic polynomial in λ,μ,

$$C_0(\lambda,\mu)=\beta_0+\beta_{1,0}\lambda+\beta_{0,1}\mu+\beta_{2,0}\lambda^2+\beta_{2,1}\lambda\mu+\beta_{0,2}\mu^2+\beta_{3,0}\lambda^3+\beta_{2,1}\lambda^2\mu+\beta_{1,2}\lambda\mu^2+\beta_{0,3}\mu^3,$$

of which we control the sign at the marked points. If $\kappa_2+\kappa_4-2\kappa_3<0$, the conditions are

$$\text{sign }\,(C_0(\kappa_1))=\text{sign }\,(C_0(\alpha_2))\neq\text{sign }\,(C_0(\kappa_j))\,,\text{sign }\,(C_0(\alpha_l))\,,\qquad \text{for } j=2,3,4,\ l=1,3,4,$$

(see also Figure 6.7 [bottom, left]). The case $\kappa_2+\kappa_4-2\kappa_3>0$ can be treated similarly. For instance, possible choices are $C_0=-(35\lambda^3+\mu^3+70\lambda^2)$ for $\mathcal{K}=\{-3,-1,2,3\}$, and $C_0=\mu^2-35$ for $\mathcal{K}=\{-3,-1,2,6\}$.

In Figure 16[left], we represent the topological model of $\Gamma(\mathcal{G}_{\rm red})$ [top], which is the partial normalization of the plane curve $\Pi_0=0$ [middle] and the oval structure of the plane curve Γ_ε as in (6.7) when $\kappa_2+\kappa_4-2\kappa_3<0$. We remark that the normalized KP wave function takes the same value at all points marked with the same symbol in Figures 14 and 16.

6.2. **Construction of $\Gamma(\xi)$ as in [3] starting from $\Gamma(\mathcal{G}_{\rm red})$.** In [3] the reducible curve $\Gamma(\xi)=\Gamma_0\sqcup\Gamma_1(\xi)\sqcup\Gamma_2(\xi)$ is obtained gluing the three rational irreducible components, $\Gamma_0,\Gamma_1(\xi)$ and $\Gamma_2(\xi)$, at prescribed real points whose position is ruled by the parameter $\xi\gg 1$. In Figure 16 [top,right], we represent the topological model of $\Gamma(\xi)$ for soliton data in $Gr^{\rm TP}(2,4)$ and call $\tilde\zeta$ the local coordinate introduced in Section 4 in [3]. For instance the point $\alpha_2\in\Gamma_1(\xi)$ has local coordinate $\tilde\zeta(\alpha_2)=\xi^{-1}$ and is glued to the point $\lambda_2^{(2)}\in\Gamma_2(\xi)$ having local coordinate $\tilde\zeta(\lambda_2^{(2)})=-1$.

The plane curve $\Gamma(\xi)$ constructed in this section satisfies $\Gamma(\infty)=\Gamma(\mathcal{G}_{\rm red})$, so it is more suitable than the one presented in [3] for comparing the two models curves and the KP divisors:

(1) Γ_0 is the same rational component both for $\Gamma(\mathcal{G}_{\rm red})$ and $\Gamma(\xi)$, and we represent it by the line $\mu=0$ in both cases;

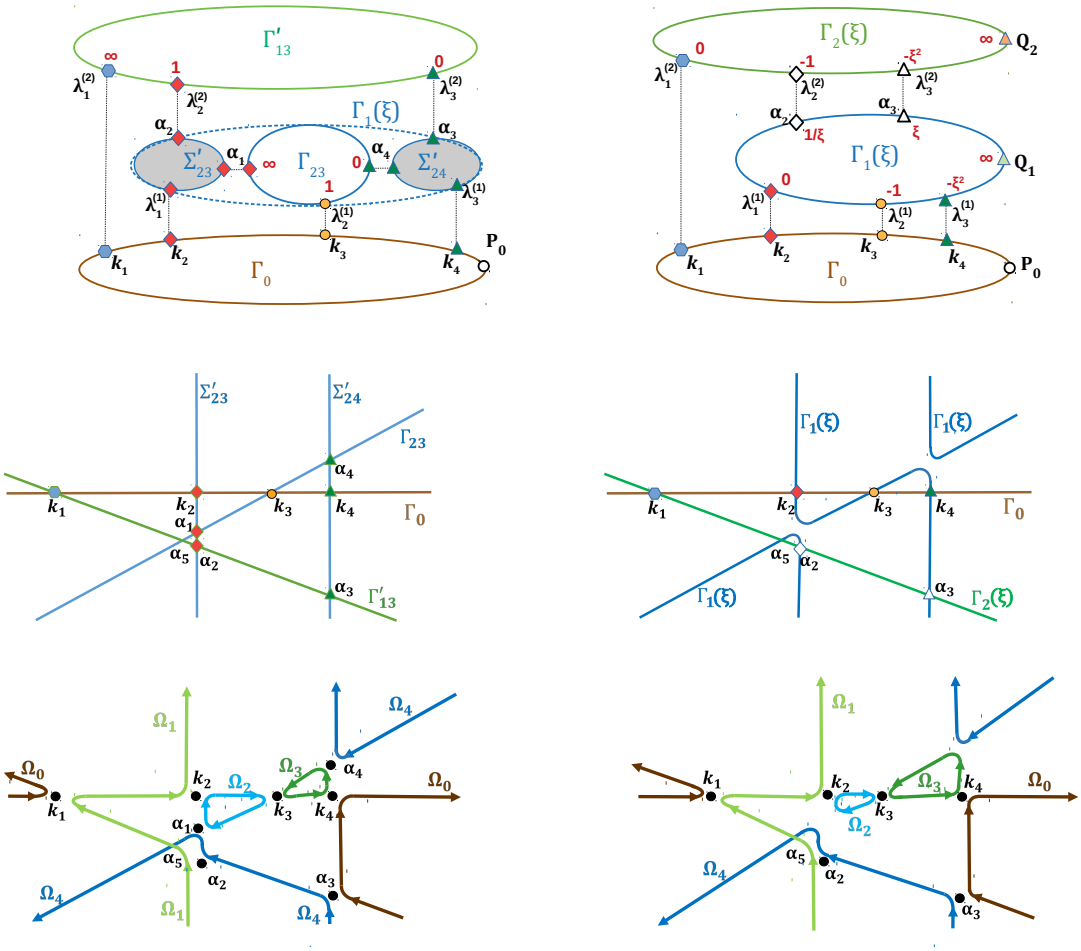

FIGURE 16. *For the same soliton data in* $Gr^{TP}(2,4)$ *we compare the topological model of the spectral curve [top], its realization as a plane curve [center] and the oval structure of the smooth genus 4* M*–curve [bottom] for the reducible rational curves* $\Gamma(\mathcal{G}_{red}) = \Gamma_0 \sqcup \Gamma'_{13} \sqcup \Gamma_{23} \sqcup \Sigma'_{23} \sqcup \Sigma'_{24}$ *[left] and* $\Gamma(\xi) = \Gamma_0 \sqcup \Gamma_1(\xi) \sqcup \Gamma_2(\xi)$ *[right]. In all figures the value of the normalized KP wave function for given soliton data in* $Gr^{TP}(2,4)$ *is equal for all times at the points marked with the same symbol.*

(2) $\Gamma_1(\xi)$ is a rational component which may be obtained from $\Gamma_{23} \sqcup \Sigma_{23} \sqcup \Sigma_{24}$ desingularising it at the double points α_1 and α_4. This transformation effects the position of the marked points $\alpha_j \equiv \alpha_j(\xi)$ and $j = 2, 3$, which have λ–coordinates $\lambda_{2,\xi} \equiv \lambda(\alpha_2) = \kappa_2 + O(\xi^{-1})$ and $\lambda_{3,\xi} \equiv \lambda(\alpha_3) = \kappa_4 + O(\xi^{-1})$ (compare with Section 7 in [3]). Then $\Gamma_1(\xi)$ may be represented by a cubic depending on ξ which tends to the product of the three lines when $\xi \to \infty$.

(3) $\Gamma_2(\xi)$ has three marked points: $\lambda_1^{(2)}$ is glued to κ_1, while $\lambda_j^{(2)}$, $j=2,3$ are glued respectively to α_j, $j=2,3$. Then $\Gamma_2(\xi)$ may be represented by a line which tends to that representing Γ'_{13} when $\xi\to\infty$.

The above ansatz is consistent with the fact that, for any fixed $\xi\gg 1$ and for all times, the normalized KP wave function on $\Gamma(\xi)$ coincides exactly with that of $\Gamma(\mathcal{G}_{\rm red})$ at the marked points κ_j, $j\in[4]$, and at leading order in ξ at the marked points α_2, α_3 (see Figure 16).

Let us now construct a plane curve $\Gamma(\xi)$ satisfying the above requirements. Γ_0 is the line $\mu=0$ as in the previous section. We require that $\Gamma_2(\xi)$ is a line passing through the point $(\kappa_1,0)$

$$\Gamma_2(\xi)\ :\ \mu - c_{13}(\xi)(\lambda-\kappa_1)=0, \tag{6.8}$$

where $c_{13}(\xi)$ tends to c_{13} as in (6.3) in the limit $\xi\to\infty$, so that the line $\Gamma_2(\infty)$ coincides with that representing Γ'_{13}.

$\Gamma_1(\xi)$ is a cubic which degenerates to the product of the three lines representing Γ_{23},Σ'_{23} and Σ'_{24} in the limit $\xi\to\infty$. We make the following choice

$$\Gamma_1(\xi)\ :\ \frac{\mu}{\xi} - c_{23}(\xi)(\lambda-\kappa_2)(\lambda-\kappa_3-\mu)(\lambda-\kappa_4)=0. \tag{6.9}$$

The coefficients $c_{13}(\xi)$, $c_{23}(\xi)$ are uniquely defined by the conditions that $\Gamma_1(\xi)$ and $\Gamma_2(\xi)$ intersect at the real points $\alpha_2\equiv\alpha_2(\xi)$, $\alpha_3\equiv\alpha_3(\xi)$ such that in the local coordinate $\tilde\zeta$ used in [3] $\tilde\zeta(\alpha_2)=\xi^{-1}$, $\tilde\zeta(\alpha_3)=\xi$ (see also Figure 16 [top,right]). In the coordinate λ used throughout this section, we have

$$\lambda_{2,\xi}\equiv\lambda(\alpha_2)=\frac{\xi^2\kappa_2(\kappa_4-\kappa_3)+(1-\xi)\kappa_3(\kappa_4-\kappa_2)}{\xi^2(\kappa_4-\kappa_3)+(1-\xi)(\kappa_4-\kappa_2)},\quad \lambda_{3,\xi}\equiv\lambda(\alpha_3)=\frac{\xi\kappa_4(\kappa_3-\kappa_2)-\kappa_3(\kappa_4-\kappa_2)}{\xi(\kappa_3-\kappa_2)-\kappa_4+\kappa_2}.$$

The third real intersection point between $\Gamma_1(\xi)$ and $\Gamma_2(\xi)$, $\alpha_5\equiv\alpha_5(\xi)$, has then λ coordinate

$$\lambda_{5,\xi}\equiv\lambda(\alpha_5)=\frac{(\lambda_{2,\xi}\lambda_{3,\xi}\kappa_1-(\lambda_{2,\xi}+\lambda_{3,\xi})(\kappa_1\kappa_2+\kappa_1\kappa_4-\kappa_2\kappa_4)-\kappa_2^2(\kappa_4-\kappa_1)-\kappa_4^2(\kappa_2-\kappa_1)+\kappa_1\kappa_2\kappa_4}{\lambda_{2,\xi}\lambda_{3,\xi}-\kappa_1(\lambda_{2,\xi}+\lambda_{3,\xi})+\kappa_1\kappa_2+\kappa_1\kappa_4-\kappa_2\kappa_4} \tag{6.10}$$

while the coefficients satisfy

$$c_{13}(\xi) = \frac{\lambda_{2,\xi}\lambda_{3,\xi}(\lambda_{2,\xi}+\lambda_{3,\xi}-\sum_{j=1}^4\kappa_j)+\kappa_1(\lambda_{2,\xi}+\lambda_{3,\xi})\sum_{j\neq 1}\kappa_j-\kappa_1(\lambda_{2,\xi}^2+\lambda_{3,\xi}^2+\sum_{1<i<j\leq 4}\kappa_i\kappa_j)+\kappa_2\kappa_3\kappa_4}{(\lambda_{2,\xi}-\kappa_1)(\lambda_{3,\xi}-\kappa_1)(\lambda_{2,\xi}+\lambda_{3,\xi}-\kappa_2-\kappa_4)}=c_{13}+O(\xi^{-1}),$$

$$c_{23}(\xi) = -\frac{c_{13}(\xi)(\lambda_{2,\xi}-\kappa_1)}{\xi(\lambda_{2,\xi}-\kappa_4)(\lambda_{2,\xi}-\kappa_2)(c_{13}(\xi)(\lambda_{2,\xi}-\kappa_1)-\lambda_{2,\xi}+\kappa_3)}=-\frac{c_{13}(\kappa_4-\kappa_1)(\kappa_2-\kappa_1)(\kappa_2+\kappa_4-2\kappa_3)}{(\kappa_3-\kappa_1)(\kappa_3-\kappa_2)(\kappa_4-\kappa_3)(\kappa_4-\kappa_2)^2}+O(\xi^{-1}).$$

Therefore $\Gamma(\xi)$ is represented by the plane curve

(6.11)
$$\Gamma(\xi)\ :\qquad \Pi_\xi(\lambda,\mu)=\mu\Big(\mu-c_{13}(\xi)(\lambda-\kappa_1)\Big)\left(\frac{\mu}{\xi}-c_{23}(\xi)(\lambda-\kappa_2)(\lambda-\kappa_3-\mu)(\lambda-\kappa_4)\right)=0.$$

We represent both the plane curve (Figure 16[right,middle]) and its partial normalization (Figure 16[right,top]) in the case $\kappa_2+\kappa_4-2\kappa_3<0$.

The genus 4 M–curve, $\Gamma_\varepsilon(\xi)$, obtained from $\Gamma(\xi)$ is then a perturbation of Γ_ε, under the genericity assumption $c_{13}\neq 1$:

$$\Gamma_\varepsilon(\xi)\ :\qquad \Pi_\xi(\lambda,\mu;\varepsilon)=\Pi_\xi(\lambda,\mu)+\varepsilon^2\left(\lambda-\lambda_{5,\xi}^2\right)^2C_0(\lambda,\mu)=0,\qquad 0<\varepsilon\ll 1, \tag{6.12}$$

where $\lambda_{5,\xi}$ is as in (6.10), and the coefficients of the cubic polynomial C_0 coincide with those in (6.12), for ξ fixed and sufficiently big. In Figure 16[right,bottom], we present the oval structure of $\Gamma_\varepsilon(\xi)$ as in (6.12) in the case $\kappa_2+\kappa_4-2\kappa_3<0$.

6.3. **The KP divisors on $\Gamma(\mathcal{G}_{\mathbf{red}})$ and on $\Gamma(\xi)$.** In [3], [5] and [2] we have computed the vacuum and the KP divisor for soliton data in $Gr^{\mathrm{TP}}(2,4)$ respectively on $\Gamma(\xi)$, on $\Gamma(\mathcal{G}_{\mathrm{red}})$ and on $\Gamma(\mathcal{G})$; therefore we do not repeat this computation here. We just verify that the KP divisors $\mathcal{D}_{\mathrm{KP},\Gamma}=(P_1^{(\mathrm{S})},P_2^{(\mathrm{S})},P_{1,\xi}^{(\mathrm{dr})},P_{2,\xi}^{(\mathrm{dr})})$ on $\Gamma(\xi)$ and $\mathcal{D}_{\mathrm{KP},\Gamma}=(P_1^{(\mathrm{S})},P_2^{(\mathrm{S})},P_{13}^{(\mathrm{dr})},P_{23}^{(\mathrm{dr})})$ on $\Gamma(\mathcal{G}_{\mathrm{red}})$, in the coordinate ζ introduced in Definition 3.1, satisfy

$$\zeta(P_{1,\xi}^{(\mathrm{dr})})=\zeta(P_{23}^{(\mathrm{dr})}),\qquad \zeta(P_{2,\xi}^{(\mathrm{dr})})=\zeta(P_{13}^{(\mathrm{dr})})+O(\xi^{-1}). \tag{6.13}$$

In the following we use the abridged notation $e^{\theta_{j,0}}=e^{\theta_j(\vec{t}_0)}=e^{\kappa_j x_0}$. By construction $\mathcal{D}_{\mathrm{KP},\Gamma}$ consists of the degree 2 Sato divisor $(P_1^{(\mathrm{S})},P_2^{(\mathrm{S})})$ defined in (2.7), $\zeta(P_l^{(\mathrm{S})})=\gamma_l^{(\mathrm{S})}$, $l=1,2$, and of 2 simple poles $(P_{13}^{(\mathrm{dr})},P_{23}^{(\mathrm{dr})})$ respectively belonging to Γ_{13} and Γ_{23}. In the local coordinates induced by the orientation of the Le–network, we have [5, 2]

$$\begin{aligned}
&\zeta(P_1^{(\mathrm{S})})+\zeta(P_2^{(\mathrm{S})})=\mathfrak{w}_1(\vec{t}_0), && \zeta(P_1^{(\mathrm{S})})\zeta(P_2^{(\mathrm{S})})=-\mathfrak{w}_2(\vec{t}_0),\\
&\zeta(P_{13}^{(\mathrm{dr})})=\frac{w_{14}(\mathfrak{D}e^{\theta_{2,0}}+w_{23}\mathfrak{D}e^{\theta_{3,0}})}{(w_{14}+w_{24})\mathfrak{D}e^{\theta_{2,0}}+w_{23}w_{14}\mathfrak{D}e^{\theta_{3,0}}}, && \zeta(P_{23}^{(\mathrm{dr})})=1+w_{23}\frac{\mathfrak{D}e^{\theta_{3,0}}}{\mathfrak{D}e^{\theta_{2,0}}}.
\end{aligned} \tag{6.14}$$

In [5, 2], we have also discussed the position of the divisor points in dependence on the signs of $\mathfrak{D}e^{\theta_{2,0}}$ and $\mathfrak{D}e^{\theta_{3,0}}$.

The relation between the local coordinates $x_{i,j}$ used in [3] and the weights w_{ij} is

$$x_{1,1}=w_{23},\quad x_{1,2}=w_{23}w_{24},\quad x_{2,1}=w_{13},\quad x_{2,2}=w_{13}w_{14}w_{23}.$$

Applying the Darboux transformation $\mathfrak{D}$ to the vacuum wave function on $\Gamma(\xi)$ computed in [3], it is not difficult to prove that on $\Gamma_1(\xi)$ the divisor point $P^{(\mathrm{dr})}_{1,\xi}$ has $\tilde\zeta$–coordinate

$$\tilde\zeta(P^{(\mathrm{dr})}_{1,\xi}) = -\frac{\xi^2\mathfrak{D}e^{\theta_{2,0}}}{\xi^2\mathfrak{D}e^{\theta_{2,0}} + w_{23}(\xi^2-1)\mathfrak{D}e^{\theta_{3,0}}}. \tag{6.15}$$

and that on $\Gamma_2(\xi)$ the divisor point $P^{(\mathrm{dr})}_{2,\xi}$ has $\tilde\zeta$–coordinate

(6.16)

$$\tilde\zeta(P^{(\mathrm{dr})}_{2,\xi}) = -\frac{\xi^3(\xi-1)\left[(w_{14}+w_{24})\mathfrak{D}e^{\theta_{2,0}} + w_{14}w_{23}\mathfrak{D}e^{\theta_{3,0}}\right]}{w_{23}(\xi-1)[w_{14}(\xi^3+\xi+1)+w_{24}(1-\xi^2)]\mathfrak{D}e^{\theta_{3,0}} + \xi^2[(\xi^2-1)w_{14}+(1-\xi)w_{24}]e^{\theta_{2,0}}}.$$

The value of the KP wave function is the same at all points marked with the same symbol in Figure 16 and coincides at leading order in ξ at the points α_2 and α_3 for $\xi \gg 1$. Therefore, for any $\xi \gg 1$, the KP divisor point $P^{(\mathrm{dr})}_{1,\xi} \in \Gamma(\xi)$ coincides with the divisor point $P^{(\mathrm{dr})}_{23} \in \Gamma(\mathcal{G}_{\mathrm{red}}) \equiv \Gamma(\infty)$, while $P^{(\mathrm{dr})}_{2,\xi} \in \Gamma(\xi)$ coincides **at leading order in** ξ with the divisor point $P^{(\mathrm{dr})}_{13} \in \Gamma(\mathcal{G}_{\mathrm{red}}) \equiv \Gamma(\infty)$. The relation between the coordinate $\tilde\zeta$ used in [3] and the coordinate ζ at the marked points $\lambda^{(1)}_s$ in Γ_{23} (resp. $\lambda^{(2)}_s$ in Γ_{23}), $s \in [3]$, is the following: $\zeta = \infty, 1, 0$, respectively correspond to $\tilde z = 0, -1, -\xi^2$. Finally, inserting the fractional linear transformation

$$\tilde\zeta = \frac{\xi^2}{(1-\xi^2)\zeta - 1},$$

in (6.15) and (6.16) and using (6.14), it is straightforward to verify (6.13).

Appendix A. The totally nonnegative Grassmannian

In this appendix we recall some useful definitions and theorems from [62] to make the paper self–contained. For more details on the topological properties of $Gr^{\mathrm{TNN}}(k,n)$ and on generalizations of total positivity to reductive groups we refer to [52, 53, 56, 63, 64]. In particular we use Postnikov rules to represent each Le–tableau D by a unique bipartite trivalent oriented network $\mathcal{N}$ in the disk. In Section 3.1 we use the Le–graph $\mathcal{G}$ of $\mathcal{N}$ to construct a curve $\Gamma(\mathcal{G})$, which is a rational degeneration of a smooth M-curve of genus equal to the dimension d of the corresponding positroid cell.

Definition A.1. The totally non–negative part of $Gr(k,n)$ [62]**.** *The totally non–negative Grassmannian $Gr^{TNN}(k,n)$ is the subset of the Grassmannian $Gr(k,n)$ with all Plücker coordinates non-negative, i.e. it may be defined as the following quotient: $Gr^{TNN}(k,n) = GL_k^+ \backslash\ Mat_{kn}^{TNN}$. Here GL_k^+ is the group of $k \times k$ matrices with positive determinant, and Mat_{kn}^{TNN} is the set of real $k \times n$ matrices A of rank k such that all maximal minors are non-negative, i.e. $\Delta_I(A) \geq 0$, for all k–element subsets $I \subset [n]$.*

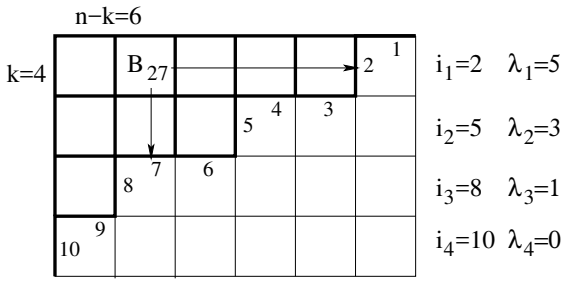

FIGURE 17. *The Young diagram associated to the partition* $(5,3,1,0)$, $k=4$, $n=10$.

The totally positive Grassmannian $Gr^{TP}(k,n) \subset Gr^{TNN}(k,n)$ *is the subset of* $Gr(k,n)$ *whose elements may be represented by* $k \times n$ *matrices with all strictly positive maximal minors* $\Delta_I(A)$.

It is well-known that $Gr(k,n)$ is decomposed into a disjoint union of Schubert cells Ω_λ indexed by partitions $\lambda \subset (n-k)^k$ whose Young diagrams fit inside the $k \times (n-k)$ rectangle (we use the so-called English notation in our text). A refinement of this decomposition was proposed in [33, 34]. Intersecting the matroid strata with $Gr^{\mathrm{TNN}}(k,n)$ one obtains the totally non-negative Grassmann cells [62] with the following property: each cell is birationally equivalent to an open octant of appropriate dimension, and this birational map is also a topological homeomorphism.

Let us recall these constructions. The Schubert cells are indexed by partitions, or, equivalently by pivot sets. To each partition $\lambda = (\lambda_1, \dots, \lambda_k)$, $n-k \geq \lambda_1 \geq \lambda_2 \dots \geq \lambda_k \geq 0$, $\lambda_j \in \mathbb{Z}$ there is associated a pivot set $I(\lambda) = \{1 \leq i_1 < \dots < i_k \leq n\}$ defined by the following relations:

$$i_j = n - k + j - \lambda_j, \quad j \in [k]. \tag{A.1}$$

Each Schubert cell is the union of all Grassmannian points sharing the same set of pivot columns. Therefore, any point in Ω_λ with pivot set I can be represented by a matrix in canonical reduced row echelon form, *i.e.* a matrix A such that $A^i_{i_l} = 1$ for $l \in [k]$ and all the entries to the left of these 1's are zero. The Young diagram representing the Schubert cell Ω_λ is a collection of boxes arranged in k rows, aligned on the left such that the j-th row contains λ_j boxes, $j \in [k]$.

Remark A.1. *In this paper we use the ship battle rule to enumerate the boxes of the Young diagram of a given partition* λ. *Let* $I = I(\lambda)$ *be the pivot set of the* k *vertical steps in the path along the SE boundary of the Young diagram proceeding from the NE vertex to the SW vertex of the* $k \times (n-k)$ *bound box, and let* $\bar{I} = [n] \backslash I$ *be the non–pivot set. Then the box* B_{ij} *corresponds to the pivot element* $i \in I$ *and the non–pivot element* $j \in \bar{I}$ *(see Figure 17 for an example).*

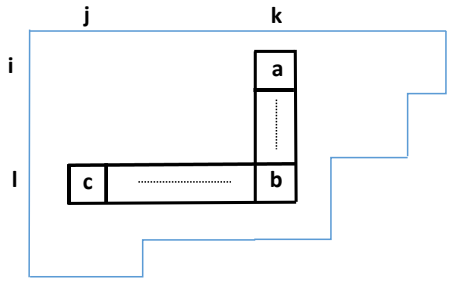

FIGURE 18. *The Le–rule $a, c \neq 0$ imply $b \neq 0$.*

Each stratum in the refined decomposition of $Gr(k,n)$ into matroid strata [33] is composed by the points of the Grassmannian which share the same set of non-zero Plücker coordinates. Each Plücker coordinate is indexed by a base, i.e. a k-element subset in $[n]$, and, for a given stratum, the set of these bases forms a matroid $\mathcal{M}$, i.e. for all $I, J \in \mathcal{M}$ for each $i \in I$ there exists $j \in J$ such that $I\backslash\{i\} \cup \{j\} \in \mathcal{M}$. Then the stratum $\mathcal{S}_{\mathcal{M}} \subset Gr(k,n)$ is defined as

$$\mathcal{S}_{\mathcal{M}} = \{[A] \in Gr(k,n) \,:\, \Delta_I(A) \neq 0 \iff I \in \mathcal{M}\}.$$

A matroid $\mathcal{M}$ is called realizable if $\mathcal{S}_{\mathcal{M}} \neq \emptyset$. The pivot set I is the lexicographically minimal base of the matroid $\mathcal{M}$. In [62], Postnikov studies the analogous stratification for $Gr^{\mathrm{TNN}}(k,n)$.

Definition A.2. ***Positroid cell.*** [62] *The totally nonnegative Grassmann (positroid) cell $\mathcal{S}_{\mathcal{M}}^{TNN}$ is the intersection of the matroid stratum $\mathcal{S}_{\mathcal{M}}$ with the totally nonnegative Grassmannian $Gr^{TNN}(k,n)$:*

$$\mathcal{S}_{\mathcal{M}}^{TNN} = \{\, GL_k^+ \cdot A \in Gr^{TNN}(k,n) \,:\, \Delta_I(A) > 0 \text{ if } I \in \mathcal{M}, \text{ and } \Delta_I(A) = 0 \text{ if } I \notin \mathcal{M} \,\}.$$

The matroid $\mathcal{M}$ is totally nonnegative if the matroid stratum $\mathcal{S}_{\mathcal{M}}^{TNN} \neq \emptyset$.

Example A.1. *$Gr^{TP}(k,n)$ is the top dimensional cell and corresponds to the complete matroid $\mathcal{M} = \binom{[n]}{k}$.*

A useful tool to classify positroid cells are Le–diagrams and Le–graphs [62].

Definition A.3. ***Le–diagram and Le–tableau.***[62] *For a partition λ, a Le–diagram D of shape λ is a filling of the boxes of its Young diagram with 0's and 1's such that, for any three boxes indexed (i,k), (l,k), (l,j), where $i < l$ and $k < j$, filled correspondingly with a, b, c, if $a, c \neq 0$, then $b \neq 0$ (see Figure 18). For such a diagram denote by d the number of boxes of D filled with $1s$.*

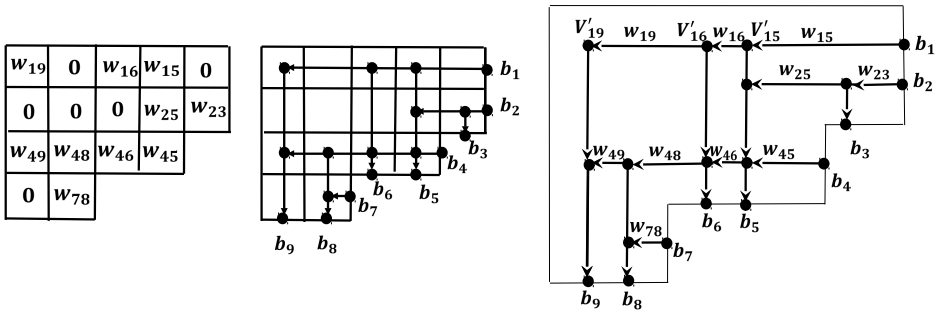

FIGURE 19. *The Le–diagram and the Le–network of Example A.2. The horizontal edges are oriented from right to left while the vertical ones from top to bottom.*

The Le–tableau T is obtained from a Le–diagram D of shape λ, by replacing all 1s in D by positive numbers w_{ij} (weights).

The construction of the Le–graph $\mathcal{G}$ associated to a given Le–diagram is as follows [62]. The boundary of the Young diagram of λ gives the lattice path of length n from the upper right corner to the lower left corner of the rectangle $k \times (n-k)$. A vertex is placed in the middle of each step in the lattice path and is marked $b_1, \ldots, b_n$ proceeding NE to SW. The vertices b_i, $i \in I \equiv I(\lambda)$ corresponding to vertical steps are the sources of the network and the remaining vertices b_j, $j \in \bar{I}$, corresponding to horizontal steps are the sinks. Then the upper right corner is connected to the lower left corner by another path to obtain a simple close curve containing the Young diagram. For each box of the Le–diagram (i,j) filled by 1 an internal vertex V_{ij} is placed in the middle of the box; from such vertex one draws a vertical line downwards to the boundary sink b_j and a horizontal line to the right till it reaches the boundary source b_i. By the Le–property any intersection of such lines is also a vertex. All edges are oriented either to the left or downwards.

To obtain a Le-network $\mathcal{N}$ from a Le–tableaux of shape λ one constructs the Le-graph from the corresponding Le-diagram, assigns the weight $w_{ij} > 0$ from the box B_{ij} to the horizontal edge e which enters V_{ij} and assigns unit weights $w_e = 1$ to all vertical edges [62]. The correspondence between the Le–tableau and the Le-network is illustrated in Figure 19.

The map $T \mapsto \mathcal{N}$ gives the isomorphism $\mathbb{R}^d_{>0} \simeq \mathbb{R}^{E(G)}_{>0}$ between the set of Le–tableaux T with fixed Le-diagram D and the set of Le-networks (modulo gauge transformations) with fixed graph $\mathcal{G}$ corresponding to the diagram D as above.

Given a Le–tableau T with pivot set I it is possible to reconstruct both the matroid and the representing matrix in reduced row echelon form using the Lindström lemma.

Proposition A.1. [62] *Let $\mathcal{N}$ be the Le-network associated to the Le–diagram D and let I be the pivot set. For any k–elements subset $J \subset [n]$, let $K = I \backslash J$ and $L = J \backslash I$. Then the maximal minor $\Delta_J(A)$ of the matrix $A = A(\mathcal{N})$ is given by the following subtraction–free polynomial expression in the edge weights w_e:*

$$\Delta_J(A) = \sum_P \prod_{i=1}^{r} w(P_i),$$

where the sum is over all non–crossing collections $P = (P_1, \dots, P_r)$ of paths joining the boundary vertices b_i, $i \in K$ with boundary vertices b_j, $j \in L$.

Let $i_r \in I$, where $r \in [k]$ and $j \in [n]$. Then the element A^r_j of the matrix A in reduced row echelon form (RREF) associated to the Le–network $\mathcal{N}$ is

$$A^r_j = \begin{cases} 0 & j < i_r, \\ 1 & j = i_r, \\ (-1)^{\sigma_{i_r j}} \sum\limits_{P: i_r \mapsto j} \left(\prod\limits_{e \in P} w_e \right) & j > i_r, \end{cases} \tag{A.2}$$

where the sum is over all paths P from the boundary source b_{i_r} to the boundary sink b_j, $j \in \bar{I}$, and $\sigma_{i_r j}$ is the number of pivot elements $i_s \in I$ such that $i_r < i_s < j$.

Example A.2. *Let us consider the Le–diagram D and Le–network represented in Figure 19. Then $I = (1, 2, 4, 7)$ and the matrix in reduced row echelon form is*

$$A = \begin{pmatrix} 1 & 0 & 0 & 0 & w_{15} & w_{15}(w_{16}+w_{46}) & 0 & -w_{15}w_{48}(w_{16}+w_{46}) & -w_{15}w_{48}w_{49}(w_{16}+w_{46}) - w_{15}w_{16}w_{19} \\ 0 & 1 & w_{23} & 0 & -w_{23}w_{25} & -w_{23}w_{25}w_{46} & 0 & w_{23}w_{25}w_{46}w_{48} & w_{23}w_{25}w_{46}w_{48}w_{49} \\ 0 & 0 & 0 & 1 & w_{45} & w_{45}w_{46} & 0 & -w_{45}w_{46}w_{48} & -w_{45}w_{46}w_{48}w_{49} \\ 0 & 0 & 0 & 0 & 0 & 0 & 1 & w_{78} & 0 \end{pmatrix}.$$

The same example is used in [47] *to illustrate the combinatorial properties of the KP–soliton tropical asymptotics in the limit $t \to -\infty$.*

Remark A.2. Reducible positroid cells *A totally non–negative cell $\mathcal{S}^{TNN}_{\mathcal{M}} \subset Gr^{TNN}(k, n)$ is reducible if its Le–diagram contains either columns or rows filled by 0s* [62]*. The Le–diagram has the j–th column filled by zeros if and only if no base in $\mathcal{M}$ contains the element j. Similarly, the Le–diagram has the r-th row filled by zeros if and only if all bases in $\mathcal{M}$ contain i_r, the r–th element in the lexicographically minimal base $I \in \mathcal{M}$.*

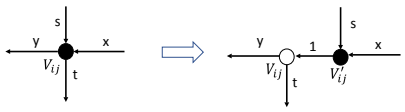

FIGURE 20. *All internal vertices of the Le–network are transformed to trivalent vertices, preserving the boundary measurement map.*

In the first case, there is no path in the Le–network with destination j, and the RREF matrix A has the j–th column filled by zeroes. One can then shift by one all indexes bigger than j in $\mathcal{M}$, call $\mathcal{M}'$ the resulting matroid of k element subsets in $[n-1]$, correspondingly eliminate the j–th column from the Le–diagram and the j–th column from the matrix A, and represent the same point in the totally non–negative cell $\mathcal{S}^{TNN}_{\mathcal{M}'} \subset Gr^{TNN}(k, n-1)$.

In the second case, there is no path in the Le–network starting from the boundary source b_{i_r}, and the r–th row of A contains just the pivot element. One can then eliminate i_r from all the bases in $\mathcal{M}$ and shift by one all the indexes greater than i_r, call $\mathcal{M}'$ the resulting matroid of $k-1$ elements in $[n-1]$, correspondingly eliminate the r–th row of the Le–diagram, eliminate the r–th row and the i_r–th columns from the matrix A and change the sign of all elements of A^i_j with $i < r$ and $j > i_r$, and represent the same point in the totally non–negative cell $\mathcal{S}^{TNN}_{\mathcal{M}'} \subset Gr^{TNN}(k-1, n-1)$.

In section 3.1 we associate an unique universal curve to each positroid cell, by modeling the construction of a rational degeneration of an M–curve on the Le–graph: vertices of the graph correspond to copies of $\mathbb{CP}^1$, whereas the edges govern the positions of the double points. To provide a construction of the curve without parameters, we require that each copy of $\mathbb{CP}^1$ associated to an internal vertex has three marked points. Moreover, the recursive construction of the wave function and the characterization of its divisor is technically simpler if modeled on a bipartite graph where black and white vertices alternate. For the above reasons we follow Postnikov's rules to transform the Le–network $\mathcal{N}$ into a planar bipartite perfect network with internal vertices of degree at most three, and we continue to denote it with $\mathcal{N}$, since this transformation is well-defined. We remark that, after such transformation, $\mathcal{N}$ is perfect since each boundary vertex has degree one and each internal vertex in $\mathcal{G}$ is either the initial vertex of exactly one edge or the final vertex of exactly one edge. For the Le–graph the only relevant transformation concerns the degree four internal vertices which become couples of trivalent vertices of opposite colour [62] (see Figure 20). Moreover, following Postnikov [62], we assign black color to each internal vertex with exactly one outgoing edge and white color to each trivalent internal vertex

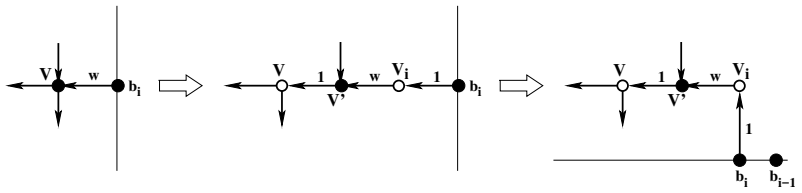

FIGURE 21. *Transformation of graph at the boundary source b_i.*

with exactly one incoming edge. We also assign black color to all boundary vertices. Finally we move all boundary vertices to the same line (see Figure 21). Therefore we get to the following definition.

Definition A.4. ***The trivalent bipartite Le–network used to construct the curve*** $\Gamma(\mathcal{G})$ *The acyclically oriented network associated to the Le–tableau T is transformed into a* **perfect trivalent bipartite network** $\mathcal{N}$ *in the disk with the following rules:*

(1) If the box B_{ij} of T is filled with 1, the vertex V_{ij} is transformed into a couple of one black vertex V'_{ij} and one white vertex V_{ij} (see Figure 20[left]); following [62] *the horizontal edge joining the black vertex V'_{ij} to the white vertex V_{ij} has unit weight, while all other weights are unchanged (see Figure 20[right]);*

(2) All boundary vertices have black colour and degree one. Any isolated boundary source b_i is joined by a vertical edge to a white vertex V_i. If the boundary source b_i is not isolated, we add a white vertex V_i to the edge of weight w starting at b_i, we assign unit weight to the edge joining b_i to V_i and weight w to the other edge at V_i (see Figure 21 middle);

(3) All internal vertices corresponding to a given row r in T, included V_{i_r}, lie on a common horizontal line;

(4) The contour of the disk is continuously deformed in such a way that all of the boundary sources and boundary sinks lay on the same horizontal segment and the edge at each boundary vertex is vertical; in this process the positions of all internal vertices are left invariant (see Figure 21 right).

In Figure 22 we show the bipartite Le–network for Example A.2.

Remark A.3. *Let $\mathcal{G}$ be the bipartite Le–graph associated to the Le–diagram D. Then in $\mathcal{G}$*

(1) Each black vertex has **at most** *one vertical edge;*

(2) Each white vertex has **exactly** *one vertical edge;*

(3) The total number of white vertices is $d + k$;

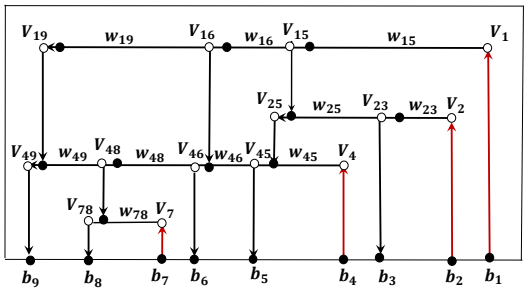

FIGURE 22. *The bipartite Le–network for Example A.2 (see Figure 19). The weights refer to the perfect orientation associated to the pivot base* $[1,2,4,7]$ *of the matroid: the vertical edges starting at the boundary sources* b_1, b_2, b_4 *and* b_7 *are oriented upwards, all other vertical edges are oriented downwards, while all horizontal edges are oriented from right to left.*

(4) If D is irreducible, then the total number of trivalent white vertices is $d-k$, while the total number of trivalent black vertices is $d-n+k$.

For any $r \in [k]$, we denote N_r the number of boxes filled with 1 in the r–th row of the Le–diagram D. By construction we have

$$d \equiv \sum_{i_r \in I} N_r, \qquad \text{with } N_r \equiv \#\{ \text{ boxes } B_{i_r j} \text{ filled by 1, for } j \in \bar{I}\} \tag{A.3}$$

We also introduce an index to simplify the counting of boxes filled by ones. For any fixed $r \in [k]$, let $1 \leq j_1 < j_2 \cdots < j_{N_r} \leq n$ be the non–pivot indexes of the boxes $B_{i_r j_s}$, $s \in \hat{N}_r$, filled by one in the r-th row. Then for any $r \in [k]$, we define the index

$$\chi_l^{i_r} = \begin{cases} 1 & \text{if there exists } s \in [N_r] \text{ such that } l = j_s, \\ 0 & \text{if } B_{i_r l} \text{ is filled by 0 or } l < i_r. \end{cases} \tag{A.4}$$

REFERENCES

[1] S. Abenda *On a family of KP multi–line solitons associated to rational degenerations of real hyperelliptic curves and to the finite non–periodic Toda hierarchy*, J.Geom.Phys. **119** (2017) 112–138

[2] S. Abenda *On some properties of KP–II soliton divisors in* $Gr^{TP}(2,4)$, Ricerche di Matematica (2018), https://doi.org/10.1007/s11587-018-0381-0

[3] S. Abenda, P.G. Grinevich *Rational degenerations of M-curves, totally positive Grassmannians and KP–solitons*, Commun.Math.Phys. **361**, Issue 3 (2018), 1029–1081, doi:10.1007/s00220-018-3123-y.

[4] S. Abenda, P.G. Grinevich *KP theory, plane-bipartite networks in the disk and rational degenerations of* M*–curves*, arXiv:1801.00208

[5] S. Abenda, P.G. Grinevich *Real periodic soliton lattices of KP-II and desingularization of spectral curves: the* $Gr^{TP}(2,4)$ *case*, Topology and physics, Collected papers. Dedicated to Academician Sergei Petrovich

Novikov on the occasion of his 80th birthday, Tr. Mat. Inst. Steklova, 302, ed. V. M. Buchstaber, I. A. Dynnikov, O. K. Sheinman, MAIK Nauka/Interperiodica, Moscow, 2018; arXiv:1803.10968

[6] E. Arbarello , M. Cornalba, P.A. Griffiths *Geometry of algebraic curves. Volume II. With a contribution by Joseph Daniel Harris*, Grundlehren der Mathematischen Wissenschaften 268, Springer, Heidelberg, (2011) xxx+963 pp.

[7] N. Arkani-Hamed, J.L. Bourjaily, F. Cachazo, A.B. Goncharov, A. Postnikov, J. Trnka *Scattering Amplitudes and the Positive Grassmannian*, arXiv:1212.5605

[8] N. Arkani-Hamed, J.L. Bourjaily, F. Cachazo, A.B. Goncharov, A. Postnikov, J. Trnka *Grassmannian geometry of scattering amplitudes*, Cambridge University Press, Cambridge, (2016), ix+194 pp.

[9] M. Atiyah, M. Dunajski, L.J. Mason *Twistor theory at fifty: from contour integrals to twistor strings*, Proc. A. **473** (2017), 20170530, 33 pp.

[10] M. Baker and S. Norine, *Riemann–Roch and Abel–Jacobi theory on a finite graph*, Adv. Math. **215**:2 (2007), 766–788.

[11] G. Biondini, S. Chakravarty *Soliton solutions of the Kadomtsev-Petviashvili II equation.* Journal of Mathematical Physics, **47**, (2006), 033514; doi:10.1063/1.2181907

[12] M. Boiti, F. Pempinelli, A.K. Pogrebkov, B. Prinari *Towards an inverse scattering theory for non-decaying potentials of the heat equation*, Inverse Problems **17** (2001), 937–957

[13] V. Buchstaber, A. Glutsyuk *Total positivity, Grassmannian and modified Bessel functions*, arXiv:1708.02154

[14] V.M. Buchstaber, A.A. Glutsyuk *On determinants of modified Bessel functions and entire solutions of double confluent Heun equations*, Nonlinearity, **29** (2016), 3857–3870

[15] V.M. Buchstaber, S. Terzic *Topology and geometry of the canonical action of T^4 on the complex Grassmannian $G_{4,2}$ and the complex projective space $\mathbb{CP}^5$,* Mosc. Math. J., **16**:2 (2016), 237–273

[16] V.M. Buchstaber, S. Terzic *Toric topology of the complex Grassmann manifolds*, (2018), arXiv: 1802.06449v2

[17] S. Chakravarty, Y. Kodama *Classification of the line-solitons of KPII*, J. Phys. A Math.Theor. **41** (2008), 275209

[18] S. Chakravarty, Y. Kodama *Soliton solutions of the KP equation and application to shallow water waves*, Stud. Appl. Math. **123** (2009) 83–151

[19] L.A. Dickey *Soliton equations and Hamiltonian systems*, Second edition. Advanced Series in Mathematical Physics, 26. World Scientific Publishing Co., Inc., River Edge, NJ, 2003. xii+408 pp.

[20] A. Dimakis, F. Müller-Hoissen *KP line solitons and Tamari lattices*, J. Phys. A **44** (2011), no. 2, 025203, 49 pp.

[21] V. S. Dryuma *Analytic solution of the two-dimensional Korteweg-de Vries (KdV) equation*, JETP Letters, **19**:12 (1973), 387–388

[22] B.A. Dubrovin *Theta functions and non-linear equations*, Russian Math. Surveys, **36**:2 (1981), 11–92

[23] B.A. Dubrovin, T.M. Malanyuk, I.M. Krichever, V.G. Makhankov *Exact solutions of the time-dependent Schrödinger equation with self-consistent potentials*, Soviet J. Particles and Nuclei, **19**:3 (1988), 252–269

[24] B.A. Dubrovin, I.M. Krichever, S.P. Novikov *Integrable systems.* Dynamical systems, IV, 177-332, Encyclopaedia Math. Sci., 4, Springer, Berlin, (2001)

[25] B. A.Dubrovin, S.M. Natanzon *Real theta-function solutions of the Kadomtsev-Petviashvili equation.* Izv. Akad. Nauk SSSR Ser. Mat. **52** (1988) 267–286

[26] V.Fock, A. Goncharov *Moduli spaces of local systems and higher Teichmüller theory*, Publ.Math. I.H.E.S. **103** (2006), 1–211

[27] S. Fomin, A. Zelevinsky *Double Bruhat cells and total positivity.* J. Amer. Math. Soc. **12** (1999) 335–380

[28] S. Fomin, A. Zelevinsky *Cluster algebras I: foundations.* J. Am. Math. Soc. **15** (2002) 497–529

[29] N.C. Freeman, J.J.C. Nimmo *Soliton solutions of the Korteweg de Vries and the Kadomtsev-Petviashvili equations: the Wronskian technique*, Proc. R. Soc. Lond. A **389** (1983), 319–329

[30] F.R. Gantmacher, M.G. Krein *Sur les matrices oscillatoires.* C.R. Acad. Sci. Paris **201** (1935) 577–579

[31] F.R. Gantmacher, M.G. Krein *Oscillation Matrices and Kernels and Small Vibrations of Mechanical Systems*, (Russian), Gostekhizdat, Moscow-Leningrad, (1941), second edition (1950); revised English edition from AMS Chelsea Publ. (2002)

[32] M. Gekhtman, M. Shapiro, A. Vainshtein *Cluster algebras and Poisson geometry*, Mathematical Surveys and Monographs, 167. American Mathematical Society, Providence, RI, 2010. xvi+246 pp

[33] I. M. Gel'fand, R. M. Goresky, R. D. MacPherson, V. V. Serganova *Combinatorial geometries, convex polyhedra, and Schubert cells*, Adv. in Math. **63** (1987), no. 3, 301–316

[34] I.M Gel'fand and V.V. Serganova *Combinatorial geometries and torus strata on homogeneous compact manifolds*, Russian Mathematical Surveys, **42** (1987), no. 2, 133–168

[35] A.B. Goncharov, R. Kenyon *Dimers and cluster integrable systems*, Ann. Sci. Éc. Norm. Supér. (4) **46** (2013), no. 5, 747–813

[36] P. Griffiths, J. Harris *Principles of Algebraic Geometry*, John Wiley & Sons, (1978)

[37] D.A. Gudkov *The topology of real projective algebraic varieties*, Russ. Math. Surv. **29** (1974) 1–79

[38] A. Harnack *Über die Vieltheiligkeit der ebenen algebraischen Curven*, Math. Ann. **10** (1876) 189–199

[39] R. Hirota *The direct method in soliton theory*, Cambridge Tracts in Mathematics, 155. Cambridge University Press, Cambridge, (2004), xii+200 pp.

[40] I. Itenberg, G. Mikhalkin, E. Shustin *Tropical algebraic geometry. Second edition*, Oberwolfach Seminars, 35. Birkhäuser Verlag, Basel, (2009), x+104 pp.

[41] B.B. Kadomtsev, V.I. Petviashvili *On the stability of solitary waves in weakly dispersive media*, Sov. Phys. Dokl. **15** (1970) 539–541

[42] S. Karlin *"Total Positivity, Vol. 1.* Stanford, (1968)

[43] R. Kenyon, A. Okounkov, S. Sheffield *Dimers and amoebae*, Ann. of Math. (2) **163** (2006), no. 3, 1019–1056

[44] Y. Kodama *Young diagrams and N-soliton solutions of the KP equation*, J Phys. A Math. Gen. **37** (2004), 11169–11190

[45] Y. Kodama *KP solitons in shallow water* J. Phys. A: Math. Theor. **43** (2010), 434004

[46] Y. Kodama, L.K. Williams *The Deodhar decomposition of the Grassmannian and the regularity of KP solitons*, Adv. Math. **244** (2013), 979–1032

[47] Y. Kodama, L.K. Williams *KP solitons and total positivity for the Grassmannian*, Invent. Math. **198** (2014) 637–699

[48] I.M. Krichever *An algebraic-geometric construction of the Zakharov-Shabat equations and their periodic solutions*, Sov. Math., Dokl. **17** (1976), 394–397

[49] I.M. Krichever *Integration of nonlinear equations by the methods of algebraic geometry*, Functional Analysis and Its Applications, **11**:1 (1977), 12–26

[50] I.M. Krichever *Spectral theory of finite-zone nonstationary Schrödinger operators. A nonstationary Peierls model*, Functional Analysis and Its Applications, **20**:3 (1986), 203–214

[51] I.M. Krichever *Spectral theory of two-dimensional periodic operators and its applications*, Russian Math. Surveys, **44**:8 (1989), 146–225

[52] G. Lusztig *Total positivity in reductive groups*, Lie Theory and Geometry: in honor of B. Kostant, Progress in Mathematics **123**, Birkhäuser, Boston, (1994), 531–568

[53] G. Lusztig *Total positivity in partial flag manifolds*, Representation Theory, **2** (1998), 70–78

[54] T.M. Malanyuk *A class of exact solutions of the KadomtsevPetviashvili equation*, Russian Math. Surveys, **46**:3 (1991), 225–227

[55] N. E. Mnëv *The universality theorems on the classification problem of configuration varieties and convex polytope varieties*, in Topology and Geometry – Rohlin Seminar, O. Ya. Viro ed., Lecture Notes in Mathematics **1346**, Springer, Heidelberg.

[56] R. Marsh, K. Rietsch *Parametrizations of flag varieties*, Representation Theory, **8**,(2004), 212–242

[57] V.B. Matveev *Some comments on the rational solutions of the Zakharov-Schabat equations*, Letters in Mathematical Physics, **3** (1979), 503–512

[58] T. Miwa, M. Jimbo, E. Date *Solitons. Differential equations, symmetries and infinite-dimensional algebras*, Cambridge Tracts in Mathematics, 135. Cambridge University Press, Cambridge, (2000), x+108 pp.

[59] S.M. Natanzon *Moduli of real algebraic surfaces, and their superanalogues. Differentials, spinors, and Jacobians of real curves*, Russian Mathematical Surveys, **54**:6 (1999), 1091–1147

[60] S.P. Novikov *The periodic problem for the Kortewegde vries equation*, Functional Analysis and Its Applications, **8**:3 (1974), 236–246

[61] A. Pinkus *Totally positive matrices*, Cambridge Tracts in Mathematics, **181**, Cambridge University Press, Cambridge, (2010), xii+182.

[62] A. Postnikov *Total positivity, Grassmannians, and networks*, arXiv:math/0609764 [math.CO]

[63] A. Postnikov, D. Speyer, L. Williams *Matching polytopes, toric geometry, and the totally non-negative Grassmannian*, J. Algebraic Combin. **30** (2009), no. 2, 173–191

[64] K. Rietsch *An algebraic cell decomposition of the nonnegative part of a flag variety*, Journal of Algebra **213** (1999), no. 1, 144–154.

[65] M. Sato *Soliton Equations as Dynamical Systems on a Infinite Dimensional Grassmann Manifolds*, RIMS Kokyuroku, **439** (1981), 30–46

[66] I. Schoenberg *Über variationsvermindende lineare Transformationen*, Math. Zeit. **32**, (1930), 321–328.

[67] I.A. Taimanov *Singular spectral curves in finite-gap integration*, Russian Mathematical Surveys, **66**:1 (2011), 107–144

[68] K. Talaska. *A Formula for Plücker Coordinates Associated with a Planar Network,* IMRN, **2008**, (2008), Article ID rnn081, 19 pages. doi:10.1093/imrn/rnn081

[69] D.P. Thurston *From dominoes to hexagons*, Proc. Centre Math. Appl. Austral. Nat. Univ., **46**, Austral. Nat. Univ., Canberra, (2017), 399–414

[70] O. Ya. Viro *Real plane algebraic curves: constructions with controlled topology*, Leningrad Math. J. **1** (1990), no. 5, 1059–1134

[71] V.E. Zakharov, A. B. Shabat *A scheme for integrating the nonlinear equations of mathematical physics by the method of the inverse scattering problem. I*, Funct. Anal. and Its Appl., **8** (1974), Issue 3, 226–235

[72] Y. Zarmi *Vertex dynamics in multi-soliton solutions of Kadomtsev-Petviashvili II equation*, Nonlinearity **27** (2014), 1499–1523

Dipartimento di Matematica, Università di Bologna, P.zza di Porta San Donato 5, I-40126 Bologna BO, ITALY

E-mail address: simonetta.abenda@unibo.it

L.D.Landau Institute for Theoretical Physics, pr. Ak Semenova 1a, Chernogolovka, 142432, Russia, pgg@landau.ac.ru, Lomonosov Moscow State University, Faculty of Mechanics and Mathematics, Russia, 119991, Moscow, GSP-1, 1 Leninskiye Gory, Main Building,, Moscow Institute of Physics and Technology, 9 Institutskiy per., Dolgoprudny, Moscow Region, 141700, Russia.